CONTROLS ON PRECIOUS-METAL MINERALIZATION,

EASTON-PACIFIC VEIN,

VIRGINIA CITY MINING DISTRICT,

MADISON COUNTY, MONTANA

by

Mark S. Lockwood

Submitted in Partial Fulfillment of the

Requirement for the Degree of Master of Science

in Geology

New Mexico Institute of Mining and Technology

Socorro, New Mexico

November 29, 1990

ABSTRACT

The Virginia City mining district in southwestern Montana
has produced economically significant amounts of placer and
lode gold, with the Easton and Pacific mines being the
largest lode producers in the district. Mining exploited
composite quartz vein structures that are spacially related
to the Brown's Gulch monzonite stock which intrudes
Precambrian metamorphic rocks. Mineralization comprises
pyrite, chalcopyrite, galena, sphalerite, acanthite,
tellurides and native precious metals and can be
characterized by two distinct mineralizing stages separated
by periods of brecciation.

Argillic alteration in the area of the Pacific mine was
produced by hydrothermal activity associated with
mineralization. Illite:smectite ratio in the zone of
argillic alteration varies inversely with respect to
distance from the Pacific vein system. The results of this
study are consistent with similar studies done on active
geothermal systems and hydrothermal ore deposits.
Systematic variations in illite/smectite ratios in zones of
argillic alteration have been documented in deposits as
diverse as Kuroko-type volcanogenic massive sulphide
deposits (Inoue and Utada, 1983) to lower temperature

epithermal deposits (Horton, 1989) and modern geothermal systems (Eslinger and Savin, 1973).

Fluid inclusion data suggest ore-forming fluids evolved with time from moderate temperature (275°C), low salinity (3-6 eq wt% NaCl) solutions to lower temperature (175°C), higher salinity (10-12 eq wt% NaCl) solutions. This suggests that Virginia City mineralization involved the mixing of fluids from different sources.

When compared to other hydrothermal ore deposits, the Virginia City deposits appear most similar to the deposits of the Cheonan district in Korea. These deposits appear to bridge the gap between model epithermal and mesothermal deposits.

Table of Contents

LIST OF FIGURES

LIST OF TABLES

ix

ACKNOWLEDGEMENTS

This work was partly supported by BHP/Utah International Inc. and also by generous donations by my parents. Larry Ott, project manager with BHP/Utah, deserves special thanks for his patience and expertise in the field and office. My graduate committee, Bill Chavez, Andy Campbell and Paul Eimon have provided expert knowledge, constructive criticisms, and motivation throughout the project. My wife, Sharon, has furnished much needed distractions and support and to her I am forever indebted. Technical support has come from many people: George Austin-clay mineralogy, Kurt Panter-fluid inclusions, Craig Beasley-geophysics, John Thede and Doug Curry-field assistance, and Randy Strong-drafting, Hugh Dresser-aerial photography. Many thanks to my fellow students who have listened to my problems and have helped provide solutions.

INTRODUCTION

Lode gold deposits in the headwaters of Brown's and Alder

Gulches have long been considered the source of placer gold

in Alder Gulch, near Virginia City, Montana. Over 2.5

million ounces of placer gold were recovered from Alder

Gulch in the late 1800's, making it one of the richest

placer deposits in the U.S. The nature of the lode

deposits in the Virginia City district have been discussed

in many reconnaissance reports (Winchell, 1914; Tansley et

al., 1933; Lorain, 1938) but no detailed studies have

described this mineralization.

The Easton and Pacific mines were the largest lode

producers in the Virginia City district. They were targeted

by BHP/Utah International as a possible low-grade bulk

tonnage deposit after reconnaissance sampling uncovered

anomalous gold values within country rock. This project is

the result of a follow up investigation of the property.

Purpose of Study

The primary goals of this research project are:

    1. Document the occurrence of gold deposits

       in the Virginia City district with emphasis on

the Easton-Pacific vein system;

2. Interpret the structural controls on the mineralization in the district and the relationship to regional structural patterns;

3. Investigate the possibility of disseminated gold mineralization in the wall rocks in the area of the Easton and Pacific mines;

4. Define the conditions and timing of mineralization and alteration at the Easton and Pacific mines.

Since much of the high-grade ore has been exploited in the Virginia City district, this study will be useful in the search for hidden ore deposits in the district and elsewhere in the Tobacco Root Mountains and similar regions.

Methodology

The first step in fulfilling these goals was a complete literature search for any and all information that was available on the Virginia City district and the Tobacco Root Mountains in general. This information was then compiled with an emphasis placed on geologic and structural controls on mineralization along with the type and

abundance of mineralization throughout the Tobacco Root mining region.

The field methods used were surface and underground mapping, soil sampling, geophysics, trenching and drilling. Laboratory methods include thin section and polished section microscopy, fluid inclusion analysis, and X-ray diffraction.

Surface and underground mapping in the area of the Easton-Pacific mine was done at several scales (1"=1000', 1"=400', 1"=100', 1"=20'). Information collected on the Virginia City district was compiled at the scale of 1"=1000'. Enlarged USGS topo maps were used as base maps, along with airphotos at appropriate scales. Tape and brunton surveys were conducted in underground workings and in trenches. Emphasis in mapping was placed on wall rock alteration and geometry of vein/wallrock contacts. Samples were collected for thin section and polished section microscopy, fluid inclusion analysis, assay and X-ray diffraction identification.

Location, Access and Physiography

The Virginia City mining district is located in central

Madison County, southwestern Montana (fig. 1). The

district, shown in figure 2, extends from Alder Gulch on

the north and east, to the west of Brown's Gulch, and to

the flanks of the Gravelly Range on the south (Cole, 1983).

The Easton and Pacific mines are located at the head of

Brown's Gulch approximately 4.5 mi south of Virginia City.

Virginia City is accessible via Montana Highway 287. The

Easton and Pacific mines and the Virginia City district are

accessible on numerous unimproved dirt roads, although

winter access is difficult in the southern portion of the

district. Many of the bedrock exposures occur in stream

cuts, along ridgetops and in mine cuts. Several adits and

crosscuts are still accessible but caution is advised in

entering them. The majority of the Easton and Pacific mine

workings are caved.

Elevations in the Virginia City district range from 5700

ft. above sea level in the north to 8561 ft. in the south.

The low-lying northern half of the district is sparsely

vegetated with sage brush and other low ground cover. This

type of vegetation grades into thick conifer stands at

higher elevations.
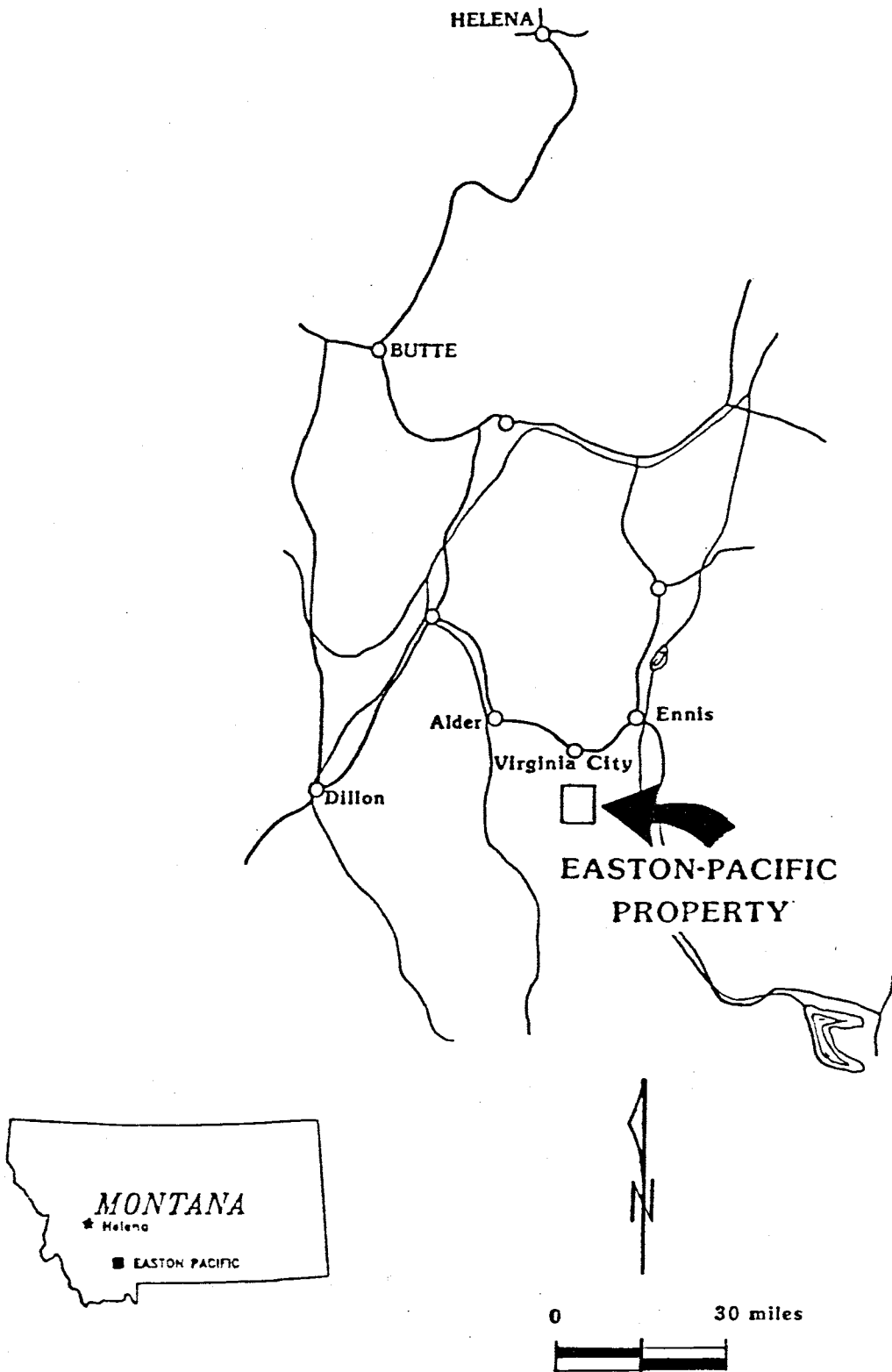
Figure 1.   Location Map.
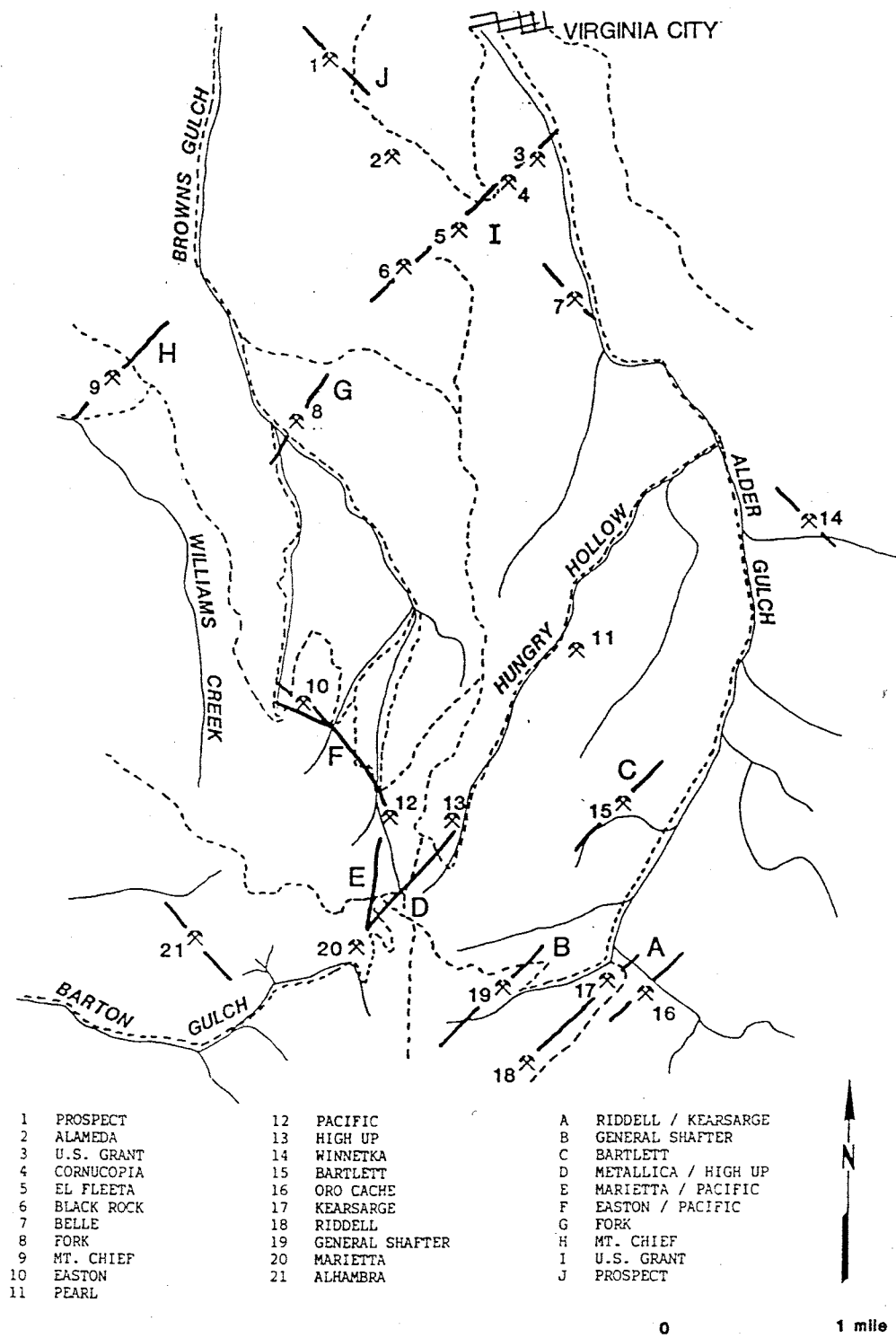
Figure 2. Map showing the location of mines and major vein trends in the Virginia City district.

#	Name	#	Name	Letter	Name
1	PROSPECT	12	PACIFIC	A	RIDDELL / KEARSARGE
2	ALAMEDA	13	HIGH UP	B	GENERAL SHAFTER
3	U.S. GRANT	14	WINNETKA	C	BARTLETT
4	CORNUCOPIA	15	BARTLETT	D	METALLICA / HIGH UP
5	EL FLEETA	16	ORO CACHE	E	MARIETTA / PACIFIC
6	BLACK ROCK	17	KEARSARGE	F	EASTON / PACIFIC
7	BELLE	18	RIDDELL	G	FORK
8	FORK	19	GENERAL SHAFTER	H	MT. CHIEF
9	MT. CHIEF	20	MARIETTA	I	U.S. GRANT
10	EASTON	21	ALHAMBRA	J	PROSPECT
11	PEARL				

The district is cut by numerous drainages, the main ones
being Alder and Browns Gulches. These are medium to small
size creeks whose level fluctuates with snow melt and
rainfall.

Property Ownership and Status

The Easton and Pacific mines and approximately 8 mi^2
surrounding them are owned by the Easton, Pacific and
Riverside Mining Company, Morrison, Colorado. The claim
block consists of 34 patented mining claims and 284
unpatented mining claims. For a discussion of past
ownership refer to section on district history.

Previous Studies

The Tobacco Root Mountains have been the subject of many
petrographic, structural and regional studies, albeit
detailed investigations of ore deposits in this region have
not been performed. The following is a compilation of work
done in the area dealing with regional geology and ore
deposits.

The first record of the Easton-Pacific lode and the
Virginia City mining district was published in Statistics

of Mines and Mining in the States and Territories West of
the Rocky Mountains, for the calendar year 1869. Records
of mining in the Virginia City district continued in this
publication, but it was not until 1914 that any geologic
investigations were conducted in the area. Winchell (1914)
reported on the mining districts in the Dillon quadrangle
and adjacent areas in southwestern Montana. Tansley,
Schafer, and Hart (1933) conducted a reconnaissance survey
of the general geology and ore deposits of the Tobacco Root
Mountains. Lorain (1937) described the geologic settings
of lode gold mines in the Tobacco Root Mountains along with
mining and processing techniques used at that time.
Levandowski (1956) investigated ore deposits in southern
Sheridan mining district. Burger (1966) conducted a
structural study of the Sheridan district and proposed
structural controls on the mineralization present there.
Hadley (1969) mapped the southern portion of the Virginia
City district in the 15 minute Varney quadrangle.
Vitaliano and Cordua (1979) mapped the southern Tobacco
Root Mountains with an emphasis on the Precambrian geology.
Weir (1982) published a preliminary map of the northern
portion of the Virginia City district. Cole (1983)
described the vein mineralogy and interpreted the
alteration assemblage at the U.S. Grant mine in the
Virginia City district. Ruppel (1985) studied the Middle

Cambrian rocks of the Tobacco Root Mountains and their relation to gold mineralization. Kinley (1987) described the geology and paragenetic sequence of gold mineralization at the Red Pine mine in the Sheridan district.

VIRGINIA CITY DISTRICT HISTORY

The 1863 discovery of gold in Alder Gulch, near Virginia City, caused an influx of miners and prospectors into the area. Within a few years lodes were discovered, and by the late 1860's a few stamp mills were in operation. Discoveries throughout the Tobacco Root Mountains made this region one of the most productive in the history of the early West (Young, 1970). By the early 1900's, 2.5 million ounces of placer gold were taken from Alder Gulch, and approximately 142,000 ounces of gold were taken from lode deposits. The most important mining areas in the Tobacco Root region were Virginia City, Pony, Norris, Renova and Sheridan districts.

Lode mining in Virginia City District began with the establishment of the Oro Cache and the Kearsarge mines in the mid-1860's at the head of Alder Gulch. Vigorous prospecting in the district resulted in the discovery of the Easton-Pacific, Prospect, U.S. Grant, Winnetka, and Marrietta mines, and numerous other smaller deposits. Figure 2 shows the location of mines in the Virginia City district. By 1890 stamp mills were installed at many of the mines. High-grade gold and silver ore was being exploited from the upper oxidized zones of these deposits (Lorain, 1937).

On May 3, 1869 the Easton lode was discovered by Joseph and D.J. Emery. The prospect was opened by two cross-tunnels, one 70 feet below the other, and a shaft. Most of the ore was treated at the mine, but select high-grade was sent to Swansea, Wales via San Francisco. Without a railroad, shipping the ore was prohibitively expensive. The Pacific lode was discovered by Joseph Emery in 1885. In 1889, a 10 stamp mill capable of processing 15 tons of ore a day was constructed on Brown's Gulch (Anon., 1889). As mining continued at Easton, the continuity and thickness of the vein was confirmed to be sufficient to warrant further upgrading of the processing facilities. By 1894, 100 men were employed at the Easton mine, and 2,200 feet of tunnels had been driven (Anon., 1894). Up to this point, very little stoping had been done as all of the ore was being extracted from the tunneling process. In late 1894, a mill capable of processing 28 tons a day was constructed at the Easton mine. Along with the mill came electric lights and power. The ore was being mined from several veins 3 to 5 feet thick with an average grade of 70 ounces silver and 1 ounce gold per ton. Some high-grade zones assayed as high as 700 oz. silver and 2 oz. gold per ton. Progress continued at Easton and development at the Pacific proved

it to be continuous and high-grade. By 1900, 1,400 feet
of tunnel was complete at the Pacific mine as shown in
figure 3 (Anon., 1900). Around this time smelter records
show the first sulfide ores were being encountered at the
Easton mine at a depth of about 400 feet. The early
1900's saw significant production from the Easton and
Pacific mines, with shipping ore averaged 62 oz. silver
and 2.7 oz. gold per ton. By the time WWI closed the gold
mines, the Easton mine had been extended to 5 levels, 500
feet below the surface; the Pacific mine had been
developed by two tunnels, 1,400 and 2,600 feet long.
After the war, production was mainly from the reworking of
old tailings. Many operators tried to reopen the mines
but none succeeded until the U.S.Grant Mining Co. took
over in 1946. They had plans to drive a 3,600 foot tunnel
that would intersect the veins at the 600 foot level and
dewater the mine which had flooded (Anon., 1947). The
tunnel was completed in 1948 and the first ore was shipped
in 1949 (fig.4). This ore averaged 0.3 oz gold and 10.8
oz silver per ton. No more records of production from the
Easton or Pacific mine are found after these shipments.
In the late 1970's, the late Ed Scheitlin operated an
small open pit at the Easton and Pacific mines with some
success.
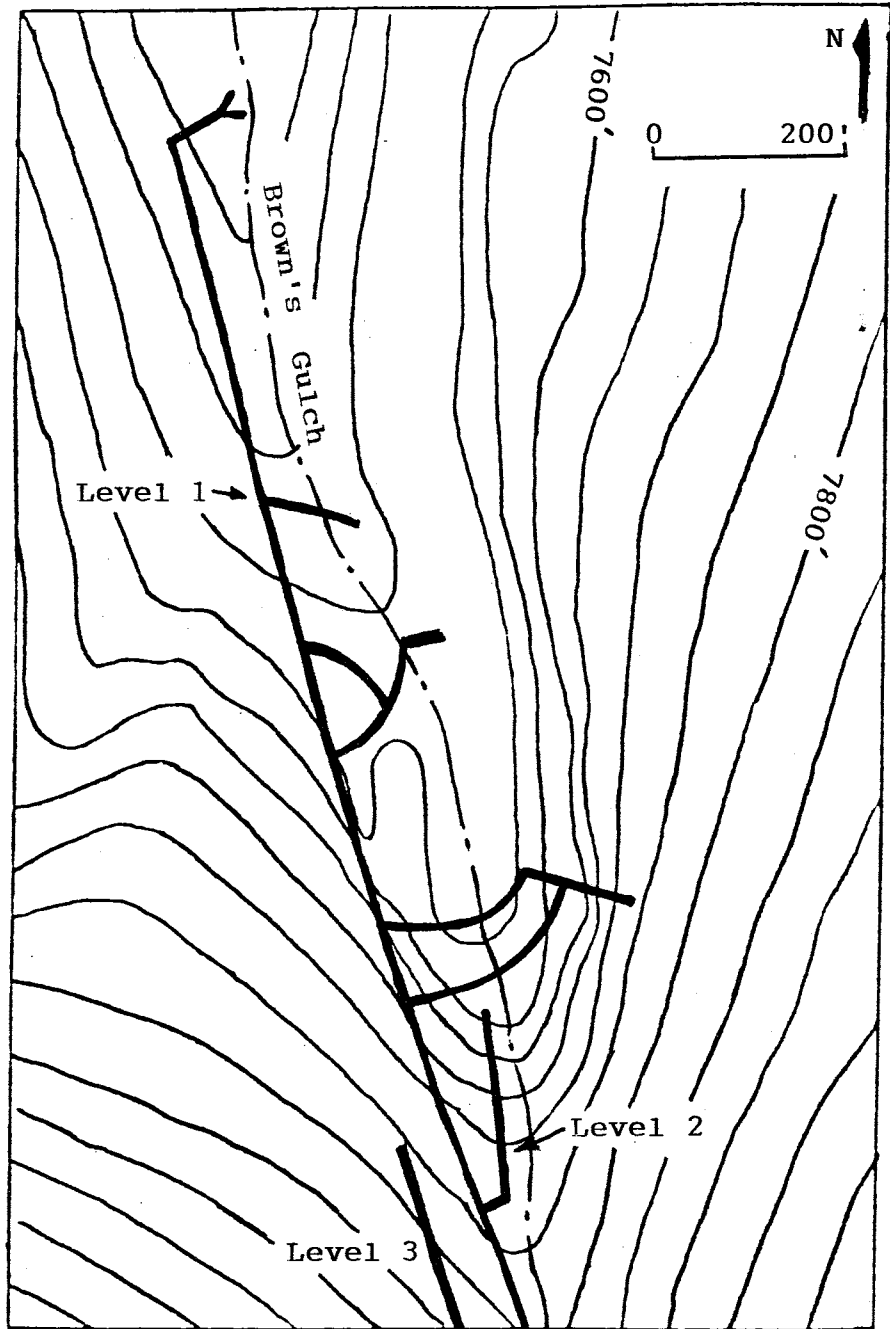
Figure 3. Plan map of the Pacific mine.
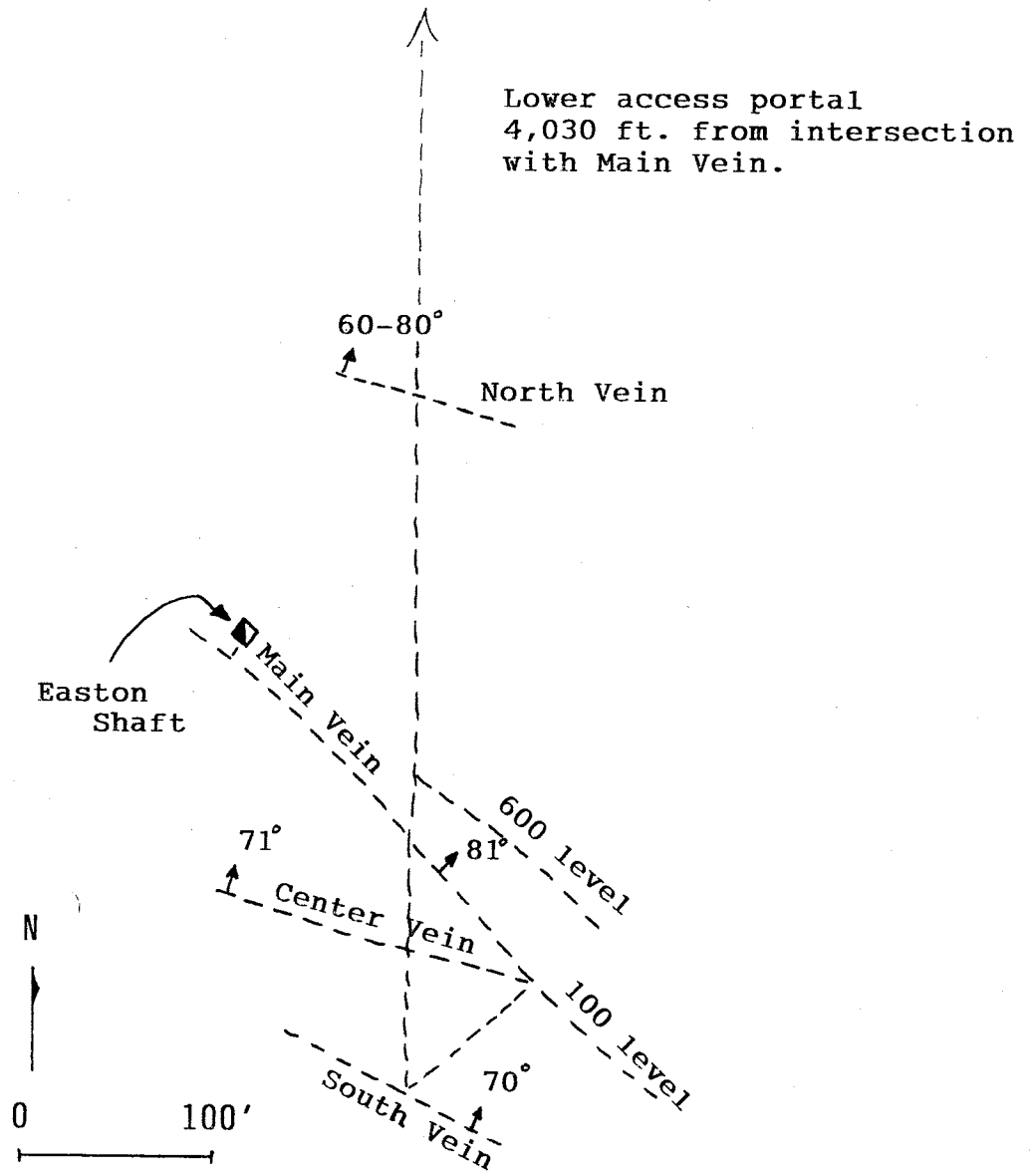
Figure 4. Plan map of the Easton mine showing the
location of major vein structures.

REGIONAL GEOLOGIC AND LITHOLOGIC SETTINGS

The Virginia City district is situated at the southern extent of the Tobacco Root Mountains and the northern extent of the Gravelly Range (Figure 5). The Tobacco Root Mountains are described by Mueller and Cordura (1976) as a large, northwest plunging domaluplift of multiply deformed and metamorphosed Archean rocks, which are concentrically surrounded by folded and thrusted Paleozoic and Mesozoic sediments. The uplift is cored by the Tobacco Root batholith, a Late Cretaceous (72-77 m.y.) quartz monzonite genetically related to the Boulder batholith (Vitaliano and others, 1980; Smith, 1970). Tertiary volcanic flows disconformably overlie Archean rocks in the area of Virginia City (Wier, 1983).

PRECAMBRIAN ROCKS

Metamorphic Rocks

Archean metamorphic rocks of the Tobacco Root Mountains belong to the Cherry Creek sequence. Pearle (1896) was the first to describe this sequence of rocks in the area of Three Forks, Montana, to the northeast of the Virginia City district. The Cherry Creek type section was later described
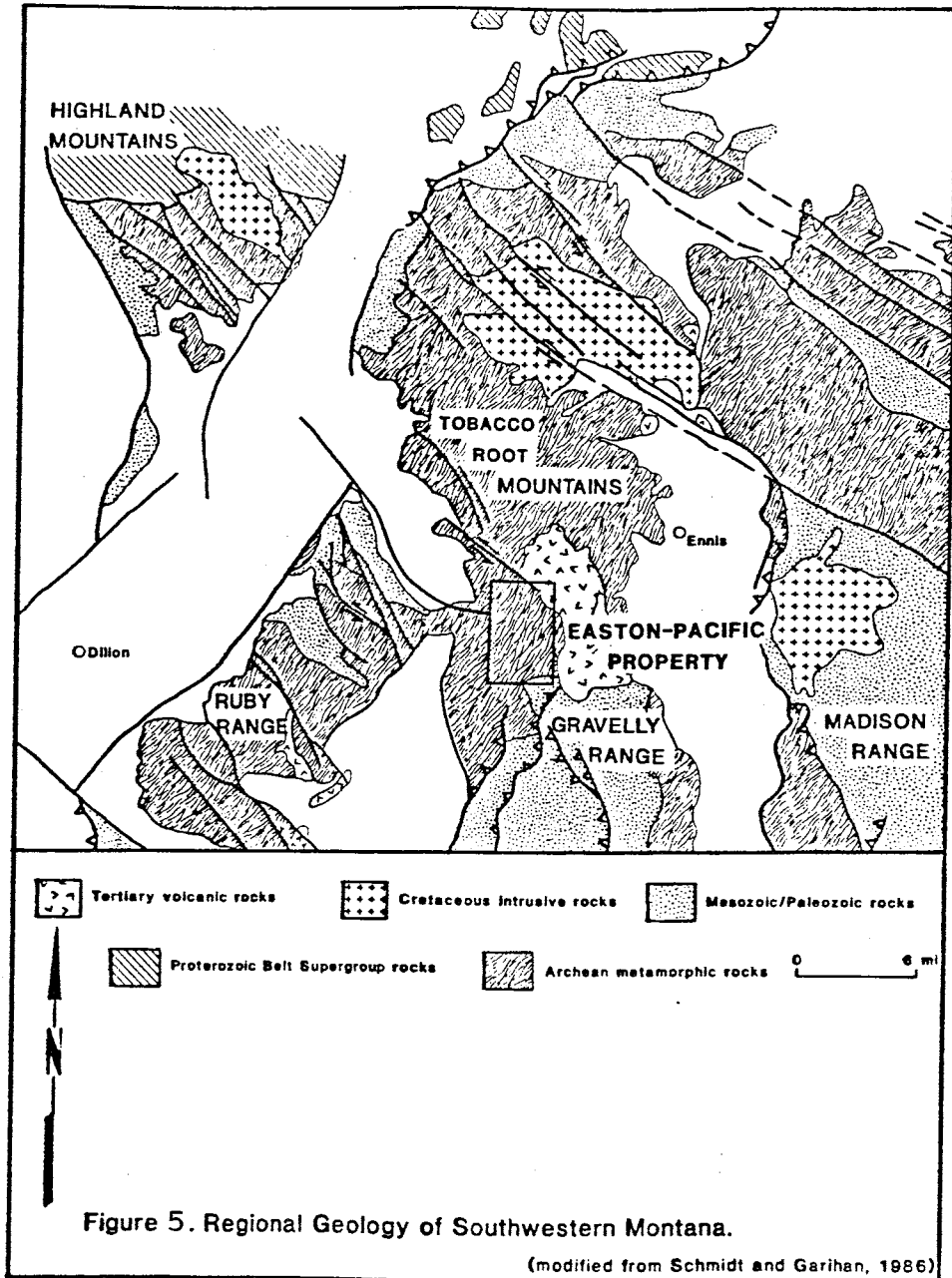
Figure 5. Regional Geology of Southwestern Montana.

(modified from Schmidt and Garihan, 1986)

Legend:
- Tertiary volcanic rocks
- Cretaceous intrusive rocks
- Mesozoic/Paleozoic rocks
- Proterozoic Belt Supergroup rocks
- Archean metamorphic rocks

0 — 6 mi

Map labels: HIGHLAND MOUNTAINS, TOBACCO ROOT MOUNTAINS, O Ennis, EASTON-PACIFIC PROPERTY, O Dillon, RUBY RANGE, GRAVELLY RANGE, MADISON RANGE

by Runner and Thomas (1928) as a sequence of
quartz-feldspar gneiss, quartz-mica schist, crystalline
limestone, quartzite, and hornblende-biotite schist.
Winchell (1914) and Tansley, et al. (1933) described the
Pony Series, an older sequence of metamorphic rocks in the
northern Tobacco Root Mountains. They reported the Pony
Series as having similar mineralogy to the Cherry Creek
sequence. Recent work by Gilette (1966), Mueller and
Cordura (1976), and James and Hedge (1980) show that the
Cherry Creek and Pony series rocks are similar in age;
differing depositional environments possibly resulted in
variations in lithology. The rocks of the Cherry Creek
series have been subjected to two major deformational
events. Cordura (1976) suggests the first event occurred at
2700-2900 m.y., which correlates with an event documented
in the Beartooth Mountains to the east. He suggests that
the second event occurred at 1600-1900 m.y., an event that
is recorded throughout southwestern Montana.

Meta-ultramafic rocks are present in the Tobacco Root
Mountains as small lenses, pods, and stocklike masses
(Vtaliano and others, 1979). They consist mainly of
serpentinized olivine, hornblende, orthopyroxene, and
clinopyroxene. The origin of these bodies is controversial.
Tendall (1978) suggests they may be tectonically emplaced

slices of the upper mantle or refractory residues from partially melted solid upper mantle. The presence of sharp contacts and the nonlinear distribution of the meta-ultramafic bodies, and the dominance of orthopyroxene over olivine favor an origin from a deep-seated magma (Vitaliano and others, 1979).

Pegmatites

Rocks of the Cherry Creek series have been intruded by numerous crosscutting and concordant pegmatite and mafic dikes. These pegmatites occur as lenses, streaks and tabular bodies. Vitaliano and others (1979) report that concordant pegmatites in the northern Tobacco Root Mountains occur as pods in the crests of subisoclinal folds and predate the latest metamorphic event. The discordant pegmatites as mapped by Vitaliano and others (1979) and Weir (1983) appear to be preferentially emplaced either along joints and faults or subparallel to the axial surfaces of open folds. In the northern portion of the Virginia City district discordant pegmatites occur as a swarm with as many as 5 dikes per 30 m which can be traced for several miles. These pegmatites are course grained and contain quartz, plagioclase, and microcline. Wier (1983) reports the pegmatite dikes to be approximately 1.9 billion

years old. Three sets of mafic dikes have been identified

by Koehler (1972, 1976) and Wooden and others (1978). These

mafic dikes range in age from 1.4 m.y. to 1.1 m.y. old.

$^{87}Sr/^{86}Sr$ ratios of these dikes range from 0.702 to

0.703 which indicate probable derivation from mantle

material (Vitaliano, 1979).

POST PRECAMBRIAN ROCKS

Sedimentary Rocks

Paleozoic sedimentary rocks unconformably overlie

Precambrian rocks in the Tobacco Root Mountains. These

sedimentary rocks comprise limestones with subordinate

sandstone and mudstone (Samuelson and Schmidt, 1981).

Paleozoic rocks are unconformably overlain by Mesozoic

rocks (Tansley and others, 1933).

Intrusive Rocks

The late Cretaceous Tobacco Root Batholith and several

smaller plutons form the central portion of the the Tobacco

Root Mountains. Vitaliano and others (1979) reports the age

of these plutons to be 74 to 71 m.y. These intrusions are

granitic in compositon and appear to zoned (Smith, 1970).

The Tobacco Root batholith crops out over a 120 mi^2 area. The composition of the batholith ranges from hornblende diorite to granite with intermediate facies of tonalitic, granodioritic, quartz monzonitic and monzonitic composition (Vitaliano and others, 1979). Smith (1970) documented a gradational concentric zoning from the periphery to the core of the batholith. Smith's study showed that the rocks become more silicic towards the core. Using this information, Vitaliano and others (1979) suggest that the batholith was emplaced by a single injection of magma and differentiated in place. This theory is also supported by the lack of primary flow structures preserved in the batholith except at the margins.

Volcanic Rocks

Tertiary volcanic rocks ranging in composition from basalt to rhyolite unconformably overlie Archean rocksd (Wier, 1983; Chadwick, 1981). These rocks comprise a series of lava flows and pyroclastic and volcanoclastic sedimentary units. Weir (1983) reports the age of these volcanics in the area of Virginia City to be approximately 51 m.y.

Unconsolidated Deposits

Alluvium and colluvium derived from local outcrops have accumulated in valley floors and hillslopes (Vitaliano and others, 1979). Glacial debris in the form of terminal and lateral moraines are present in the valleys draining the highest peaks of the central Tobacco Root Mountains.

REGIONAL STRUCTURAL SETTING

Structures in the Tobacco Root Mountains show evidence of activity dating back to the Precambrian (Vitaliano and others, 1979) with intermittent activity along the same structures through the Eocene (Schmidt and Garihan, 1986). Two major thermal events (2.7 and 1.6 b.y.) folded the Archean rocks (Vitaliano and others, 1979) and brittle and semibrittle deformation has occurred along two sets of faults; northeast and northwest (Schmidt and Garihan, 1986).

FOLDS

Regional scale folding in the southern Tobacco Root Mountains is dominated by the Mill Gulch antiform, a north trending broad open fold that is flanked by a series of subisoclinal folds which are nearly parallel (Vitaliano and others, 1979). Drag folds are present along northwest trending fault zones that have experienced movement during the Laramide orogeny (Vitaliano and others, 1979).

Vitaliano and others (1979) interpret recumbent isoclinal folds as the result of a compressional event at approximately 2.7 b.y. Later in the Precambrian (1.6 b.y.)

this isoclinally folded strata was deformed into a set of northeast-trending open folds. Evidence for the refolding of Archean rocks along with overlying Phanerozoic rocks during the Laramide orogeny is recognized as drag folds along major transcurrent faults.

FAULTS

The major faults in southwestern Montana, shown in figure 6, can be classified into two sets: northwest-trending and northeast-trending (Vitaliano and others, 1979). The majority of these faults are steeply dipping, with dips varying between 50° and 80° to the north. These faults have been active since the Precambrian and show evidence for movement as recently as the Holocene (Schmidt and Garihan, 1986). In addition, these structures, especially those trending northwest, have been important in localizing mineralized quartz veins and igneous intrusions as well as sedimentary deposits and volcanic centers. Although ample conduits for fluid flow existed since the Archean mineralizing events appear to be related to the emplacement of the Tobacco Root batholith.

Vitaliano and others (1979) determined the earliest age of fault activity to be Precambrian through the fact that
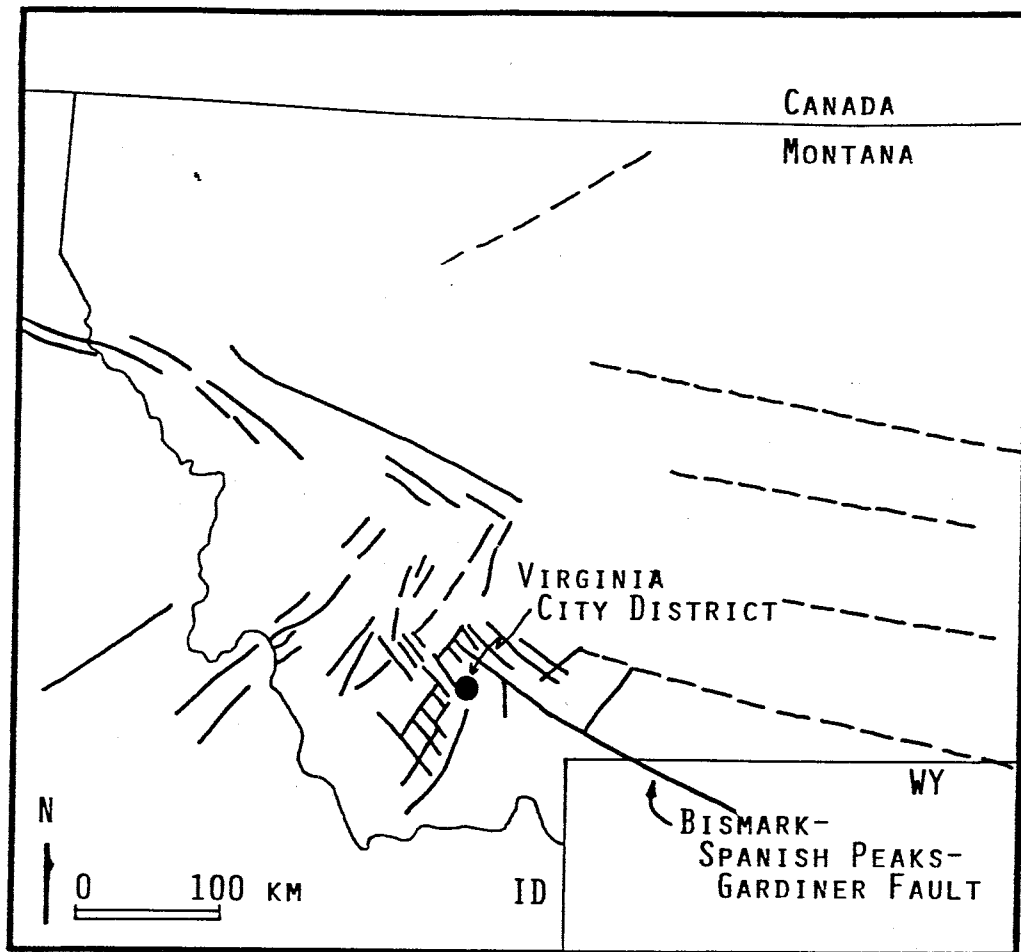
Figure 6. Regional map showing major recurrent fault zones in southwestern Montana (after Schmidt and Garihan, 1986).

dikes and dikes swarms of late precambrian age are localized in northwest-trending fault and fracture zones. Schmidt and Garihan (1986) add other evidence to the theory of middle Proterozoic movement by noting that there are faults which offset Archean units but do not affect Palezoic units. Emplacement of dikes indicate an extensional component to movement during this time. This extension also appears to have influenced the deposition of Middle Proterozoic Belt Supergroup rocks (fig. 7).

Schmidt and Garihan (1986) have documented the occurrence of Late Cretaceous movement along the Precambrian faults in southwestern Montana. They conclude that the northwest-trending fault set is the principal Laramide fabric in the region. Vitaliano and others (1979) note more recent movement by the offset of the Cretaceous-age Tobacco Root batholith with relation with the surrounding Archean rocks. Reactivation of this Precambrian faulting is also responsible for the localization of Eocene volcanic centers (Chadwick, 1970).

The geometry of the northwest-trending faults is very similar. The longest of the northwest faults, the Bismark-Spanish Peaks-Gardiner fault, can be traced for 150 km (Schmidt and Garihan, 1986). The majority of these
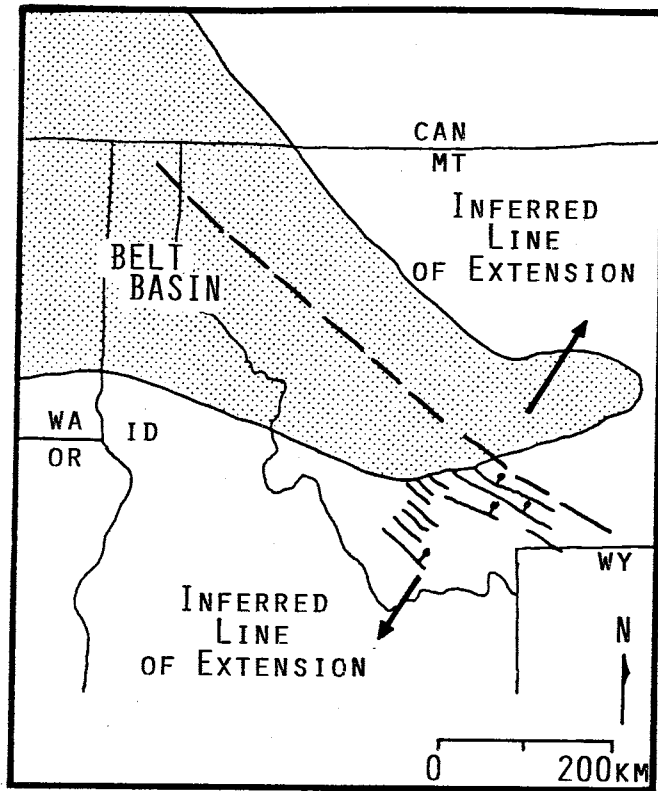
Figure 7. Tectonic controls on the location of
the Belt Basin (after Schmidt and
Garihan, 1986).

faults are on the order of 10's of kilometers long. Most faults strike between N30°W and N70°W and dip 50° to 70° to the northeast. Schmidt and Garihan (1986) show that fault dips are usually 5° to 10° greater in Palezoic rocks than in older Archean rocks. They also suggest a slightly listric geometry for the Precambrian faults through evidence in the southern Highland Mountains and the Ruby Range.

Figure 8 shows the development of structures in the Ruby Range as interpreted by Schmidt and Garihan (1986). They determined that middle Proterozoic activity was dominated by crustal extension which produced northwest-trending northeast dipping listric normal faults (fig. 8A). Crustal shortening during Late Cretaceous and Paleocene time was accomplished partly by left-reverse slip motion on the earlier normal faults and folding (fig. 8C). East-west extension during the Eocene resulted in the formation of major north to north-east trending basins and ranges (fig. 8D).

Schmidt and Garihan (1986) conclude that the Laramide movement along these faults was reverse left-lateral with equal reverse and sinistral components, but occurrence of dip-slip as opposed to strike-slip is correlated with fault
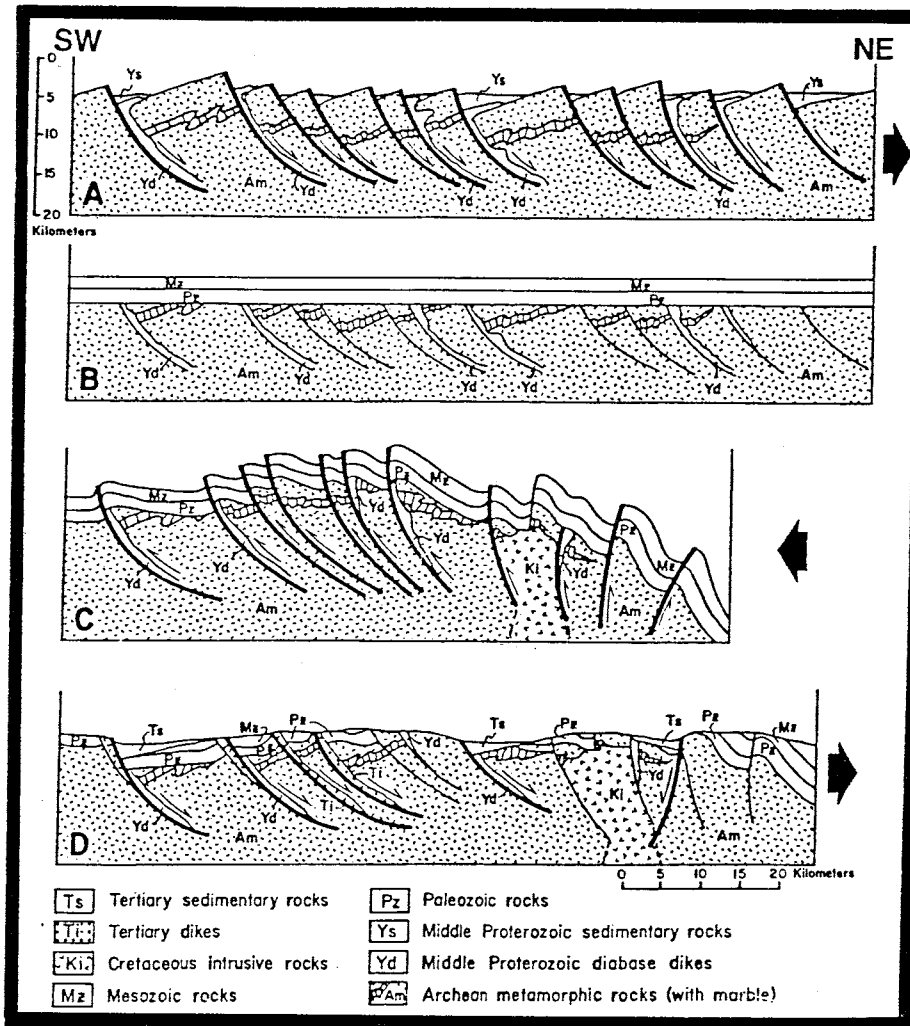
Figure 8. Schematic northeast-southwest sections
showing the recurrent activity and intrusion
associated with northwest-trending fault set
in southwestern Montana (from Schmidt and
Garihan, 1986). Refer to text for
discussion of sequence.

strike. More northerly striking faults have greater
components of dip-slip, whereas faults with a more
east-west strike have greater components of strike-slip.
These slip directions are compatible with compressive
deformation suggested by Hamilton (1981).

REGIONAL MINERALIZATION PATTERNS

The Tobacco Root precious-metal mining region is comprised of the Virginia City, Pony, Norris, Sheridan and Renova districts (Figure 9). The precious-metal deposits of this region show many similarities (Lorian, 1937).

Winchell (1914) and Lorian (1937) report that the deposits in the Tobacco Root mining region are mainly quartz vein systems occurring in fractures in Precambrian metamorphic rocks or Laramide intrusions. The vein morphology varies from tabular bodies concordant with metamorphic foliation to quartz lens and stringers in crushed and sheared fracture zones which crosscut metamorphic foliation. The veins commonly contain gold, silver, pyrite, galena, sphalerite, and chalcopyrite. All deposits show variable depth and intensity of oxidation. Replacement deposits are also found where reactive host rocks are cut by these mineralized fracture systems. Orientation of the veins varies, but is controlled by either local foliation (northeast) or regional fracture pattern (northeast and northwest).

The following is a brief description of the host rocks and the mineralization in each of the districts in the Tobacco Root region.

BUTTE
DISTRICT ⚒ Butte

GOLDEN ⚒
SUNLIGHT

RENOVA
DISTRICT

⚒ ⚒ ⚒
PONY
DISTRICT Pony

ROCHESTER
DISTRICT ⚒

TIDAL WAVE ⚒
DISTRICT ⚒

NORRIS
DISTRICT

Norris

Twin Bridges

⚒

SHERIDAN ⚒
DISTRICT ⚒ ⚒

Sheridan

Alder

Ennis

Virginia City

⚒
VIRGINIA CITY
DISTRICT
⚒ ⚒
⚒ ⚒

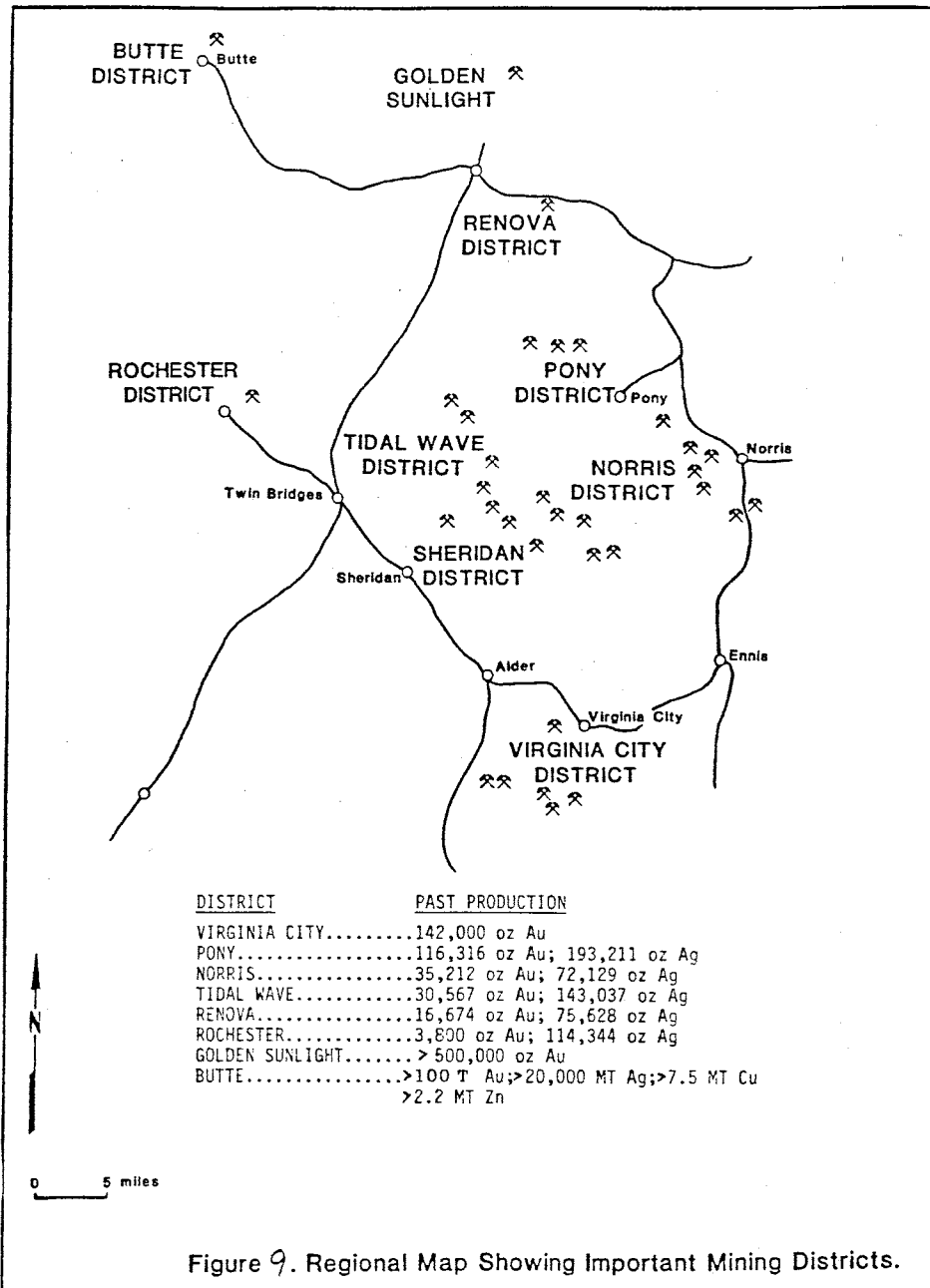| DISTRICT	PAST PRODUCTION
VIRGINIA CITY	142,000 oz Au
PONY	116,316 oz Au; 193,211 oz Ag
NORRIS	35,212 oz Au; 72,129 oz Ag
TIDAL WAVE	30,567 oz Au; 143,037 oz Ag
RENOVA	16,674 oz Au; 75,628 oz Ag
ROCHESTER	3,800 oz Au; 114,344 oz Ag
GOLDEN SUNLIGHT	> 500,000 oz Au
BUTTE	>100 T Au;>20,000 MT Ag;>7.5 MT Cu >2.2 MT Zn

N

0   5 miles

Figure 9. Regional Map Showing Important Mining Districts.

Virginia City District

The Virginia City district was the largest producer in the region. The combined production from the Easton-Pacific, Oro Cache, Kearsarge, Marrietta, Prospect, U.S.Grant and many other smaller operations totalled approximately 142,000 oz. gold and 1.1 million oz. silver.

The Virginia City district is underlain by multiply deformed Precambrian gneiss with abundant crosscutting and concordant narrow pegmatite bodies. In the area of the Easton and Pacific mines the gneiss is intruded by a monzonite stock.

The deposits occur as quartz vein systems, localized by fractures in the gneiss. Veins show evidence of multiple stages of quartz emplacement, and comprise sulfides with native gold and silver. Supergene enrichment near the surface was significant and a large portion of the production was from oxidized ores (Lorain, 1937). Very little wall rock alteration is present in the district, except in the area of the Pacific mine where argillic alteration is pervasive over area approximately 75 m by 300 m with a minimum depth of 125 m.

Pony District

The Pony district has been one of the most important
producers of lode gold in the Tobacco Root region. The
major producers in the district were the Mammoth, Boss
Tweed-Clipper, and the Strawberry-Keystone mines.

The district is underlain by Precambrian gneiss which has
been intruded by the Cretaceous Tobacco Root quartz
monzonite and pegmatite dikes. With exception of the Boss
Tweed-Klipper, deposits in this district can be
characterized as quartz veins in fracture zones which are
parallel to the gneiss-quartz monzonite contact or the
banding in the gneiss. Mineralization is confined to the
veins and wall rock alteration is poorly developed (Hart,
1933). The Boss Tweed-Klipper system mineralization occurs
in fractured and silicified gneiss (Lorian, 1937).

Hart (1933) proposed a district scale zoning pattern with
respect to the intrusion. He noted that mineralization
closest to the contact was typically gold-containing
pyrite, chalcopyrite, and quartz (fig. 10). This pattern
grades into a galena- and silver- dominant zone.
Mineralization that occurs within the intrusion is
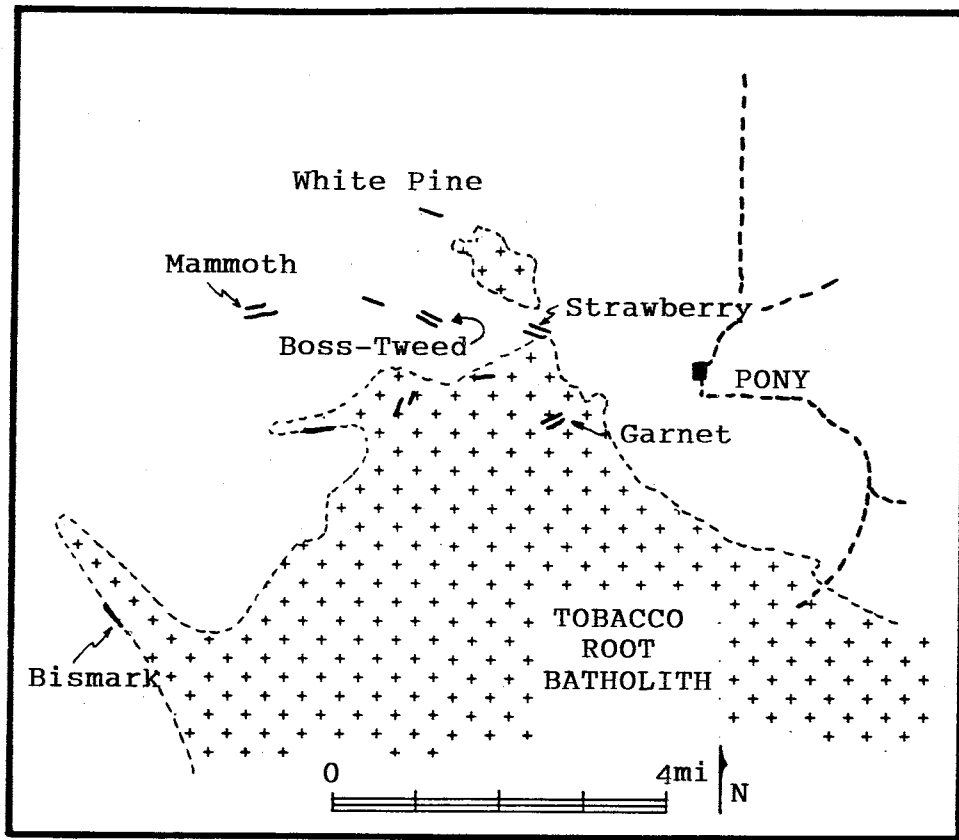characterized by the presence of fluorite and hubnerite.

Figure 10. Plan map showing the relationship of vein deposits in the Pony district to the Tobacco Root batholith.

(after Lorain, 1937)

Norris District

Lode mining in the Norris district began shortly after the discovery of placer gold there in 1864 (Hart, 1933). The main producers of the Norris district were the Revenue, Boaz, Rosebud and Galena mines.

The geology of the Norris district can be grouped into two distinct units, Precambrian gneiss and the Tobacco Root quartz monzonite. The majority of the deposits occur in the gneiss (Hart, 1933). Gold mineralization is localized in quartz veins of various orientations. At the Galena mine quartz veins are present as narrow stringers occupying a zone up to 3 m wide. The greatest producer, the Revenue mine, is a quartz vein system within the quartz monzonite that has been cut by post mineralization shear zones. High-grade gold is present at the intersection of the veins and the shears (Hart, 1933). Secondary enrichment has been an important factor in the formation of economic concentrations of gold in the Norris district.

Sheridan District

Discovery of lode deposits in the Sheridan district occured shortly after the discovery of gold in Alder Gulch in 1863.

The most important producers, although small, were the Red
Pine, Smuggler, Belle, Sunnyside, and Tamarack-Broadguage
mines. Lorian (1937) noted that although the deposits in
this district were smaller, ore was being produced from
five times as many mines as the other districts in the
Tobacco Roots. He suggests that this represents the
affects of a weakening mineralizing system related to the
Tobacco Root batholith.

The principal rock types in the Sheridan district are
Cherry Creek schists and gneisses. Limestones of the
Cherry Creek series crop out throughout the district.
Outcrops of the Tobacco Root batholith are limited to a few
small areas in the eastern portion of the district.

The deposits are characterized as veins and replacements in
limestones (fig. 11). The presence of limestone seems to
be the most important factor in controlling the location of
an ore deposit in the Sheridan district. Localization of
mineralization is controlled by bedding plane faults and at
contacts between the limestone and other members of the
series. In the replacement type deposits disseminated gold
is found in silicified limestone.

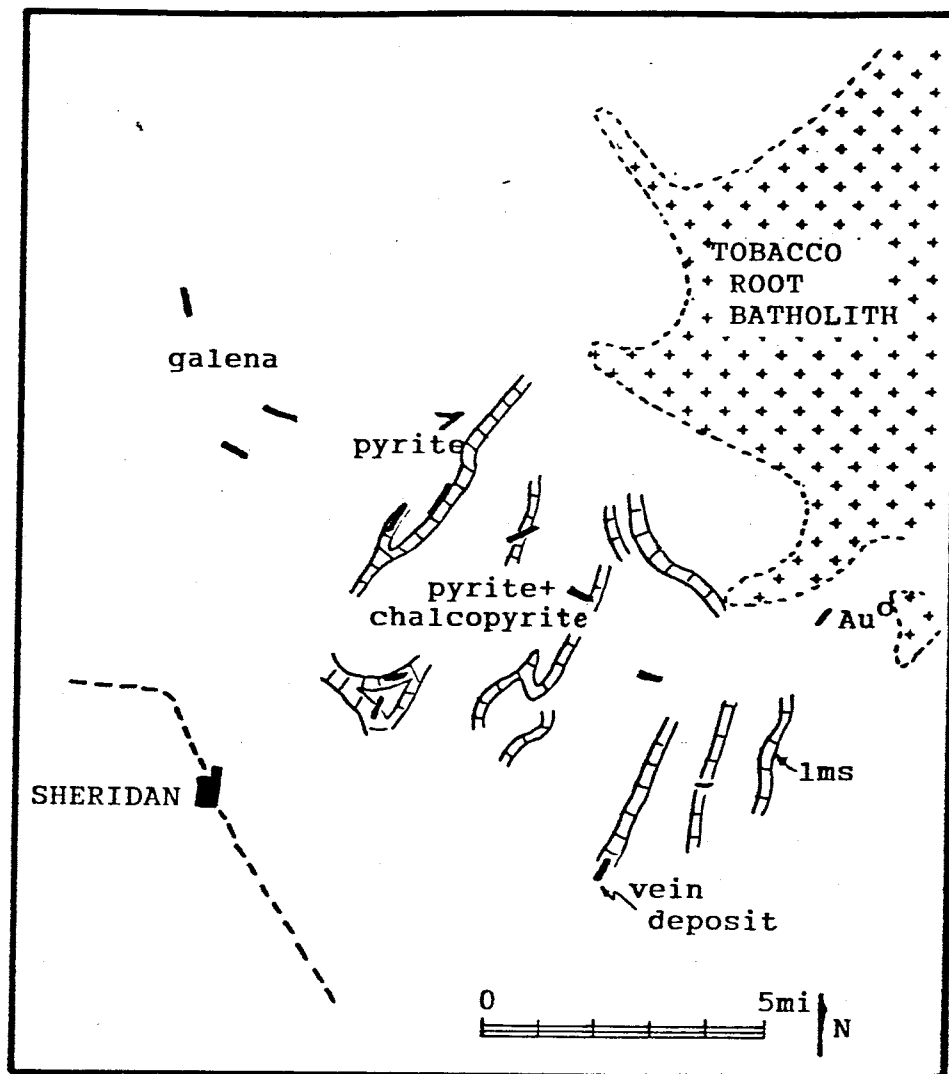Lorian (1937) noted a district scale zoning pattern with

Figure 11. Plan map showing the relationship of vein deposits in the Sheridan district and the Tobacco Root batholith. Also shown, major ore minerals at various deposits.

(after Lorain, 1937)

respect to distance from the Tobacco Root batholith.
Deposits close to the batholith contain
pyrite-chalcopyrite, whereas pyrite-galena ore becomes more
abundant with distance. Further to the west the deposits
in Goodrich Gulch are primarily galena.

Renova District

The Renova District is in the northern end of the Tobacco
Root Mountains. Important mines in the district include
the Gold Hill, Surprise, Mary Ingabar, Colorado, Blue Bird
and Mayflower (Lorain, 1937). Of these the Mayflower was
the largest producer. Hart (1933) reports that the
Mayflower Mine produced approximately 65,000 oz. of gold
between 1896 and 1901. Ore at the Mayflower was very
high-grade, averaging 7 oz/ton gold.

Geology at the Mayflower Mine is atypical of Tobacco Root
deposits as they occur in Palezoic rocks. Winchell (1914)
reports the geology in the vicinity of the mine as slates
of the Belt Series which are overlain by Cambrian
conglomerates and sands and massive blue limestone. The
ore is hosted in this limestone and along a fault that
brecciated the limestone nearly parallel to bedding.
Northwest of the fault the limestone is unaltered, but on

the southeast side it is brecciated, silicified and mineralized. The gold in the Mayflower ore was almost exclusively in the form of tellurides. Oxidation played an important role in concentrating gold and silver near the surface. At depth hypogene mineralization was encountered, but was to low grade to mined at a profit.

The other mines in the Renova district are located in Beltian arkosic sandstones which are crosscut by porphyritic dikes (Winchell, 1914). Mineralization occurs as fissure veins which crosscut bedding. The majority of ore mined was oxidized with free gold occurring in hematite and limonite and quartz.

VIRGINIA CITY DISTRICT GEOLOGY

The Virginia City district is underlain by multiply deformed Precambrian gneiss with abundant narrow pegmatite bodies both crosscutting and concordant with metamorphic foliation (fig.12; plate I). In the area of the Easton and Pacific mines the gneiss is intruded by a monzonite stock. The southern border of the district is formed by Mississippian Madison limestone in thrust contact with the gneisses. The eastern boundary of the district is formed by Tertiary volcanics which unconformably overlie the gneisses.

Precambrian Rocks

Gneiss

Quartzofeldspathic gneiss, as mapped by Weir (1983), is the dominant lithology in the district. It contains, in order of decreasing abundance: feldspar (orthoclase and plagioclase), quartz, biotite, amphibole, chlorite, pyroxene, garnet, and magnetite. The term quartzofeldspathic gneiss is used here in a general way denoting a variety of different combinations of the previously mentioned minerals.
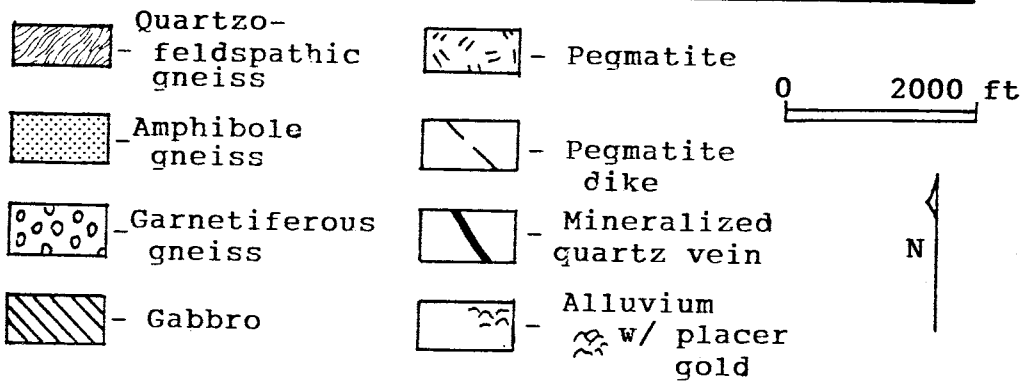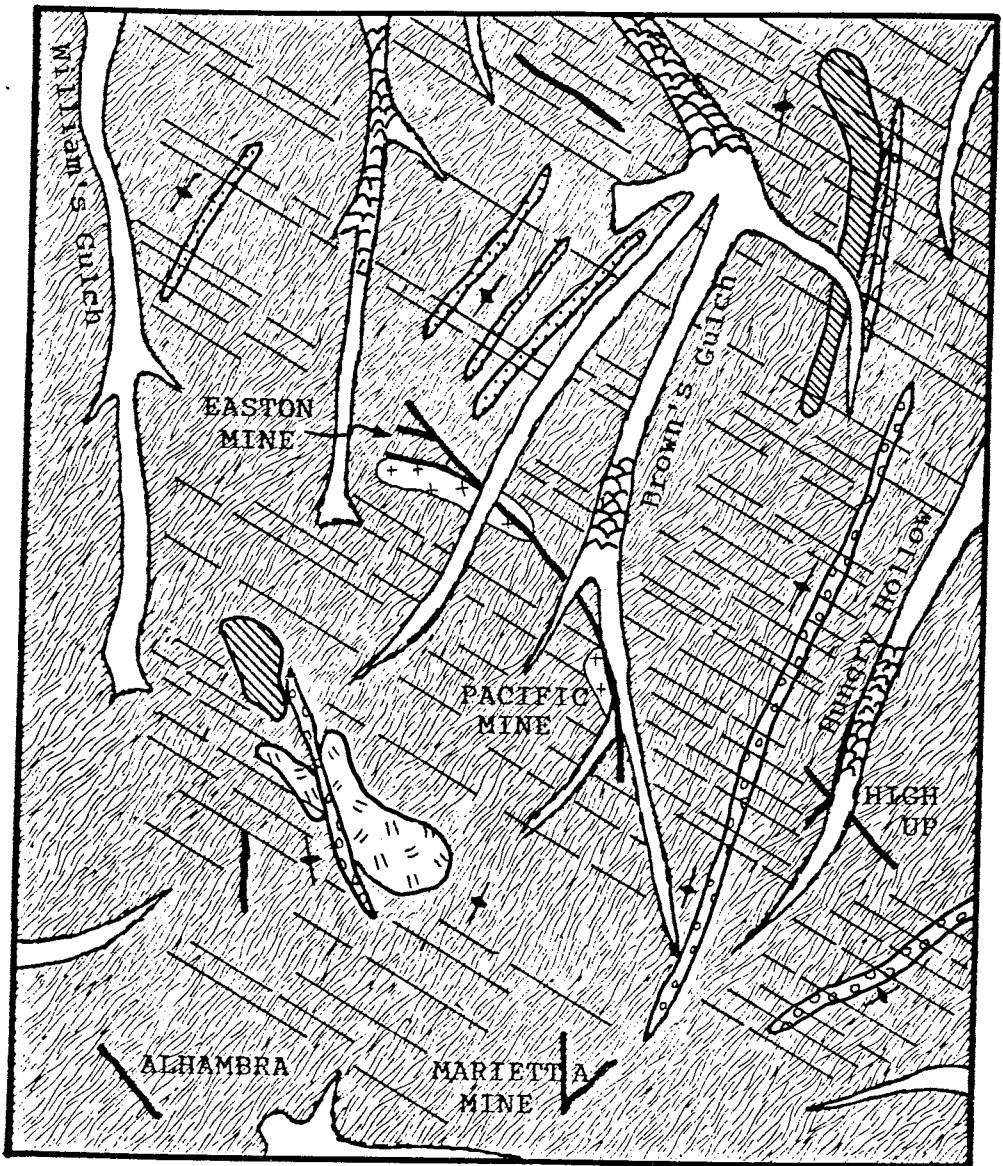
Figure 12. Generalized geologic map of the area around the Easton and Pacific mines.

Three distinct units of quartzofeldspathic gneisses have been delineated for mapping purposes: quartz-feldspar -biotite (QFB) gneiss, amphibolite gneiss, and garnet bearing QFB gneiss.

The most mappable and abundant unit is the quartz-feldspar-biotite gneiss, recognized by its light tan color. This unit underlies approximately 90% of the Virginia City district. In outcrop it weathers brown/orange and exhibits coarse foliation in the form of cm- to m-thick banding. Figure 13 shows a typical exposure of QFB with intercalated amphibole-rich layers.

Amphibole-rich gneiss, which has a black to mottled appearance is the second most abundant gneissic rock type. It contains abundant (usually greater than 50% volume) mafic minerals and feldspar. In outcrop it appears massive but on close inspection foliation is obvious. The amphibole-rich gneiss occurs as lens in QFB which can be traced for several 100 meters. Thickness of the lens varies from about 1 meter up to several tens of meters.

Garnet-bearing gneiss is the least common and forms lenses in the other gneissic units. In outcrop it appears similar to QFB with a slight red tint from the garnets. Garnet

Figure 13. Photograph of quartzofeldspathic gneiss
with amphibole-rich interlayers which is
exposed in Brown's Gulch.

porphroblasts range in size from a maximum of 3 cm to 5 mm
with an average of 50 mm. Garnets occur as distinct layers
and disseminations within the gneiss.

Pyroxenite

Medium to coarse grained pyroxenites crop out throughout
the district. These rocks are composed of pyroxene $\pm$
feldspar. They are massive with little or no foliation
developed. Poor exposures make the geometry of this unit
difficult to ascertain.

Gabbro

Gabbro, which has been serpentinized, was mapped at several
localities in the district. In outcrop it weathers buff to
white. A fresh surface reveals dark green very fine grained
pyroxenes, feldspar, and magnetite. Faint foliation can be
noted on the weathered surface. Serpenite occurs as veins
up to 1 cm thick. Outcroppings of gabbro coincide with
large amplitude dipole anomalies generated by a total field
magnetic survey of the map area. This magnetic data
verifies the observation that the gabbro occur as elongated
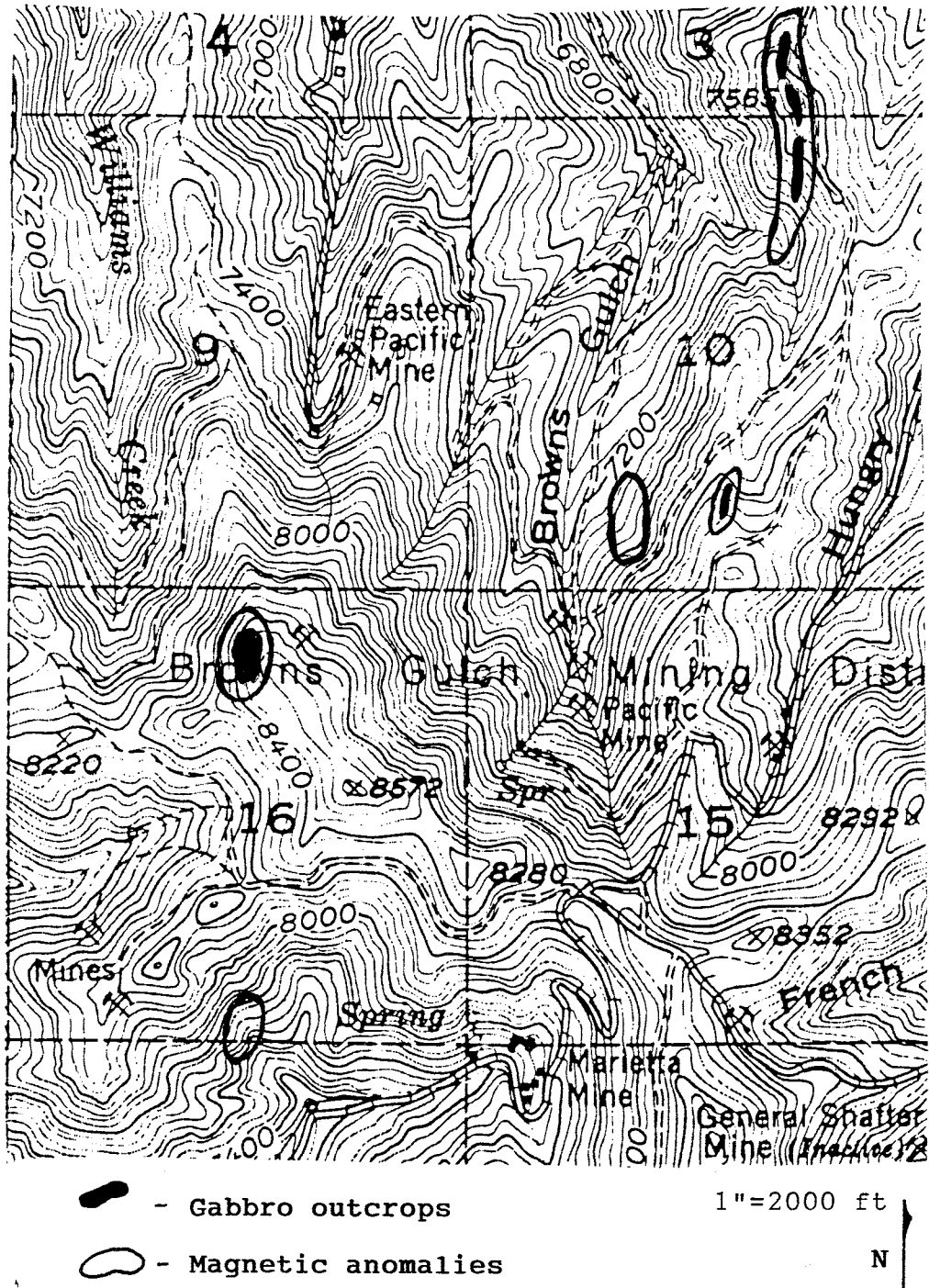bodies, concordant with foliation (fig. 14).

- Gabbro outcrops

- Magnetic anomalies

1"=2000 ft

N

Figure 14. Map showing gabbro outcrops and magnetic anomalies in the area of the Easton and Pacific mines. Anomalous areas are assumed to be underlain by gabbro.

Carbonates

Tan to brown meta-dolomites and marbles crops out
discontinuously on the west side of Brown's Gulch and in
upper Alder Gulch (Cole, 1983). Thickness varies from 1
meter to 20 meters, but is commonly less than 1.5 meters.
These units are important marker units used to recognize
structures in the relatively homogeneous quartzofeldspathic
gneisses

Pegmatites

Pegmatite dikes, which vary in thickness from a few
centimeters to over 8 meters crosscut all of the
forementioned rock units. They trend west-north-west and
can be traced for several miles. These pegmatites are
composed of quartz and feldspar with minor biotite and/or
muscovite ± minor pyrite. They exhibit graphic texture or
rough zonation of quartz-rich centers to feldspar-rich
margins. In outcrop they are iron stained and weather to
gruss. In many locations they are devoid of vegetation and
therefore can be mapped on airphotos and on the ground
easily (fig.15). Cole (1983) determined the age of one of
these dikes in the area of the U.S. Grant mine as 1.6
billion years old using K-Ar dating. The density of diking

Figure 15. Aerial photograph of northwest-trending
pegmatite dikes in the northern Virginia
City district.

48

varies with a maximum of about 5 dikes per 30 meters.
Figure 16 shows the density of·dikes in the area of Marble
Knob.

A small stock of pegmatitic rock composed of quartz and
feldspar crops out on the ridge south of the Easton-Pacific
mine. It is medium to coarse grained, with porphyritic
texture. Feldspar phenocrysts range from several
centimeters up to 0.3 meters in length. Many xenoliths of
gneissic rock are present within this stock. The xenoliths
are typically elongated along foliation with lengths up to
15 meters.

Post-Precambrian Rocks

Sedimentary Rocks

The district is bordered on the south by Paleozoic and
Mesozoic sedimentary rocks in thrust-fault contact with
underlying Precambrian metamorphic rocks.

Intrusive Rocks

The Brown's Gulch stock, a monzonite intrusion, crops out
as an elongate mass in the vicinity of the Easton and

MONZONITE
QUARTZ–FELDSPAR–BIOTITE GNEISS
GARNETIFEROUS GNEISS
AMPHIBOLITE
PEGMATITE
QUARTZ VEIN

0   160ft   N

Trench #15

Trench #13

Trench #14
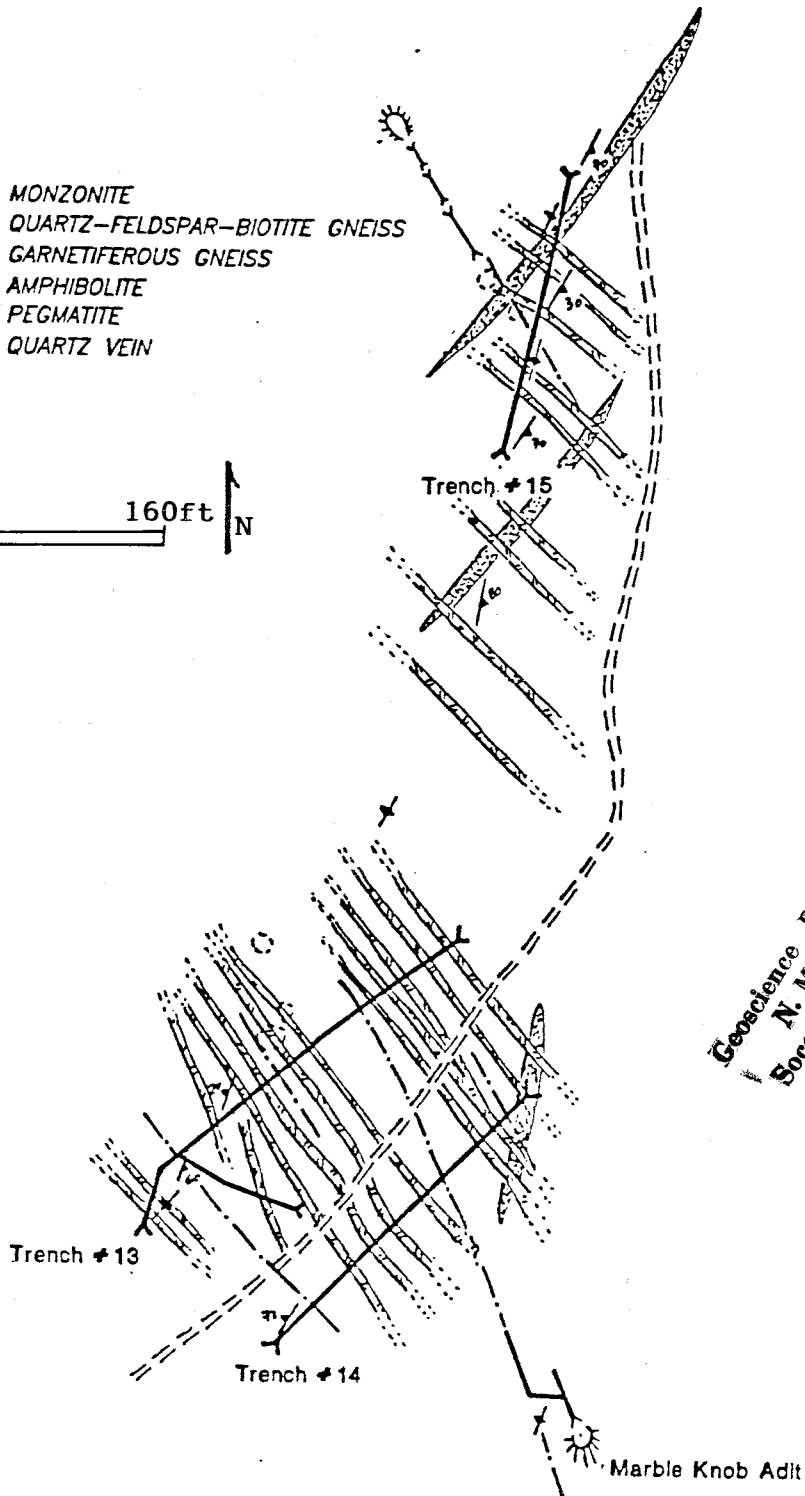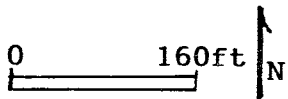
Marble Knob Adit

Geoscience Department
N. M. I. M. T.
Socorro, N. M. 87801

Figure 16. Geologic map of the Marble Knob area
showing the density of pegmatite dikes.

Pacific mines. This stock was previously referred to as
alaskite or aplite by earlier workers (Winchell, 1914;
Tansley, 1933). The stock trends NW and crosscuts gneissic
rocks. In outcrop it is difficult to distinguish from
mafic-poor gneissic rocks because of their similar
mineralogy and fine grained textures. The stock typically
weathers orange-brown and forms blocky outcrops. Previous
workers consider this stock to be coeval with the Tobacco
Root batholith of Cretaceous age (72-77 m.y.; Vitaliano and
others, 1980).

VIRGINIA CITY DISTRICT STRUCTURE

The major structures in the Virginia City district are northeast-trending isoclinal folds in Archean rocks and fault and fracture zones which crosscut (northwest-trending) and parallel these folds.

Folds

Cole (1983) and Weir (1982) documented the presence of two deformational events that produced folds in the northern portion of the Virginia City district. The first deformational event produced tight isoclinal folds. The second event refolded this strata into a northeast-trending southwest-vergent antiform. Fold limbs are easily traced by the location of resistant marble outcrops.

This structure was mapped in the area of the Easton-Pacific mine (fig.17). Garnet-rich layers within quartzofeldspathic gneisses adequately define the structure. Small scale isoclinal folds appear to be concentrated in rubble crop along the inferred axis of this structure.

The detailed geometry of folding is still poorly defined in the Virginia City district because of the limited extent of
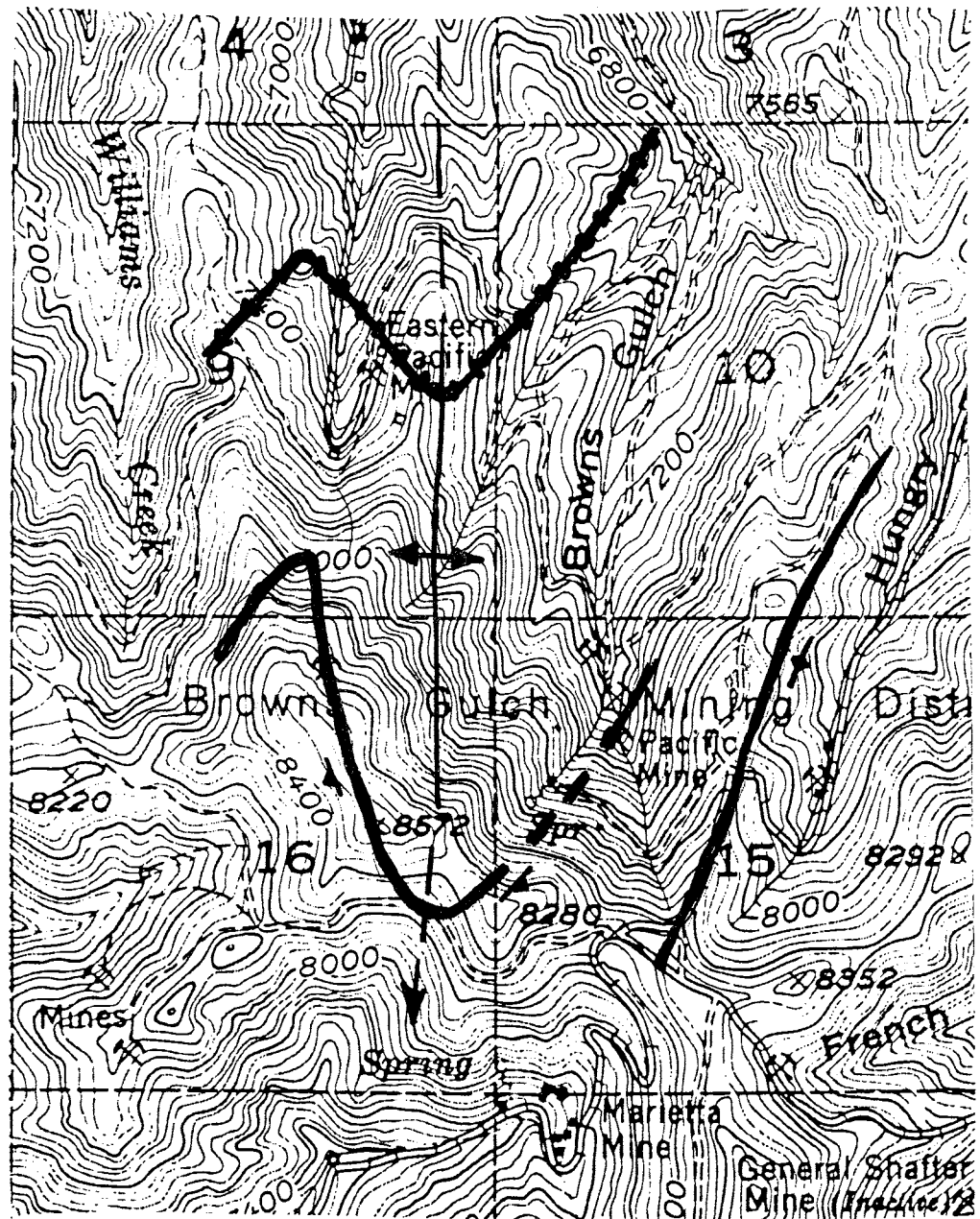
1"=2000 ft.

N

**Figure 17.** Generalized map showing the location of folds in the area of the Easton and Pacific mines. Bold lines represent marker units.
—garnet-rich
—amphibole-rich

outcrop in the southern portion and the homogeneous nature
of the quartzofeldspathic gneiss which makes up a majority
of the country rock. On a small scale, folding does not
appear to be a major factor in the localization of
mineralization.

Faulting and Fracturing

Brittle deformation in the district is best represented by
a prominent northeast-northwest conjugate fracture set.
Faults and fractures of the Virginia City district are
important for localization of ascending fluids and can be
broken down into 4 groups: northwest, northeast, north
-south, east-west with the majority dipping to the north.
Figure 18 is a rose diagram which shows the trend of veins
in the Virginia City district. The northwest and northeast
trending fractures have controlled the emplacement of
Archean pegmatite dikes, the Brown's Gulch stock, and
mineralized and unmineralized quartz veins. The other
trends influenced the emplacement of mineralized quartz
veins and drainage patterns throughout the district. These
structures parallel or are segments of the regional scale
structures discussed earlier.
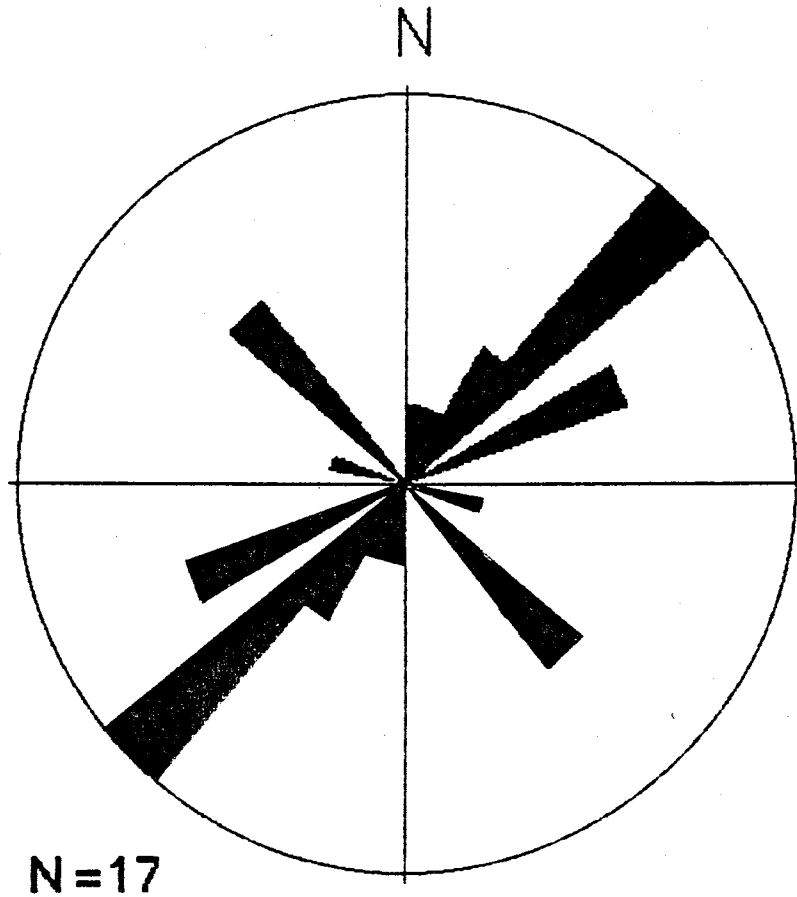
Figure 18. Rose diagram showing trend of mineralized
quartz veins in the Virginia City District.

Displacement along these faults is not well documented
because of the homogeneity of the country rocks and the
accelerated rate of weathering of the fault zones. Cole
(1983) has documented the presence of right-lateral offset
along the northeast-trending structure of the U.S. Grant
mine. Weir (1981) mapped left-lateral offset of marble
units in the northwest corner of the district. Slickensides
in the area of the Pacific mine indicate a reverse
component of slip. Judging from the age of the district
scale structures, their displacement histories are probably
complex.

In the area of the Pacific mine, low angle fault zones were
detected. Drill core data indicates that low-angle fault
zones crosscut mineralized veins. This is evidenced by the
presence of mineralized clasts within the fault gouge.
Flat lying pegmatites are also noted in the area of the
Pacific mine. This might indicate that these flat lying
structures are reactivated portions of listric faults
developed during the Precambrian. Brecciation is abundant
along the fault zone associated with the Pacific mine, and
to a lesser extent along most veins of the district.

Dilatant zones developed along fault and fracture zones
are important in localizing mineralizing fluids in the

Virginia City district. These zones of dilatancy are occur
at bends and jogs along linear structures. The tectonic
origin of these zones is evidenced by the tabular geometry
of the brecciated zones, the abundance of fine grained
cataclasites (gouge), and the presence of slickensides
(Sillitoe, 1985).

DISTRICT MINERALIZATION PATTERNS

The precious metal deposits of the Virginia City district
show many similarities in morphology and mineralization
(Lorian, 1937). They are characterized by quartz vein
systems which occupy shear zones and fractures in Archean
gneisses. The veins average 1 meter in width and 100 meters
several hundred feet in length. Vein morphology ranges from
single-stage syntaxial quartz veins with sulphides filling
open spaces to brecciated and rebrecciated quartz-carbonate
veins with multiple stages of sulphide mineralization. The
hypogene mineralogy of the veins consists of quartz and
pyrite ± varying amounts of galena, sphalerite, acanthite,
chalcopyrite, and gold. Appendix I lists the minerals
historically reported from the Virginia City district.
Hydrothermal alteration is limited to areas around the
veins. Oxidation was an important factor in developing
higher grade ores near the surface.

The Easton and Pacific mines are located the center of the
Virginia City district and have been the greatest lode
producers in the district. As with the other deposits in
the district, they exhibit the characteristics previously
mentioned.

LARGE SCALE MORPHOLOGY

The mineralized and unmineralized quartz veins of the
Virginia City district are located within northeast,
northwest, north-south and east-west trending structures.
The majority of these structures are linear but many show
the development of second order shear zones, jogs and bends
(Hodgson, 1989) (fig 19). The veins are vertical to steeply
dipping in various directions, mainly to the north. The
average length of the mineralized veins is one hundred
meters with the longest trend, the Kearsarge-Oro Cache,
being approximately 1.5 km. Maximum depths of the veins are
not known but depths of mining indicate that some veins are
continuous to 220 meters. The veins vary in thickness from
0.25 meters to 7 meters with an average width around 1
meter. In the area of the Kearsarge mine the veins are
sheeted, with several veins occupying a 12 meter wide zone.

The Easton-Pacific vein trend occupies a northwest trending
curvalinear structure which crosscuts foliation and the
Brown's Gulch stock. The structure is readily traceable
using very-low-frequency electomagnetics (VLF). The results
of a VLF survey over the area are shown in figure 20. The
data shown has been modified by a Fraser filter which
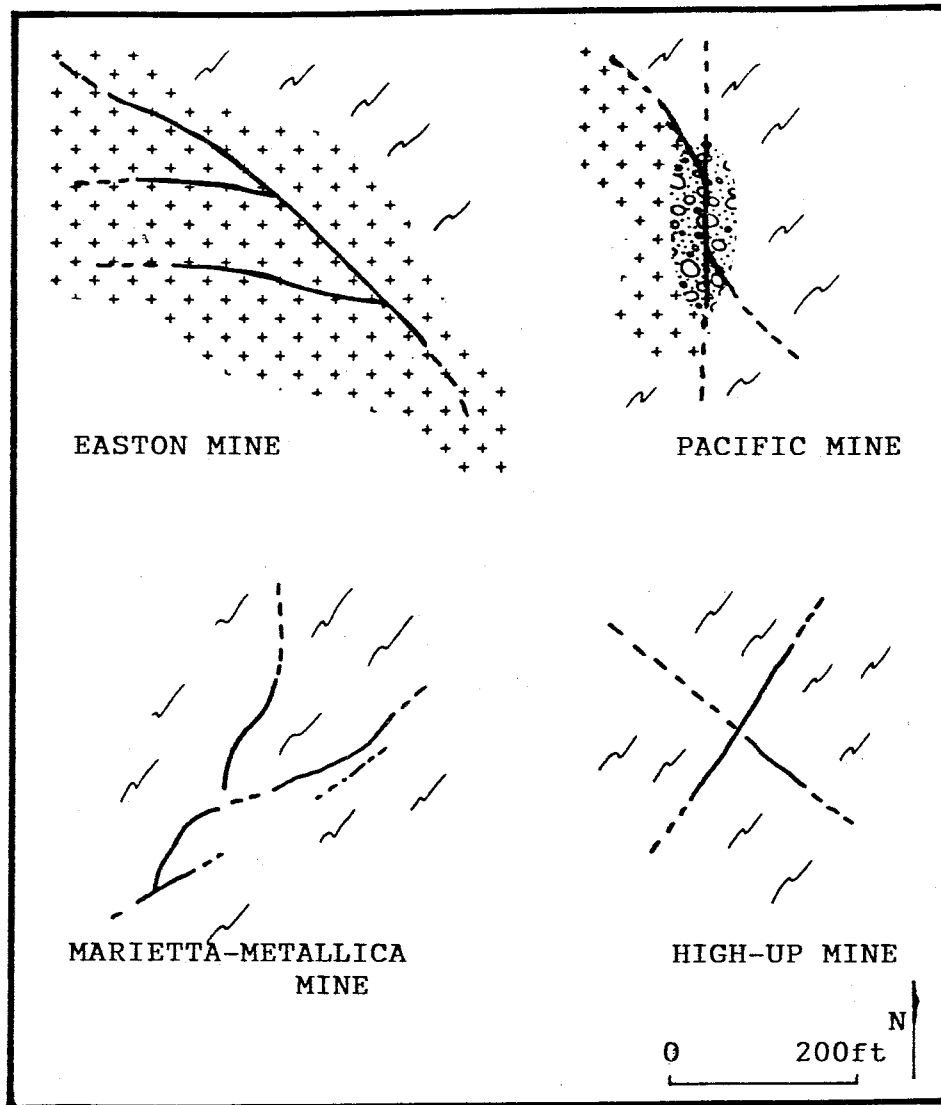performs a phase shift so that the source of the data is

Figure 19. The nature of second-order structures responsible for localizing ore deposits in the Virginia City district.
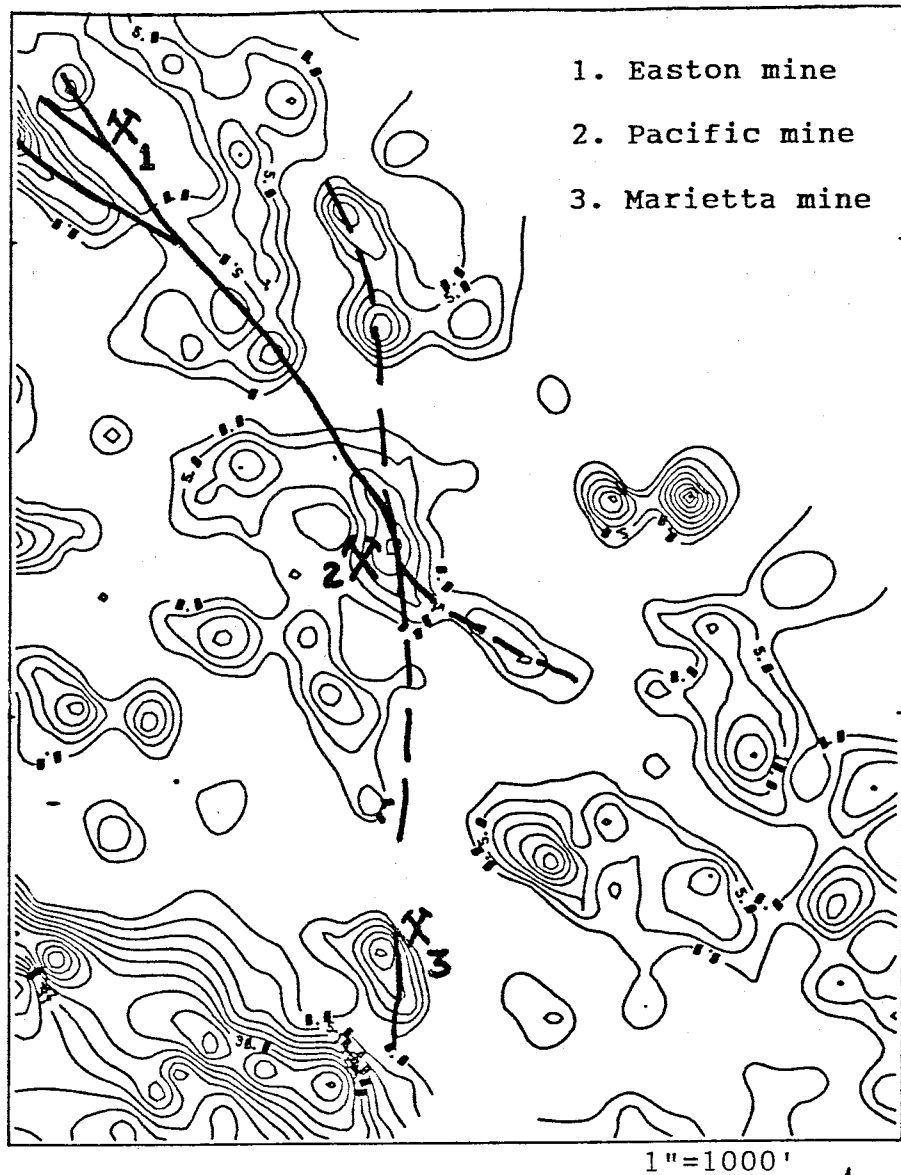
Figure 20. Extent of VLF anomalies in the area of the Easton and Pacific mines. Heavy lines represent known vein locations. Positive values only.

located at a positive peak rather than at an inflection
point. The Fraser filter also removes anomalies that are
the result of topography. The survey succeeded in showing
that the Easton and Pacific mines are located on the same
structure. It also shows the horsetail geometry of the
veins in the area of the Easton mine and the intersection
of north-south, northwest, and east-west trending
structures in the area of the Pacific mine. It should be
noted that both the Easton and Pacific mines are located at
the apex of the curves in the structure.

SMALL SCALE MORPHOLOGY

Morphology of individual mineralized veins throughout the
district were investigated by drilling, trenching, and
underground and surface mapping. The majority of the veins
are hosted by gneisses with exception of the Easton-Pacific
vein which cuts the Brown's Gulch stock. The veins occur as
tabular bodies, lenses and pods in shear zones and
fractures. Quartz is the dominant gange with subordinate
calcite. Quartz occurs as euhedral to subhedral syntaxial
crystals oriented perpendicular to the vein trend. In areas
of brecciation, massive quartz and rock flour forms the
matrix. Sheeted, 1 to 5 cm, quartz veinlets typically
parallel major vein trends. Calcite occurs as a late
fracture filling.

The nature of the contact between vein and wallrock is dependent on the amount of shearing within the structure. Veins in structures with little shearing have frozen contacts, that is the vein adheres closely to the wallrock. If high degrees of shearing were present in the structure, the contact is typically clay/gouge-rich where the vein can be easily separated from the wallrock. Figure 21 shows the smooth nature of the contact developed from a narrow selvage of clay in the Marble Knob adit.

Figure 22 shows a cross-sectional veiw of several quartz veins exposed in a trench #1 in the area of tha Pacific mine. The veins strike approximately N10W and dip 55° to the east. At the surface the dip of the veins appears to be flattening out. Figure 23 shows an east-west cross-section through the Pacific mine. This cross-section is based on surface mapping and diamond drill-hole data. Drill-hole data suggests that the veins do flatten out, but this flattening is exaggerated by post-mineralizing low-angle faulting.

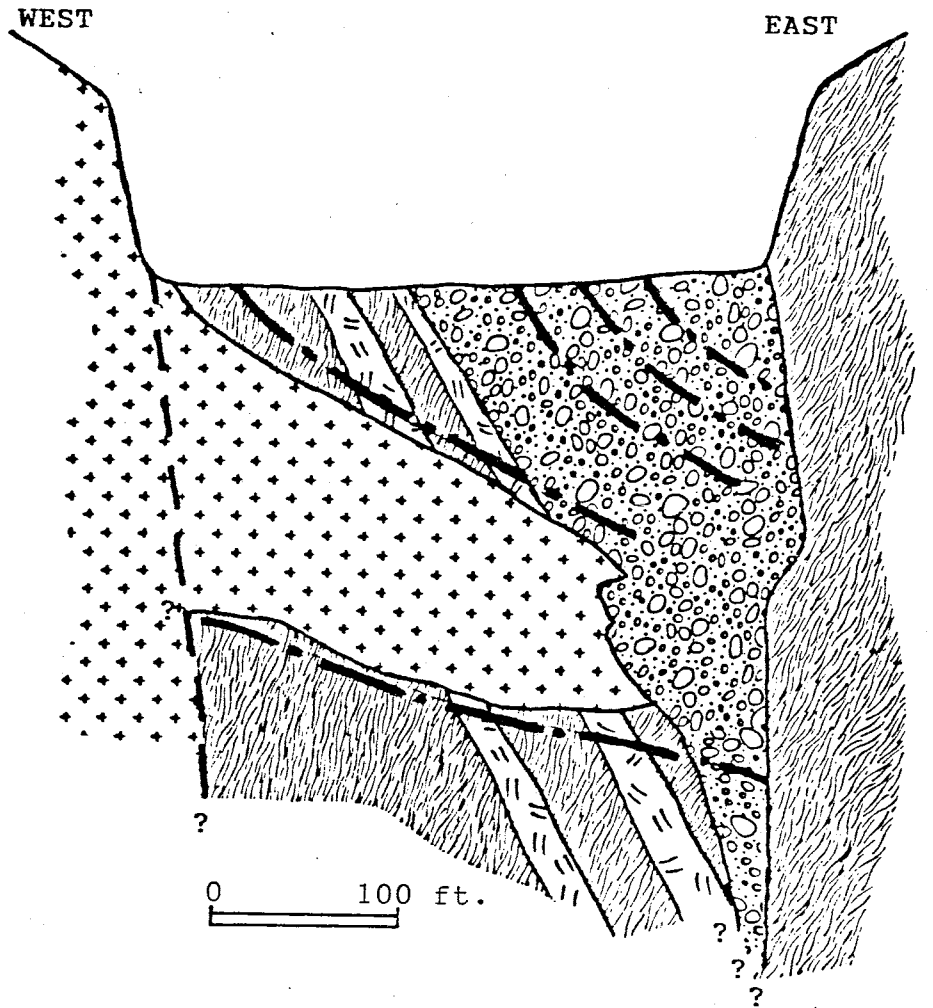The veins and wallrock show textures which typify tectonic breccias (Sillitoe, 1985). Figure 24 shows various brecciated textures from the Pacific mine area. The variety

Figure 21. Photograph of stoping in the Marble Knob
adit showing the smooth nature of the
contact between the wall rock and the vein.

Figure 22. Photograph of Trench #1 in the Pacific Pit.

Figure 23. Generalized cross-section through the
Pacific Pit.
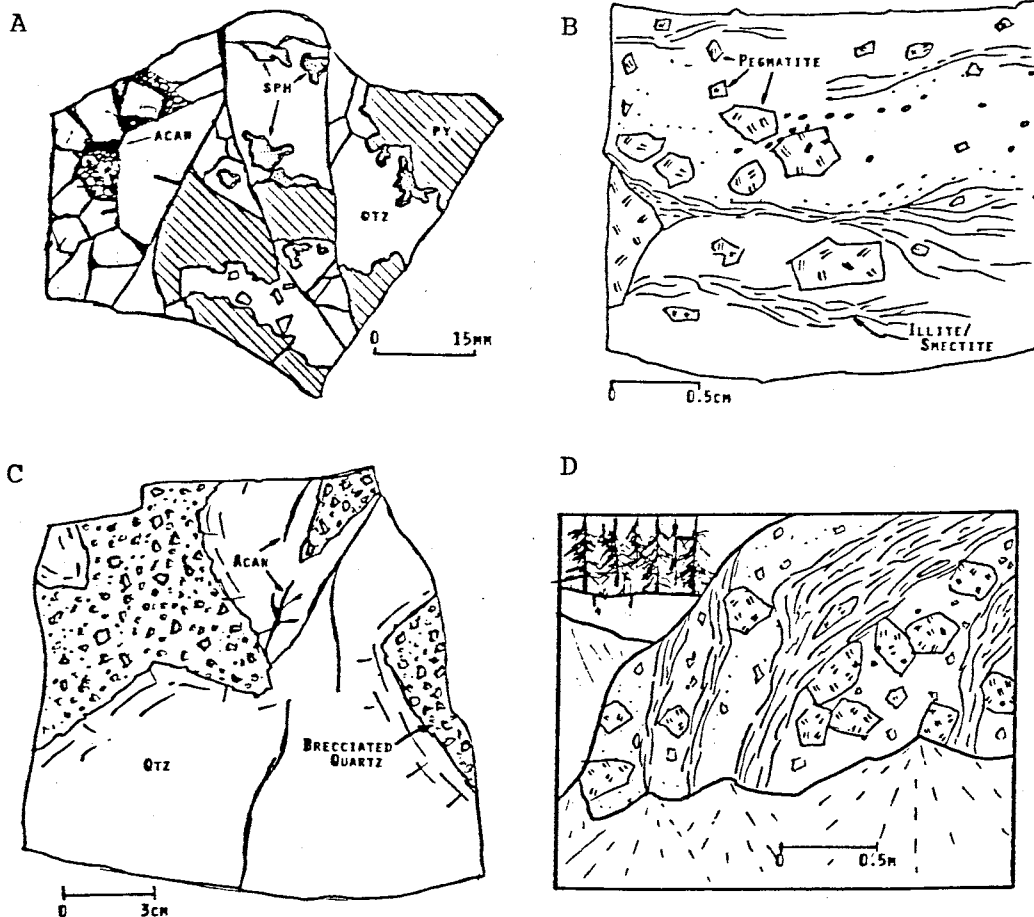
Figure 24. Various breccia textures in the area of the Pacific mine: A) Angular quartz and pyrite in vein; B) Rounded pegmatite clasts in rock flour matrix; C) Subangular quartz cemented by later quartz in vein; D) Pegmatite breccia with zones of illite/smectite in matrix of rock flour.

of breccias present indicate multiple stages of brecciation (Hodgson, 1989). Early stage brecciation is best preserved in pyrite where angular clasts appear to be floating (matrix supported) in dark gray quartz. Later fault breccias are characterized by rounded clasts with abundant black gouge as matrix. Abundant slickensides are present along the vein contacts and in fault zones.

Two other types of quartz veins are present in the Virginia City district. Narrow, sheeted, gray to white bladed quartz veins occur as distinct zones in the gneisses. These veins characteristically have selvages of salmon-pink K-feldspar which are typically about the same width as the veins. The longitudinal extent of these veins seems to be limited. No sulphide minerals were noted in these veins. These veins show no evidence of brecciation or deformation, as do most of the mineralized veins, therefore they are consider to be younger than the mineralized veins of the district. Also present are bull-quartz veins which occupy northwest trending fractures. These bull-quartz veins can be traced for several hundred feet as they form blocky, very obvious outcrops. The width of these veins is about 1 meter. The genetic relationship of these bull quartz veins to the other veins of the district was not determined.

MINERALIZATION

Macro- and microscopic features of ore minerals can be used
to unravel the sequence of mineralizing events responsible
for ore deposition. Polished sections of ore were examined
from the Easton and Pacific mines as well as other veins
throughout the district. Location of these ore samples are
shown on Plate 1.

Ore minerals occur as blebs, brecciated clasts, stringers
and fracture fillings in quartz. Typically they constitute
less than 10% of the vein material.

Pyrite occurs as an early sulphide phase in the veins. It
is noted with quartz, brecciated and crosscut by later
quartz and sulphide phases. Its texture is typically
angular but in areas of intense brecciation it can appear
quite rounded. In areas where veins are emplaced into
pyroxenite, pyrite occurs as euhedral crystals forming a
selvage around the vein. Pyrite also forms as the result of
the sulphidization of biotite which occurs when mineralized
quartz veins crosscut biotite-rich country rocks. Figure 25
shows biotite being replaced by pyrite.

Galena occurs as euhedral crystals, blebs and vein
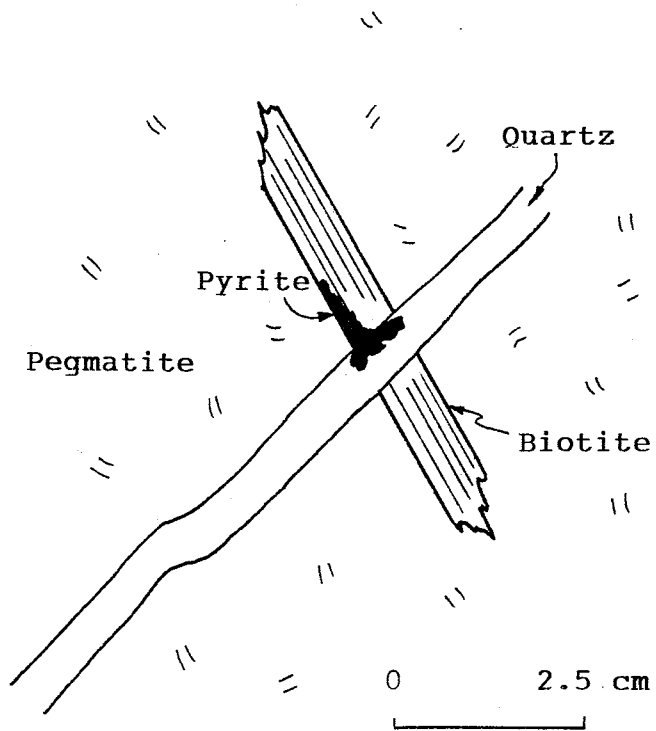
Figure 25. Illustration showing biotite being replaced by pyrite.

fillings. Deformation has caused bending of individual crystals. Galena appears to be late in the paragenic sequence as it is seen filling voids and in crosscutting veinlets.

Sphalerite and tetrahedrite, in massive form, are present in the voids formed by early brecciation. Deformation has caused some bending of these minerals.

Acanthite, (Ag_2S), is observed, associated with chalcopyrite, filling voids in brecciated quartz and in veins with galena and chalcopyrite.

The sequence in which these minerals were deposited was determined through the correlation of their textures and mode of occurrence. Figure 26 shows the paragenetic relationship of the individual ore and gangue minerals and deformational events. The sequence of mineralizing events can be broken into two main periods separated by a period of brecciation. Photomicrographs of polished sections showing the various textures and relationships are presented in Appendix II.

MINERALS	PERIOD 1	PERIOD 2	SUPERGENE
Quartz	▬▬▬▬	▬▬▬	▬
Calcite			▬
Pyrite	▬▬		
Galena		▬	
Sphalerite		▬	
Tetrahedrite		▬	
Chalcopyrite		▬···▬	
Acanthite		▬···▬	
Goethite			▬
Malachite			▬
Chalcocite			▬
Illite		▬	
Smectite		▬	
Kaolinite			▬
DEFORMATION			
Brecciation	✗	✗	
Ductile		✗	
Fracturing		✗	

FIGURE 26. Paragenetic sequence of mineralization for the Easton-Pacific Vein.

Period 1

Quartz and pyrite are the main minerals deposited during Period 1 mineralization. Quartz appears to be milkly to gray. Pyrite is euhedral to massive. Quartz and pyrite are brecciated and healed by more quartz before the onset of Period 2.

Period 2

Period 2 begins with brecciation which forms open space. This open-space is filled with galena, sphalerite, tetrahedrite, chalcopyrite and acanthite. These minerals occur as euhedral to anhedral grains which infill available space between breccia fragments. These early Period 2 minerals are then deformed and fractured. Fractures are filled with galena, acanthite and chalcopyrite veinlets. Late chalcopyrite and acanthite appear to fill any remaining voids. Quartz is ubiquitous through Period 2, seen filling fractures. Late calcite, in the form of veins up to 2.5 cm thick, crosscuts both period 1 and 2 mineralization.

ALTERATION

Three types of alteration were noted in the Virginia City
district: potassic, argillic and supergene. The intensity
of this alteration varies throughout the district.
Alteration seems to be restricted to areas of veining but
not all veins have alteration associated with them.
Potassic alteration is the most pervasive on a district
wide scale. Argillic alteration is restricted in its
occurrence and appears to be best developed in the area of
the Pacific mine. Supergene alteration is noted at most
deposits.

Potassic Alteration

Potassic alteration is the most common alteration type in
the Virginia City district. It occurs along vein structures
as a selvage surrounding the vein. The selvage is typically
wider than the vein it surrounds and appears to be
laterally continuous. Close examination of the selvage
shows that K-spar is selectively replacing existing
feldspars in the wallrock whereas quartz remains
unaffected. Figure 27 shows veins with the K-spar selvage
characteristic of potassic alteration. This potassic
alteration is associated mainly with narrow quartz veins
and stringers.

Figure 27. Photograph of quartz vein with K-spar selvage.

Argillic Alteration

Pervasive argillic alteration is present around mineralized quartz veins in the area of the Pacific mine. It is characterized by pale green mixed-layer illite/smectite in the form of clots and wispy veinlets (fig 28). Clots appear to be replacing K-spar whereas veinlets crosscut all minerals present. Argillic alteration post dates brecciation since clasts and matrix appear to be altered. Veinlets average approximately 5-10 mm and can be traced for several feet where they pinch out. Clay minerals occur as platy masses within the veinlets.

Supergene

Supergene processes have affected a majority of the deposits in the Virginia City district. The extensive development of supergene enrichment of gold and silver has apparently been important in making many deposits profitable (Lorian, 1937). Oxidation is the dominant process in the conversion of primary sulphide phases to oxides. Goethite and limonite appear to be the dominant oxides. Malachite is in close association with chalcopyrite. Oxides occur as blebs completely replacing
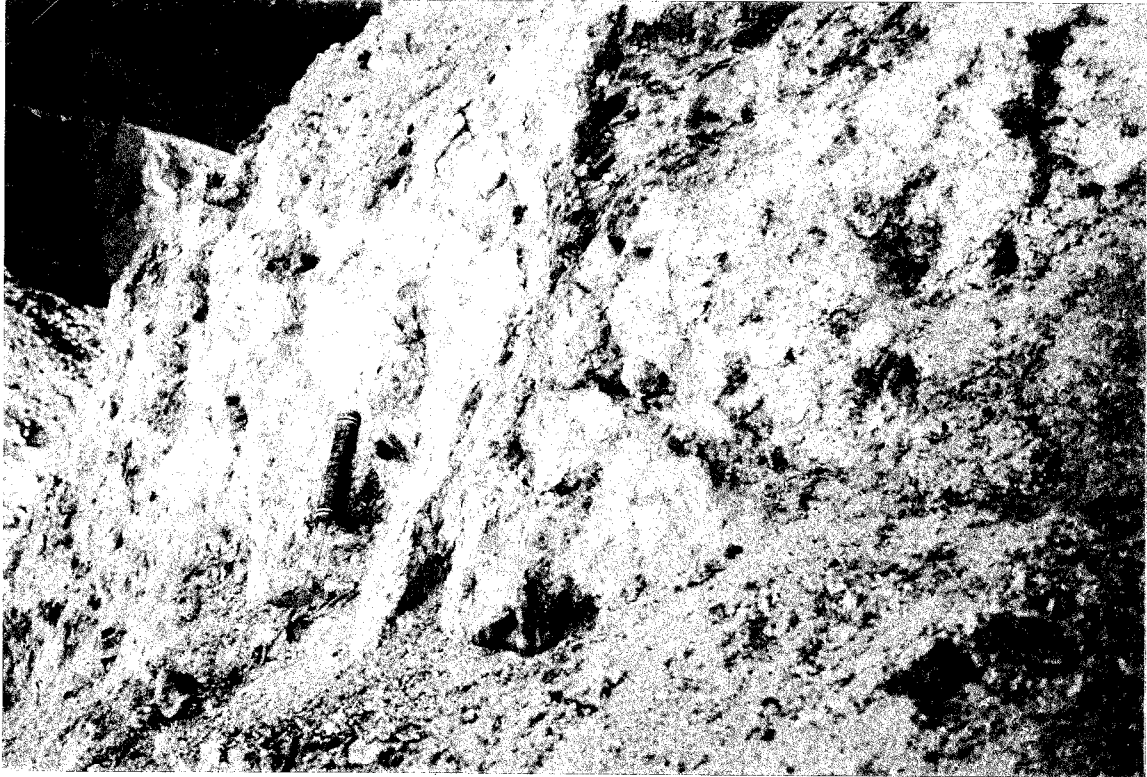
Figure 28. Photograph of argillically altered pegmatite
in the Pacific pit.

sulphides, as replacement rims around sulphides, and as spongy masses. The depth at which primary ore is encountered varies from mine to mine. At the Easton mine unoxidized ores were encountered at 120 meters (Winchell, 1914). Unoxidized ores were encountered at 40 meters at the Kearsarge mine. This may reflect the difference in elevations of the two deposits.

LITHOGEOCHEMISTRY

Channel samples were collected across the major veins in the Easton-Pacific area. The host rock was also sampled, in many cases for up to 20 meters from the vein. Elemental analysis of these samples were conducted by Chemex Labs, in Butte, Montana.

Samples of mineralized veins are anomalous in Au-Ag-Cu-Pb-Zn-As-Sb-Bi. Figures 29 shows the distribution of Au, Ag, As, and Hg in Trench #1 which is located in the area of the Pacific mine. Also shown are background levels for Au and Ag, and detection limits for As and Hg. Anomalous precious-metal values appear to be restricted to the veins but a very. low grade halo is also present surrounding the veins. Figure 30 shows the distribution of elements in Trench #10 above the Bear Adits. Again the

78
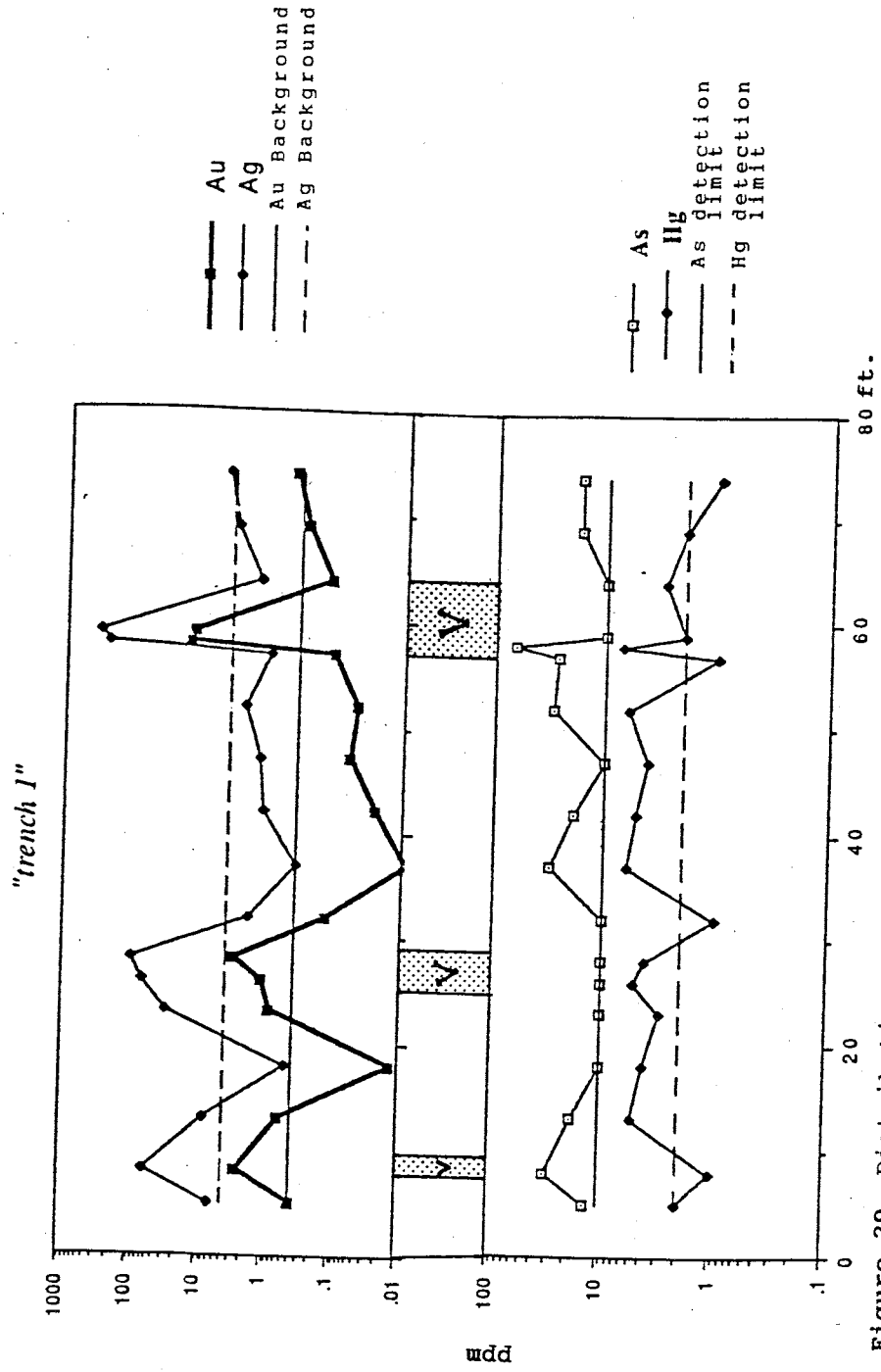
Figure 29. Distribution of elements in Trench #1.
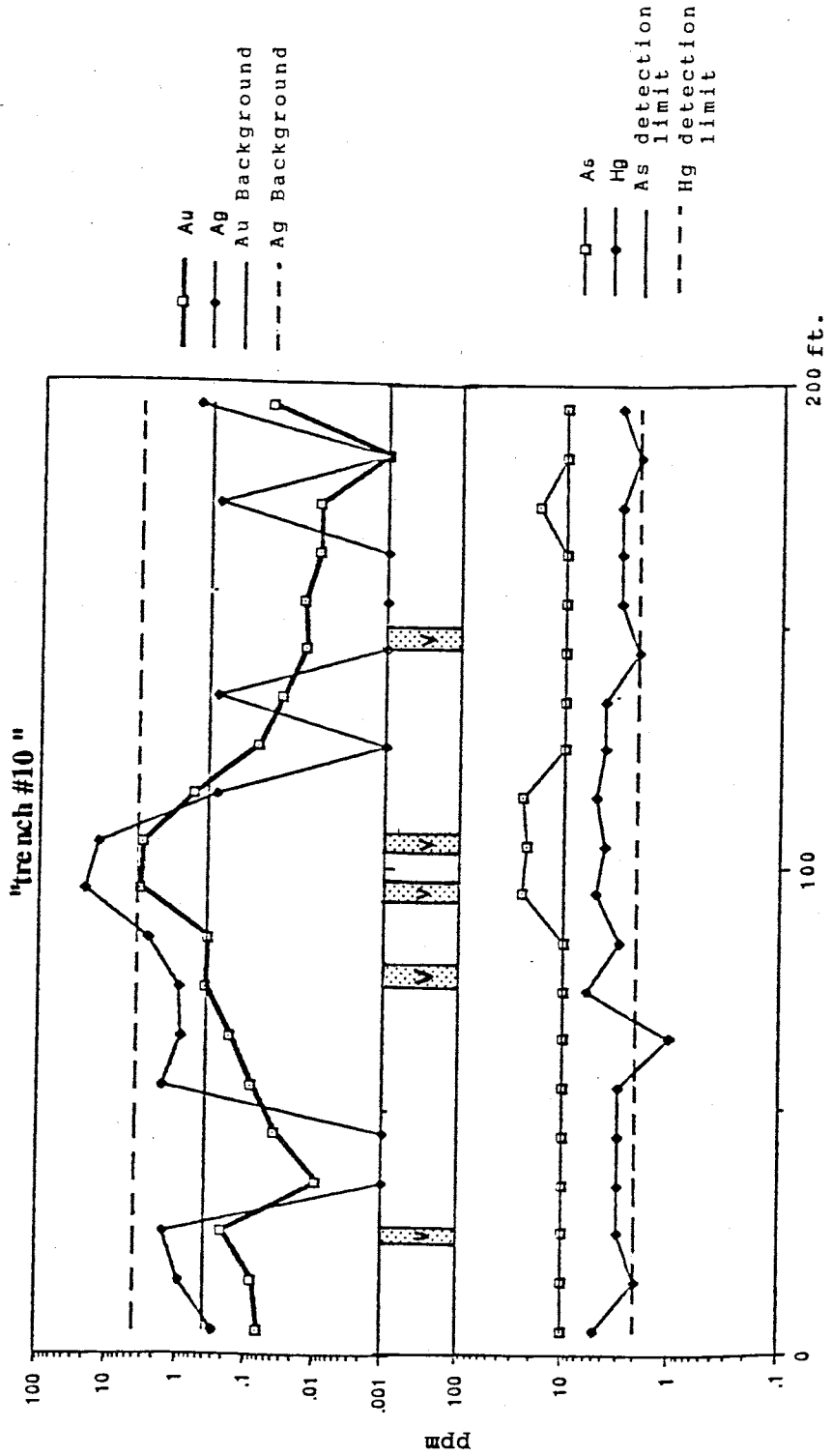
Figure 30. Distribution of elements in Trench 10.

precious-metal values are restricted to the veins but the halo is more obvious because more samples were collected away from the vein. Arsenic varies sporadically throughout the trenches and is not preferentially localized by veins. Mercury appears to be elevated in most samples and does not appear to concentrated in the veins. Figure 31 shows the relationship of As, Hg and Ag to Au in all the trench samples. It can be seen that Au and Ag vary linearly with respect to each other with a ratio of approximately 1:10 (Au:Ag). Hg is elevated in most samples containing Au, with a consistent concentration of approximately 2 ppm. As is present in samples that contain Au and those that do not contain Au. The importance of these relationships is realized in developing a soil sampling program which targets hidden vein deposits. Hg which forms a widespread consistent halo would be more useful than As which occurs sporadically in and around the veins. Appendix III lists trench sample geochemical data.

ILLITE/SMECTITE RATIOS

To determine what the relationship is between the argillic alteration and the mineralized veins, a detailed study of the clay minerals present was conducted. Also, since the majority of the Pacific vein system is covered or
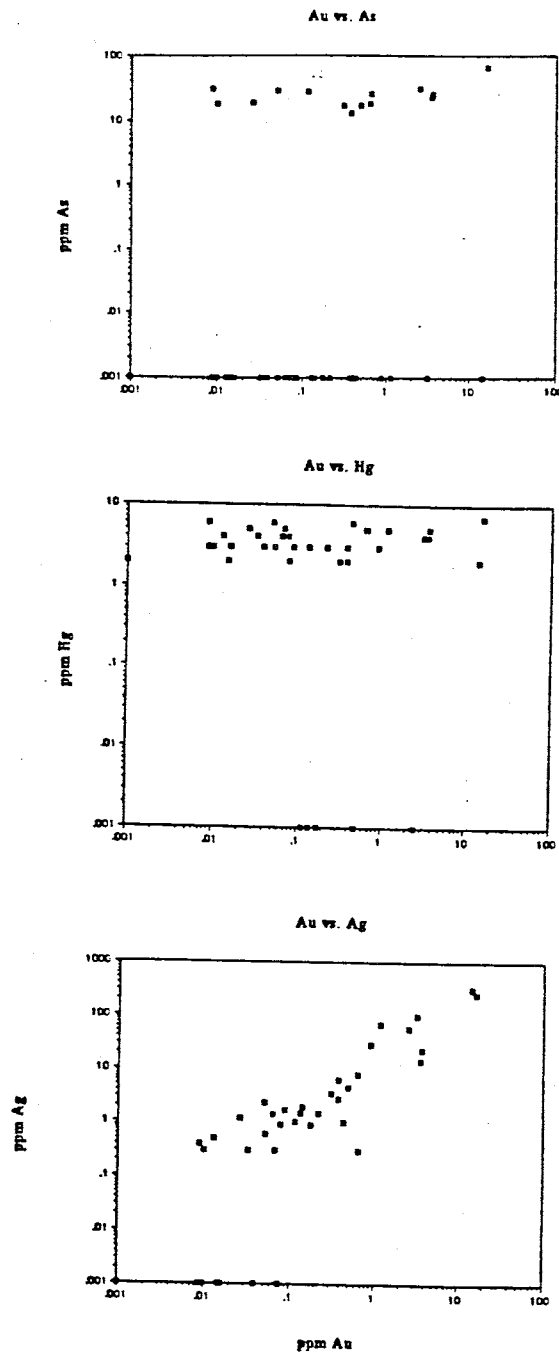
Figure 31. Graphs showing the relationship of gold to arsenic, mercury, and silver in trench samples.

inaccessible because of caved workings an exploration tool that would be able to determine the proximity to the high-grade veins in drillholes was needed. Illite/smectite ratios were examined to test for systematic variation with respect to the veins.

Background

The formation of illite/smectite as an alteration product, or newly precipitated phase under a variety of relatively low temperature ($100^{\circ}C$-$300^{\circ}C$) petrologic conditions has been well documented in the literature (Horton, 1985). It has also been shown that systematic variations in composition and structure of mixed-layer illite/smectite exist with changing temperature and depth in modern geothermal systems (Steiner, 1968; Eslinger and Savin, 1973; McDowell and Elders, 1980). Less work as been done in the area of illite/smectite systematics as related to ore deposits. Modern geothermal systems have been used as analogs for hydrothermal ore deposits (White, 1981). To better understand the correlation, Tooker (1963), Inoue and Utada (1983) and Horton (1985) have investigated the relationship of illite/smectite in modern geothermal systems to fossil geothermal systems.

Methods

Clay samples that were used in this study were collected
from diamond drill core in the area of the Pacific mine.
Sample locations are shown in Figure 32 and 33.

Samples were prepared for XRD analysis by soaking
approximately 10 grams of sample in approximately 100ml of
distilled water for several days. The samples were then
gently dispersed into the water with a glass stirring rod.
This clay and water slurry was then allowed to stand for 10
minutes to allow coarser grained particles to settle. An
eyedropper was used to remove enough material from the
surface to cover a glass slide. The upper most portion of
the suspension should be 2μm fraction (equivalent
spherical diameter) (Moore and Reynolds, 1989). The slides
were air-dried, which allows the individual clay particles
to become oriented parallel to the glass slide. This allows
for measuring the c-axis thickness of the individual clay
species. For a complete discussion of this methodology see
Moore and Reynolds (1989).

X-ray diffractograms of air-dried, ethylene glycol-solvated
and heated specimens were produced for each of the samples.
First, the air-dried sample was run from 35° to
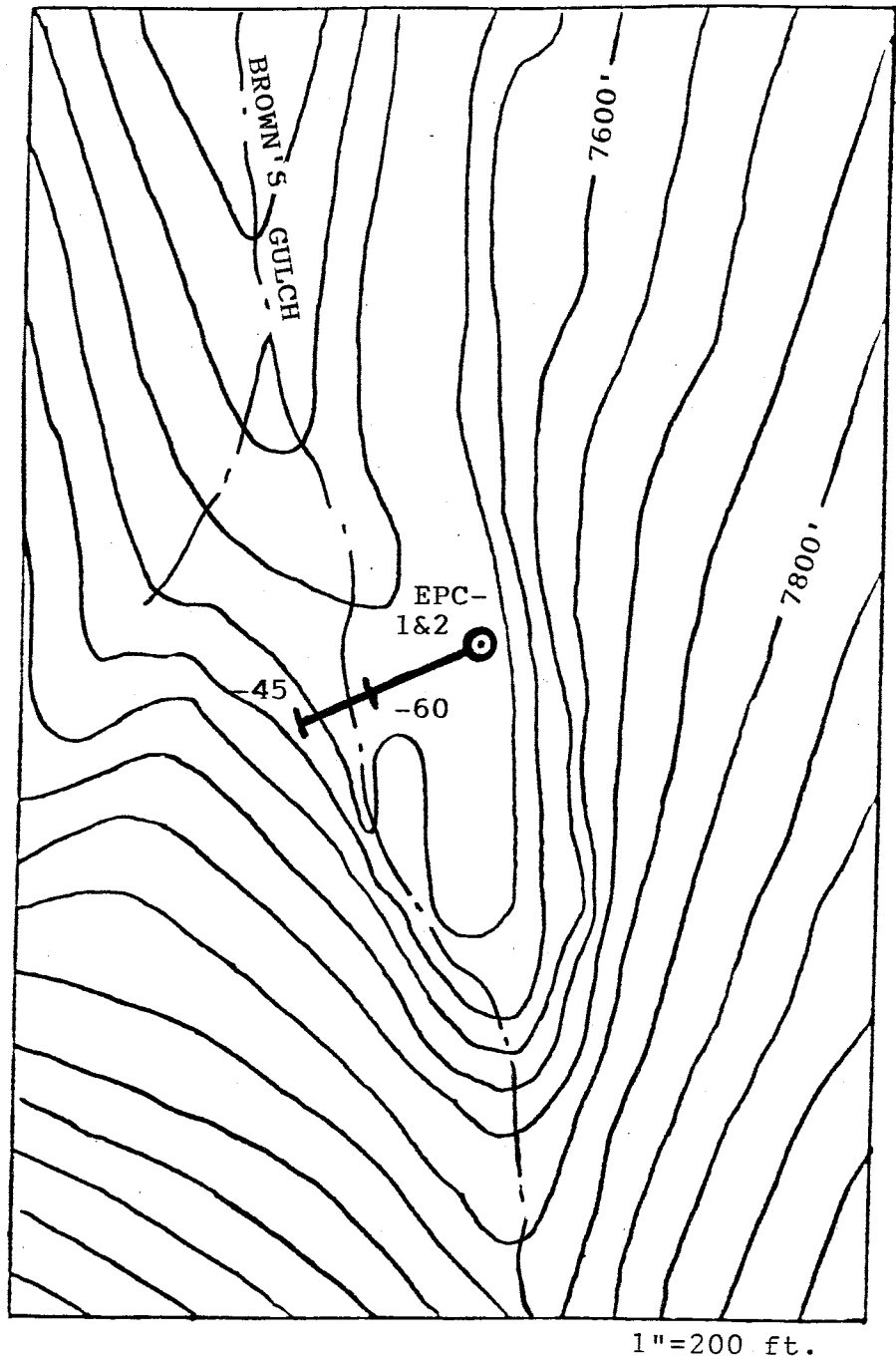
Figure 32. Plan map of the Pacific Pit showing the location of drill holes.

West   East

EPC-2-52

EPC-1-88

EPC-1-121

EPC-2-235
EPC-2-246

EPC-2-273

0   50 ft.
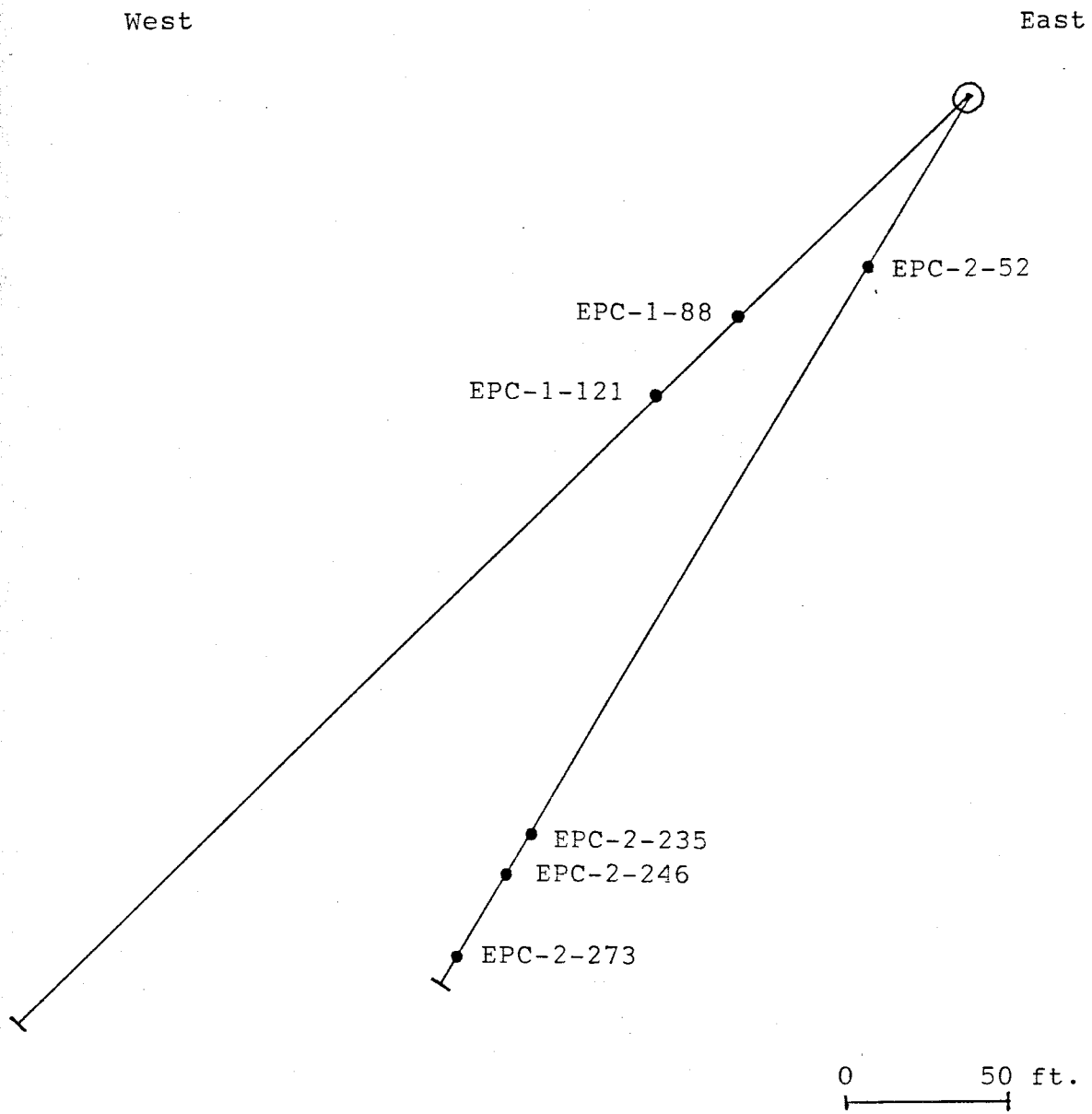
Figure 33. Cross-section showing the location of
samples used for clay analysis.

$2^{o}2\theta$/minute. The same sample was then placed in an ethylene glycol atmosphere for 24 hours at ambient temperature. This allows for the expansion of smectities and mixed-layer clays. The slide is run from 15° to $2^{o}2\theta$/minute. Expanded vs. the unexpanded thickness of the clay minerals are then compared. From this the amount of expandable clay species can be determined by analyzing the intensity of the shifted peak. The slide is then heated for 30 minutes at $375^{o}C$ to collapse the expandable clays. The slide is then run from 9.5^{o} to $7.5^{o}2\theta$/minute while still hot and the from 15° to $2^{o}2\theta$/minute. The comparison of this diffractogram with that of the glycol-treated clay was used to calculate the ratio of expandable to nonexpandable clays. The abundance of individual clay species, expressed in parts in 10, were calculated following the semiquanitative approach of Austin (Appendix III).

X-ray diffraction data were obtained with a Rigaku diffractometer using monochromatic Cu radiation, a scintllation counter, a 1° divergence silt, a 0.1mm scatter silt, a 0.3 mm receiving silt and a 0.3 mm detector silt. Samples were scanned at $2^{o}2\theta$/minute and the data was recorded by a strip chart recorder at the rate of 20mm minute.

Results

A plan view of the extent of argillic alteration in the area of the Pacific mine is shown in Figure 34. Throughout the sampled interval light green, scaly illite/smectite occurs as veinlets and pods which crosscut foliation. Argillic alteration is restricted to the zone of brecciation which is outlined on the geologic map of the Pacific mine area (Fig. 35). The intensity of argillic alteration appears to be consistent throughout this zone.

A schematic representation of drill holes EPC-1 and EPC-2 is shown in Figure 36. Also shown are XRD patterns which illustrate the clay mineral peaks.

The proportion of illite and expandable clays (smectite and mixed-layer clays) shows a systematic change with respect to distance from the Pacific vein system. The amount of illite increases as the veins are approached. Expandable clays increase distally from the veins. This relationship is shown graphically in Figure 37. Kaolinite is also present in the zone of argillic alteration possibly as a weathering product but no definite patterns have been noted.
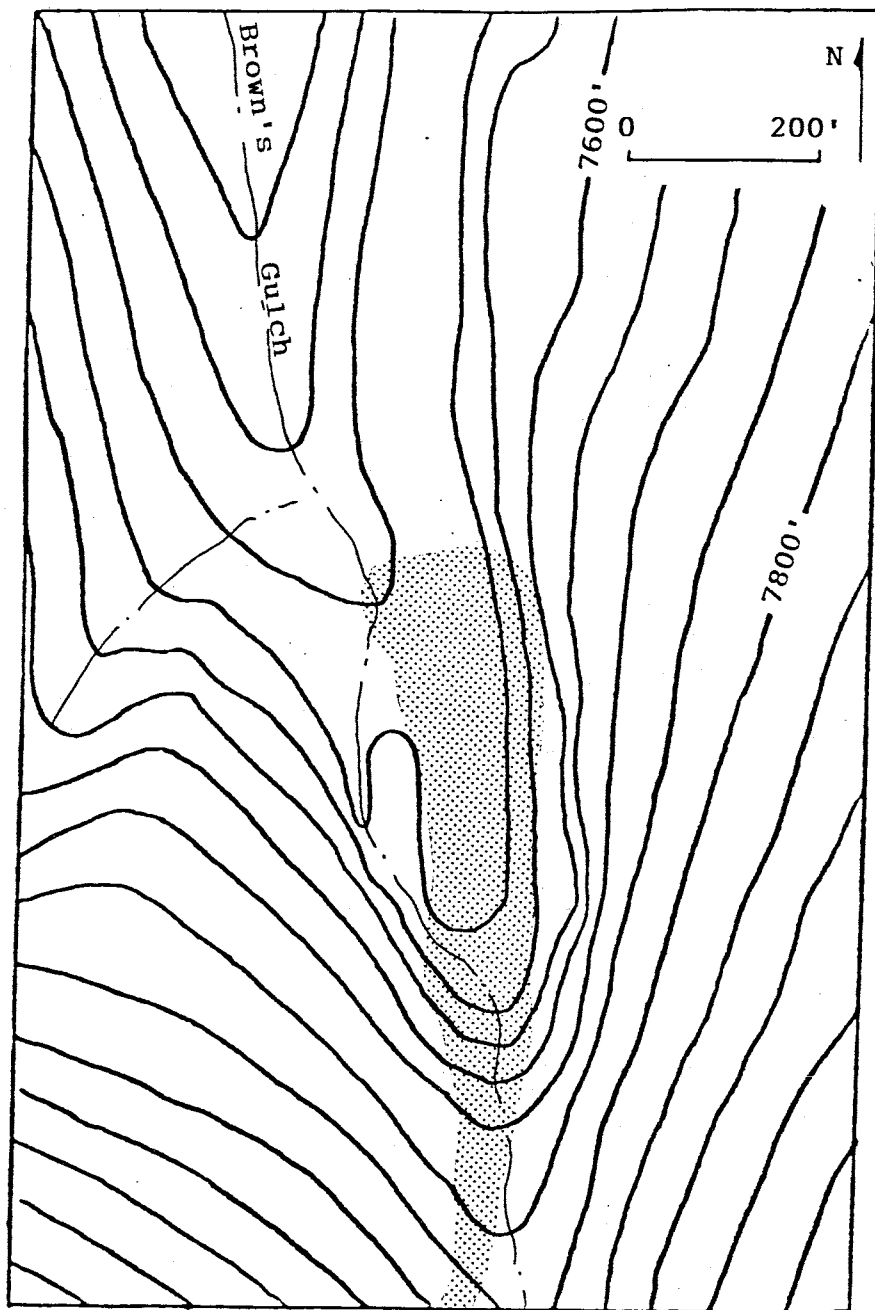
- Zone of argillic alteration

Figure 34. Plan map of the Pacific Pit showing the
extent of argillic alteration.
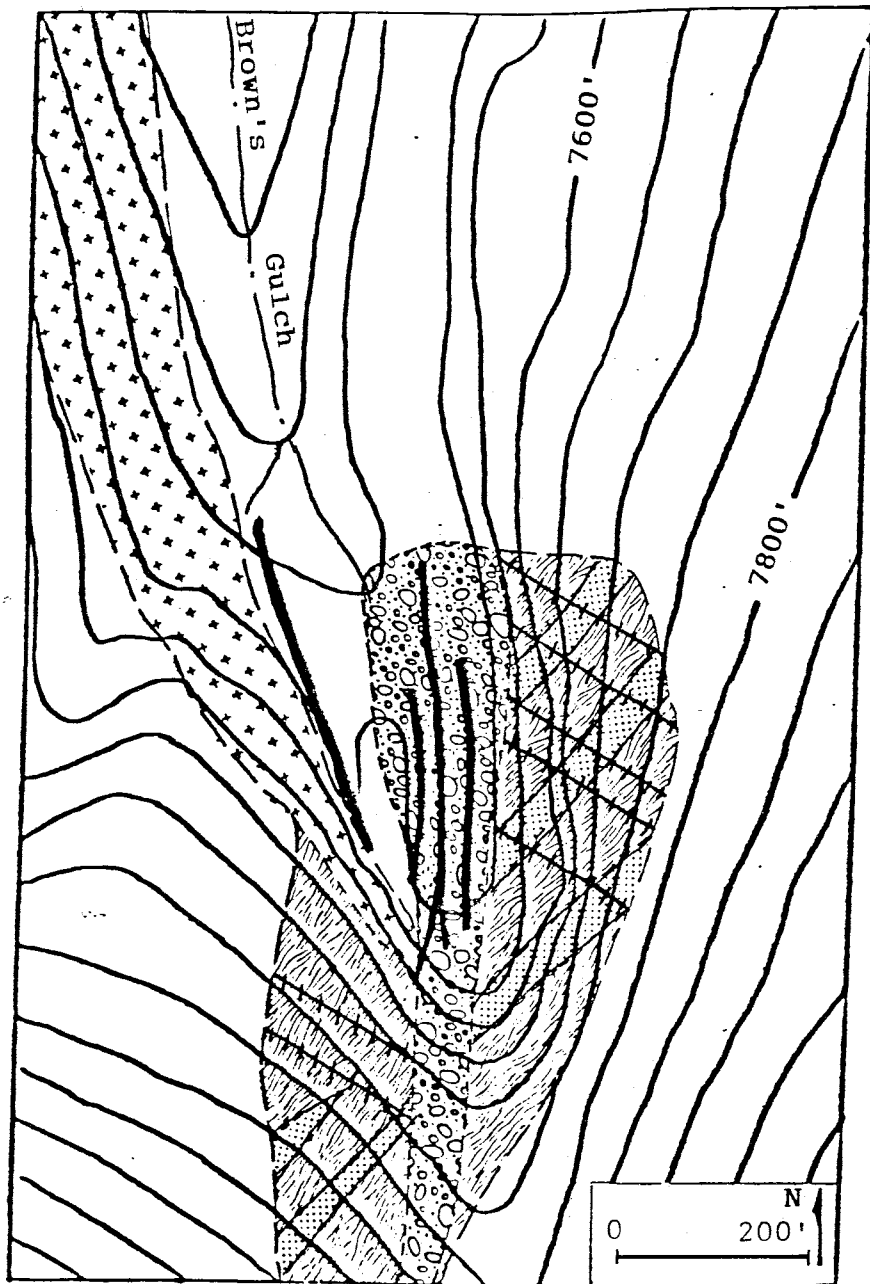
Figure 35. Generalized geologic map of the Pacific Pit.
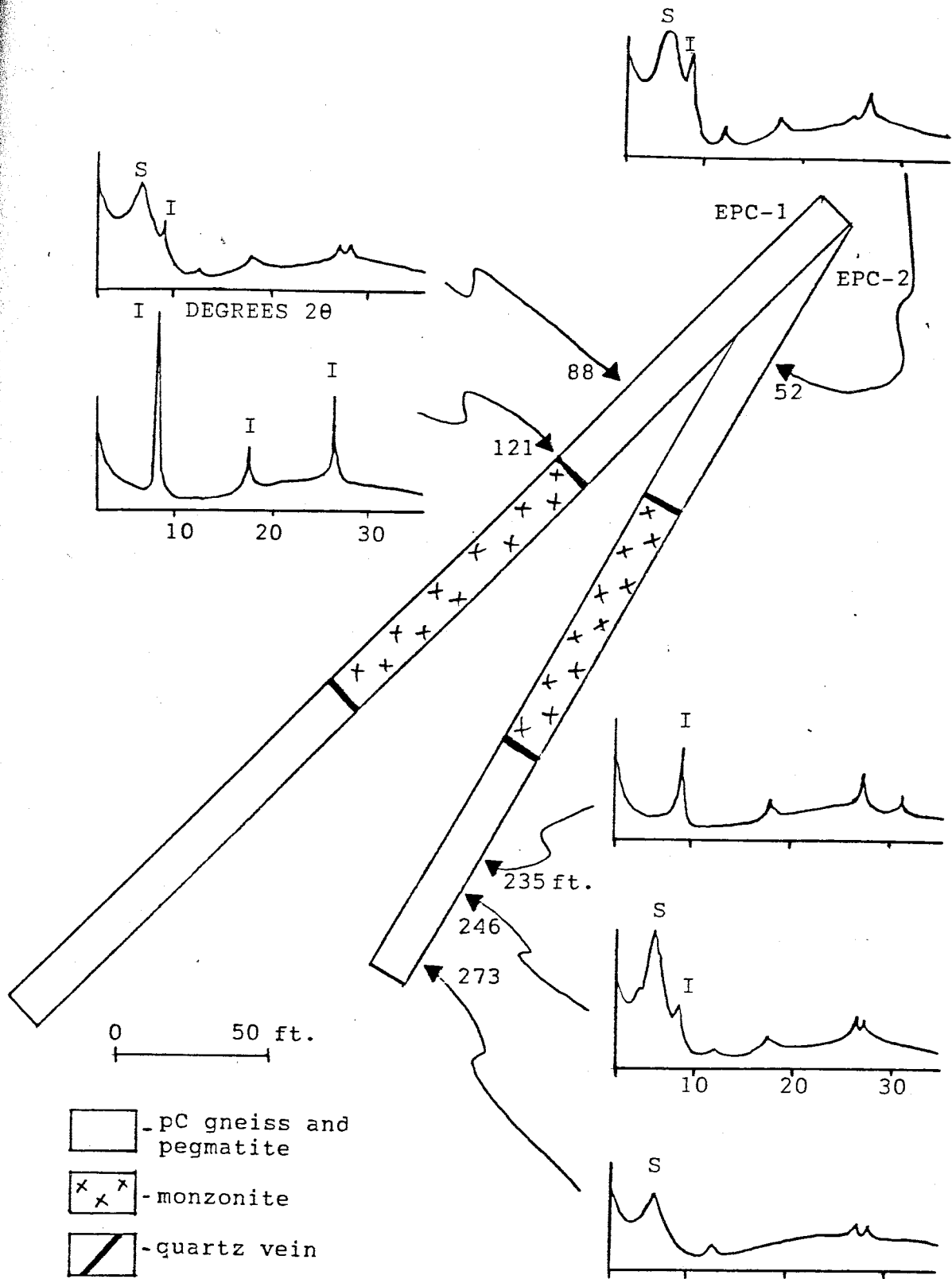
Figure 36. Schematic representation of drill hole geology and results of XRD.

parts in ten
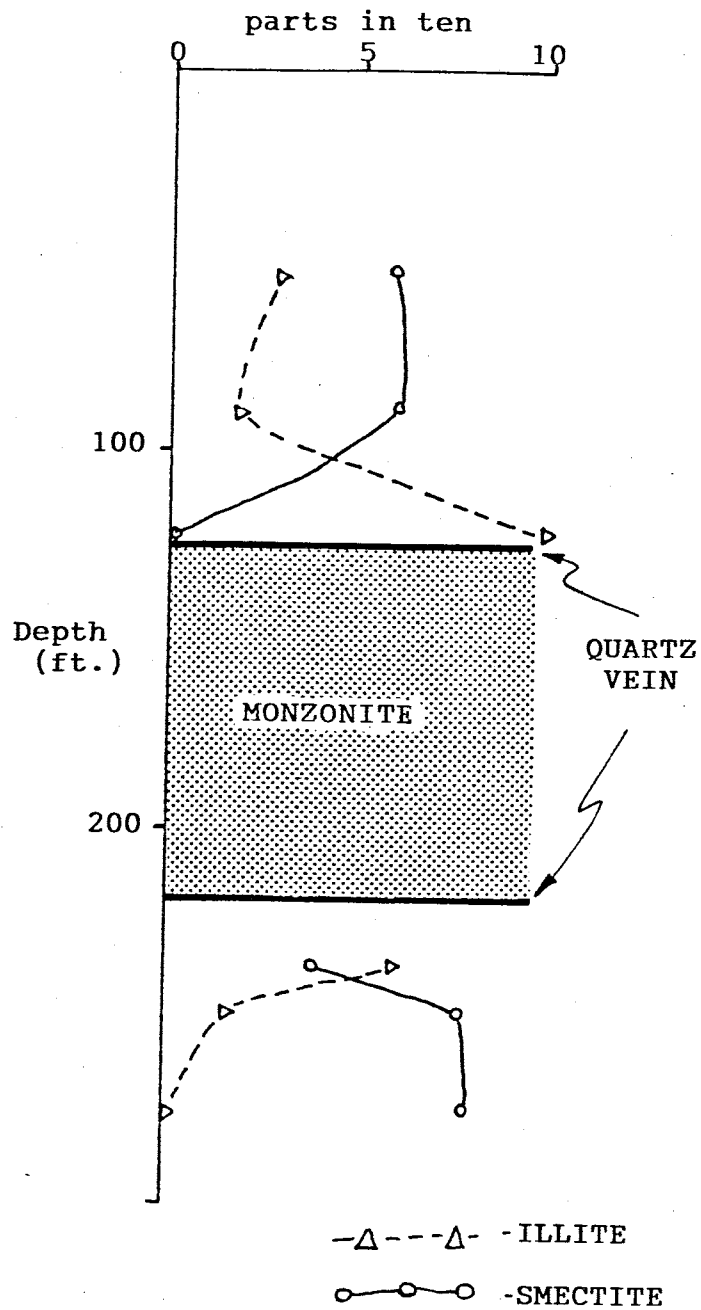
Figure 37. Graph showing the relationship of illite and expandable clays to quartz veins.

Discussion

Horton (1985) compiled the results of several studies on
illite/smectite relationships in modern geothermal fields
and in burial metamorphosed shales (fig.38). The results
of these studies showed that smectite is dominant at
temperatures from $50^{\circ}C$ to $120^{\circ}C$. As temperature
increases mixed-layer illite/smectite where illite is most
abundant is stable. Around $180^{\circ}C$ minor smectite is
present and all expandable clays are lost at $250^{\circ}C$ to
$270^{\circ}C$.

Horton also investigated the relationship of
illite/smectite in the argillic alteration halo surrounding
the Amethyst vein in the Creede district, Colorado. He
found that the percentage of illite increased as the vein
was approached. The random nature of illite/smectite
interlayering (ordering) became more ordered (1 to 1) as
the vein was approached. He was able to estimate thermal
gradients which were consistent with those observed modern
geothermal fields. Inoue and Utada (1983) studied a
Kuroko-type deposit in northeast Japan. They found a zonal
arrangement of increasing expandable clays distal to the
center of hydrothermal activity.
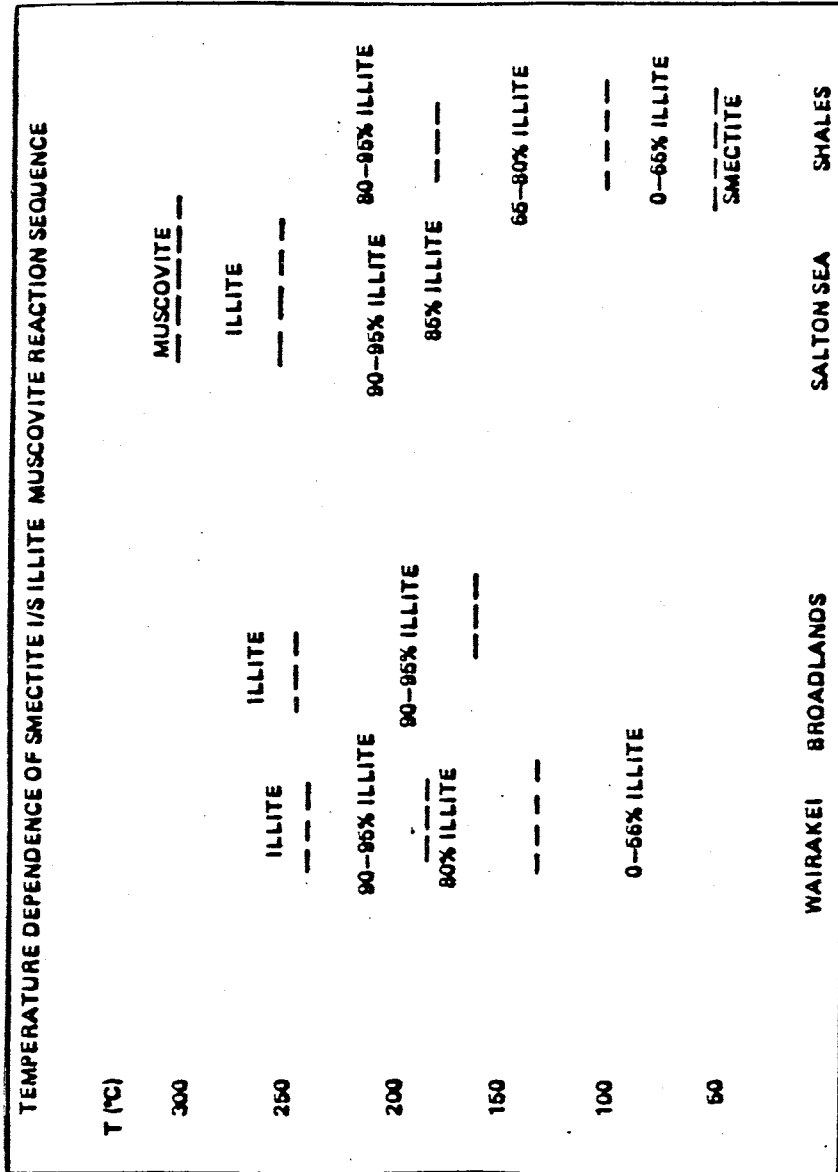
FIGURE 38. TEMPERATURE DEPENDENCE OF THE SMECTITE TO ILLITE/
SMECTITE TO ILLITE TO MUSCOVITE REACTION SEQUENCE
AT THREE MODERN GEOTHERMAL AREAS AND IN BURIAL
METAMORPHOSED SHALES (MODIFIED FROM HORTON, 1985)

The zoning of illite/smectite with respect to the Pacific vein system is consistent with the results of Horton (1985) and Inoue and Utada (1983). Comparison of the illite/smectite compositions present around the Pacific vein and those found in modern systems shows that the temperature of formation of clay adjacent to the Pacific vein can be estimated at $250^{\circ} \pm 40^{\circ}$. This is based on the purity of illite in sample EPC-1-121.

Temperature is not the only controlling factor in the formation of various clay species. Solution chemistry could have also affected the zoning around the Pacific vein. Eberl (1978) found that the absence of available potassium retards the smectite to illite transformation. The lack of available potassium should not have been a limiting factor at the Pacific mine, since K-spar constitutes a major portion of the host rock. The abundance of K^{+} is well documented with the presence of K-spar selvage around many veins in the district. With is available potassium it can be assumed that the I/S recorded the temperature at which the reaction took place.

Conclusions

Illite/smectite can be used in the area of the Pacific mine

to determine proximity to the Pacific vein system. It has

been shown that illite increases as the vein is approached.

This increase can be attributed to higher temperatures in

proximity to the vein at the time of emplacement. From the

purity of the illite temperatures can be estimated at

approximately $250^{\circ}\pm40^{\circ}C$. This range is consistent

with the temperatures determined by fluid inclusion

investigations.

FLUID INCLUSIONS

Fluid inclusions in quartz veins from the Easton-Pacific

area were investigated. The samples analyzed represent

different types of quartz veins with and without

mineralization. Five samples were prepared and analyzed to

determine the trapping temperature and salinity of the

trapped fluids.

Samples were selected from several different quartz veins

in hopes of determining a genetic relationship between the

various types. Samples 001508 and 001514 are representative

of narrow (up to 1 cm), unmineralized quartz veins with a

K-spar selvage. The quartz occurs as syntaxial subhedral

crystals oriented perpendicular to the vein trend. This

type of quartz vein occurs randomly and is associated with

major producing veins throughout the district. Sample
001524 is similar in morphology and occurrence to 001508
and 001514 but has anomalous gold content (2.4 ppm). Sample
89 MSL 010 represents mineralized quartz from the
Easton-Pacific vein. It is gray, fine-grained quartz that
has been brecciated, silicified, and cross cut by later
quartz veinlets. Sulphides occur as disseminations, blebs
and fracture fillings. ML-G1 is from a highly mineralized
vein at the Little Lode mine in Alder Gulch. Open space in
subhedral quartz is filled with native gold and telluride
minerals.

Microthermometric measurements were performed, by Kurt
Panter at New Mexico Tech. The temperature of
homogenization (T_h) was determined for 65 inclusions.
Salinities of the fluids were calculated from the
temperature at which the frozen fluid melted (T_m).
Determination of the primary versus secondary nature of the
inclusions were made following criteria outlined by Roedder
(1984).

Temperatures of homogenization for both primary and
secondary inclusions range from 143° to 312°.
Calculated salinities vary from 1.0 to 13.3 eq. wt.% NaCl.
The size of the individual inclusions used for the

measurements ranged from 2 to 9 micrometers. The majority
of inclusions are liquid-rich, two phase (NaCl eq. + H_2O
liquid + H_2O vapor). Subordinate to these are liquid-rich
two phase inclusions that contain variable amounts of
CO_2. Although a separate, visible CO_2 phase was not
observed, the presence of CO_2 was determined by presence
of clathrate and positive T_m values. CO_2 content of the
inclusions varies with no perceivable pattern but is
present in some yet not others. This indicates that the
CO_2 content of the solutions was low.

Figures 39 thru 43 show plots of salinity vs. T_h for the
individual samples. In general gold bearing veins appear to
have high T_h's and low to moderate salinities. The
unmineralized veins tend to have higher salinities and
lower T_h's. This trend is shown in figure 44 with a
combined plot of all the samples. It should be noted that
secondary inclusion in sample ML-G1 are similar to primary
inclusions in 001508. Based on paragenetic relationships of
the quartz veins this could indicate that ore-forming
fluids evolved from a higher temperture, low salinity
solution to a low temperature, high salinity solution with
time. A mechanism for this change could involve mixing of
water from various sources. The present limited data base
makes impossible to define the sources of these waters.

"001508"
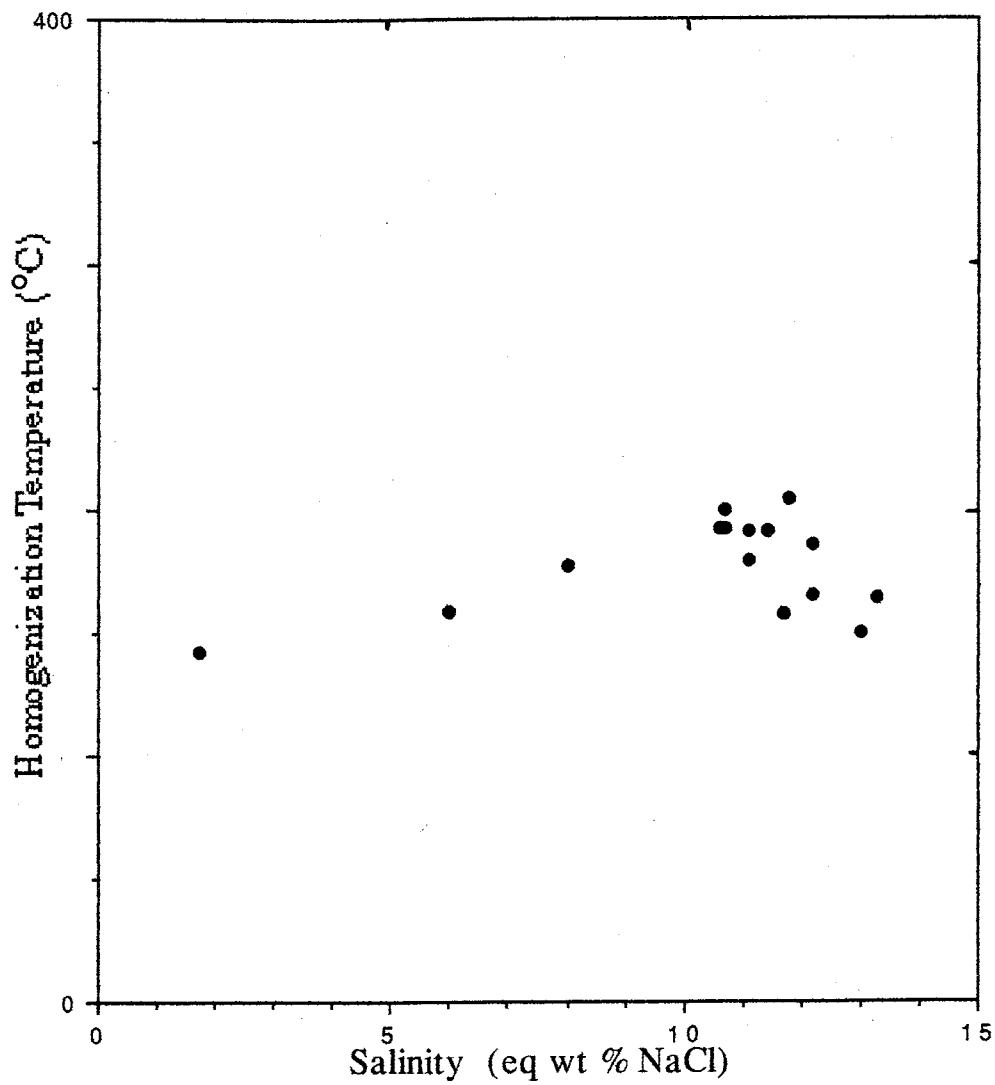
Figure 39. Salinity vs. T_h - sample #001508

"001514"
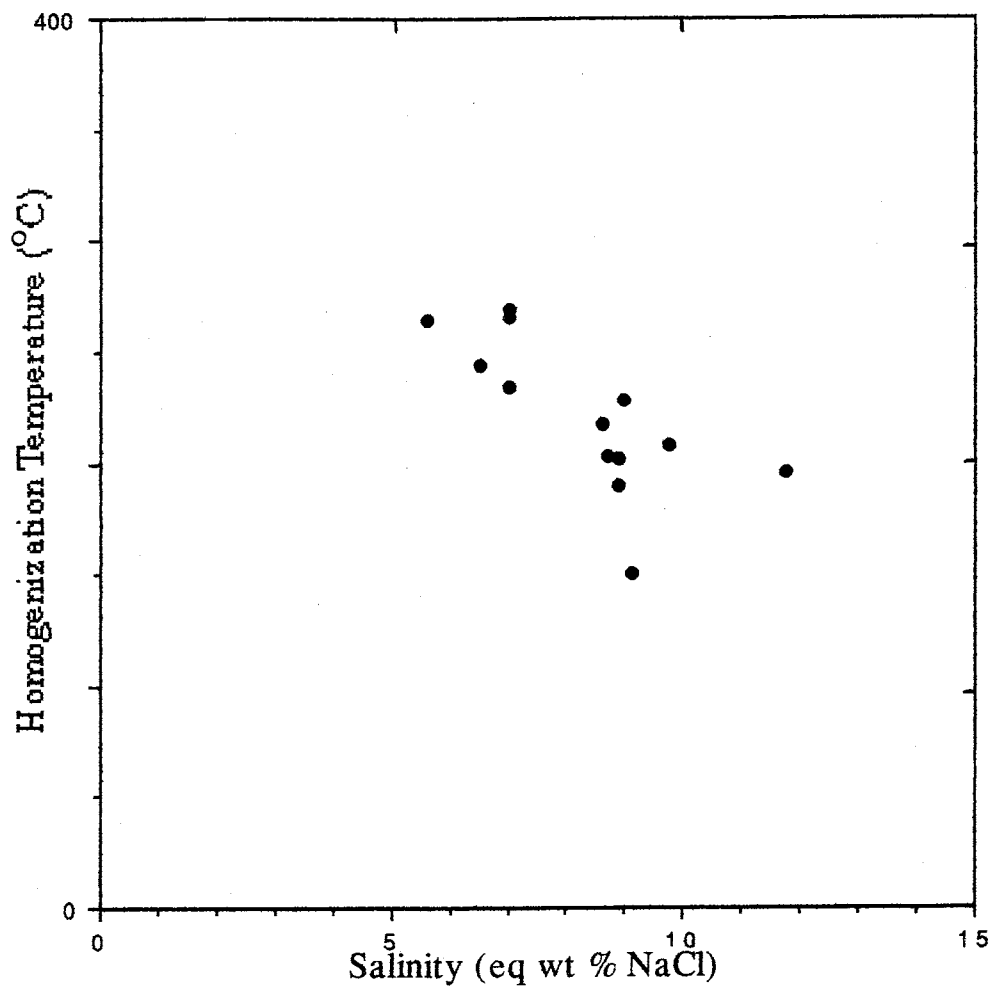
Figure 40. Salinity vs. T_h – sample #001514

"001524"
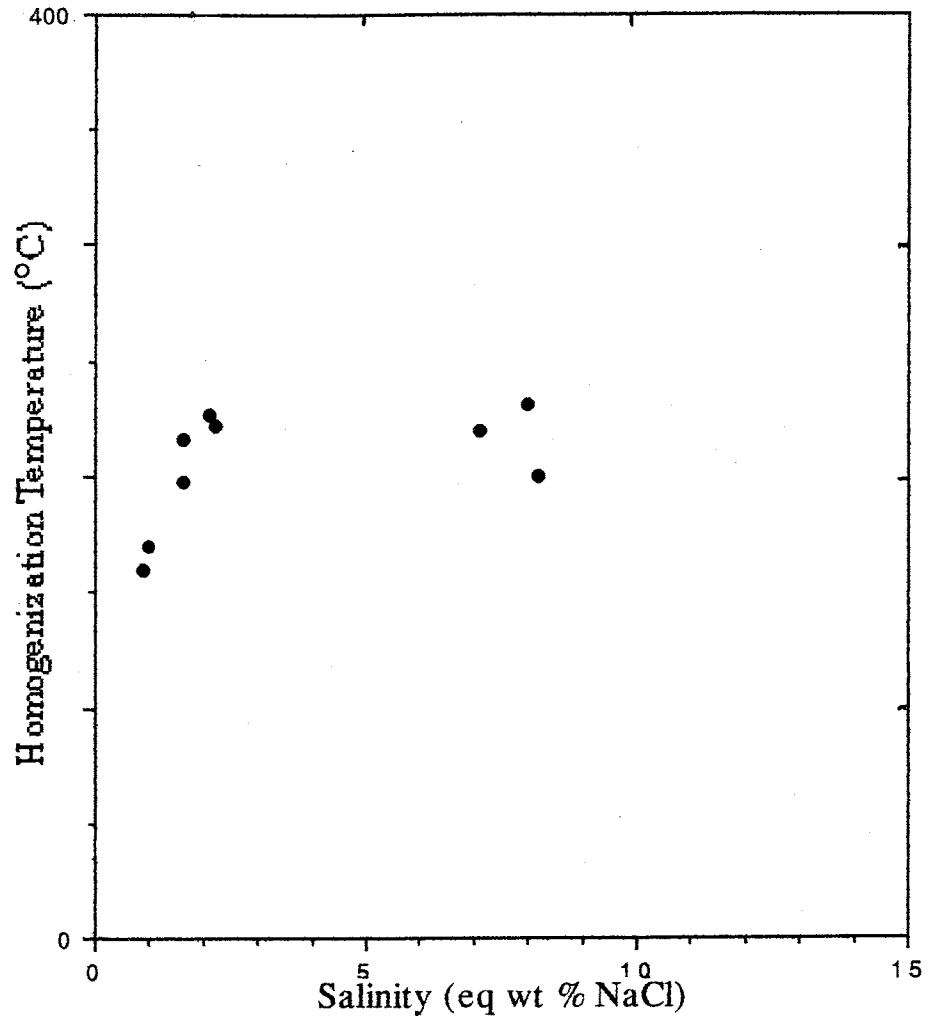
Figure 41. Salinity vs. T_h - sample #001524.

"89 msl 010"
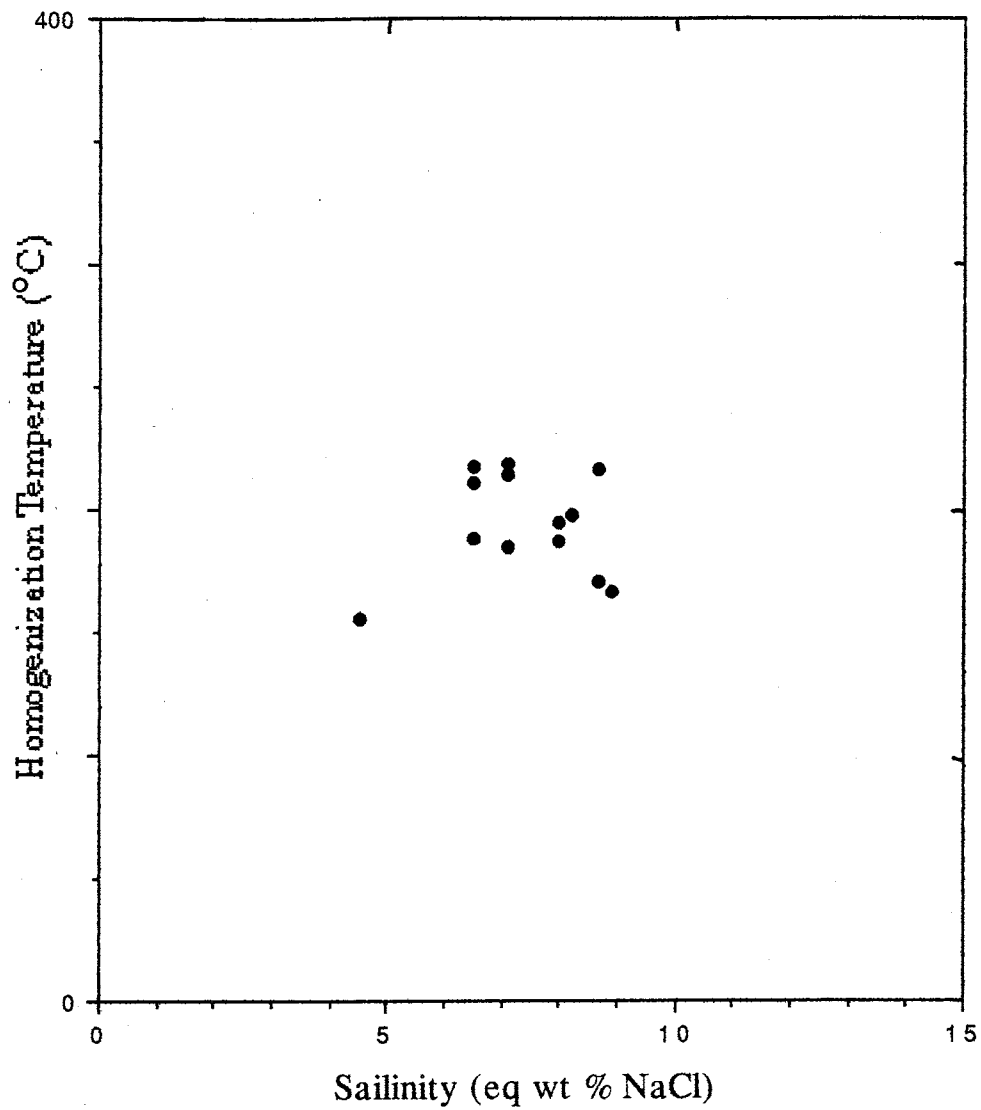
Figure 42. Salinity vs. T_h- sample # 89 MSL 010.

"mlg1"
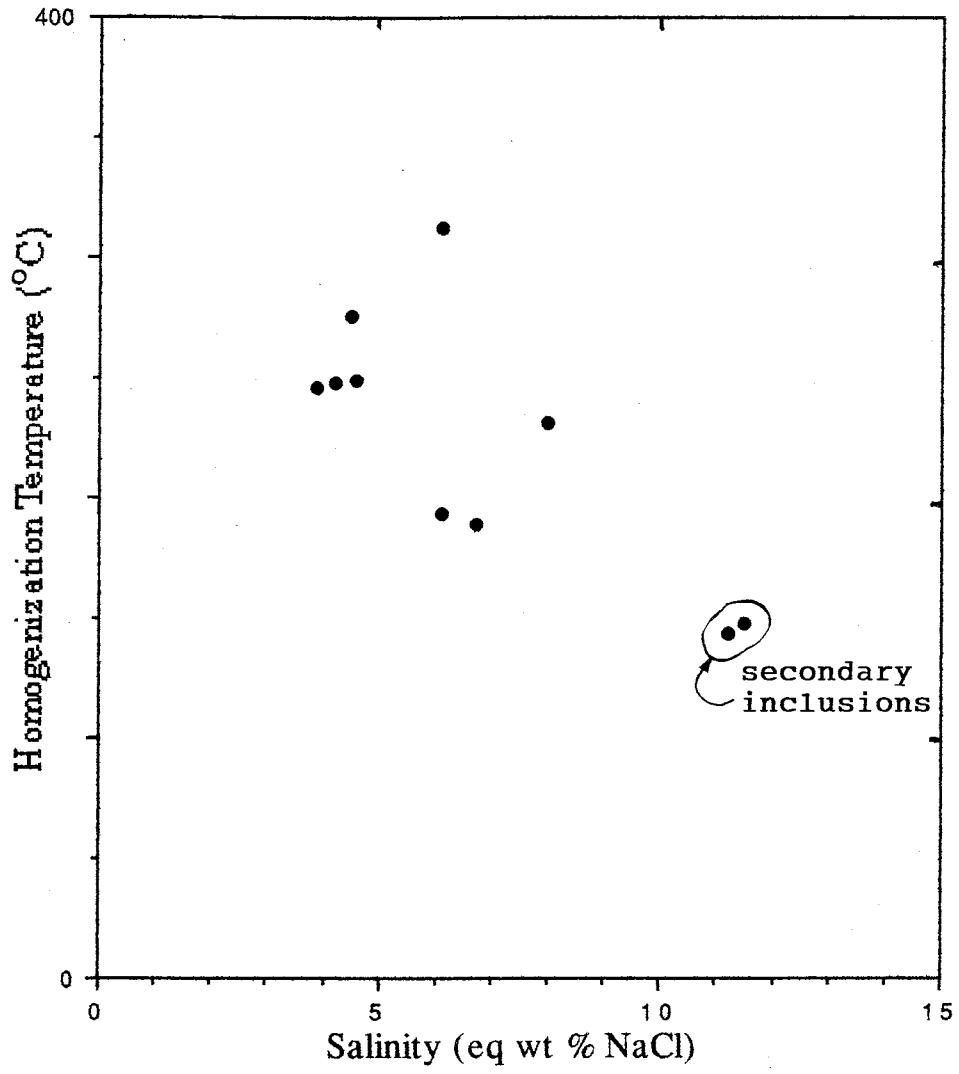
Figure 43. Salinity vs. T_h - sample # ML-G1.
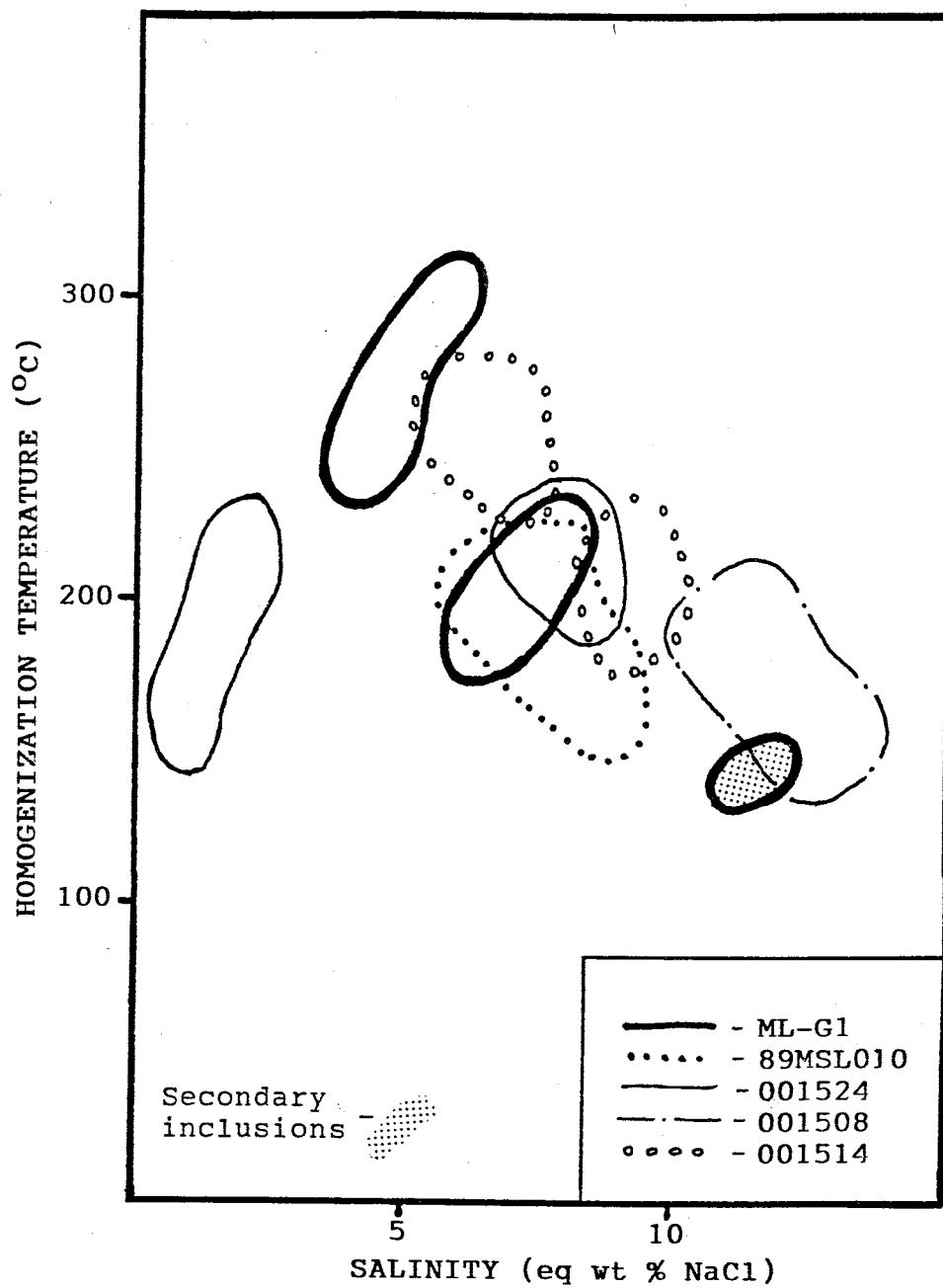
Figure 44. Combined plot of salinity vs. homogenization temperature for all fluid inclusion samples.

DISCUSSION

The precious metal deposits of the Tobacco Root mining region show many similarities in their host rocks, structural controls, and mineralization patterns. The lithology of the host rocks appears to have influenced the style of mineralization (i.e. vein vs. replacement), regional scale fracture patterns have controlled the location of deposits in most cases, and the association with the Tobacco Root batholith and its satellite intrusions has developed vein deposits typical of a near-plutonic environment.

Lithology

Host rock lithology appears to have influenced the style of mineralization in the Tobacco Root mining district. Quartzofeldspathic gneiss and quartz monzonite are the most common host rocks and appear to restrict the development of disseminated type deposits because of their low permeability. As result deposits are typically located in zones where secondary permeability was increased through fracturing.

Reactive host rocks such as limestone appear to favor the

development of replacement type deposits like the Bear

Gulch deposits in the Sheridan district (Winchell, 1914).

Since limestone is subordinate to the typical

quartzofeldspathic gneisses, these replacement type

deposits are limited.

The host rock lithology in the area of the Easton-Pacific

vein system is of the relatively "unreactive" variety

therefore the majority of the mineralization is restricted

to the veins.

Structure

In the Tobacco Root mining region, long-lived Precambrian

fracture zones that have periodically been reactivated have

served as conduits for ascending solutions through time.

These structures and structural zones have localized the

emplacement of plutons, dikes and veins systems.

Second-order structures are important sites for mineral

deposition on a deposit scale.

Precious metal deposits of the Tobacco Root mining district

occur over a large area but all exhibit strong structural

control. NW and NE trending fracture zones were important

in localizing ore-forming fluids. Reactivation of these

fracture zones developed dilatant zones in which vein material could form. Why then are the length of veins on the order of hundreds of feet and the length of the fractures on the order of miles? The location of these dilatant zones within main fracture appear to control the location of veins and the location of dilatant zones can best be explained by the mechanism of bulk, inhomogeneous shortening proposed by Hodgson (1989). On a smaller scale brecciation and opening along jogs and bends in the structure appear to be important mechanisms for developing dilantancy.

In the Virginia City district the presence of many relatively short veins (compared to the length of regional scale structures) can be explained using Hodgson's mechanism. Hodgson suggests that dilation can occur along individual segments of a conjugate fracture set. Figure 45 shows a diagrammatic representation of the results of bulk, inhomogeneous shortening. The dilatant zones developed in this model could represent the quartz veins of the Virginia City district (fig. 46). Evidence for the throughgoing nature of the veins but the limited extent of wide mineralized zones can be seen in the area of the Pacific mine. Geophysics was able to trace the veins away from the Pacific mine but only narrow veins were encountered in trenching and drilling away from the main structure.
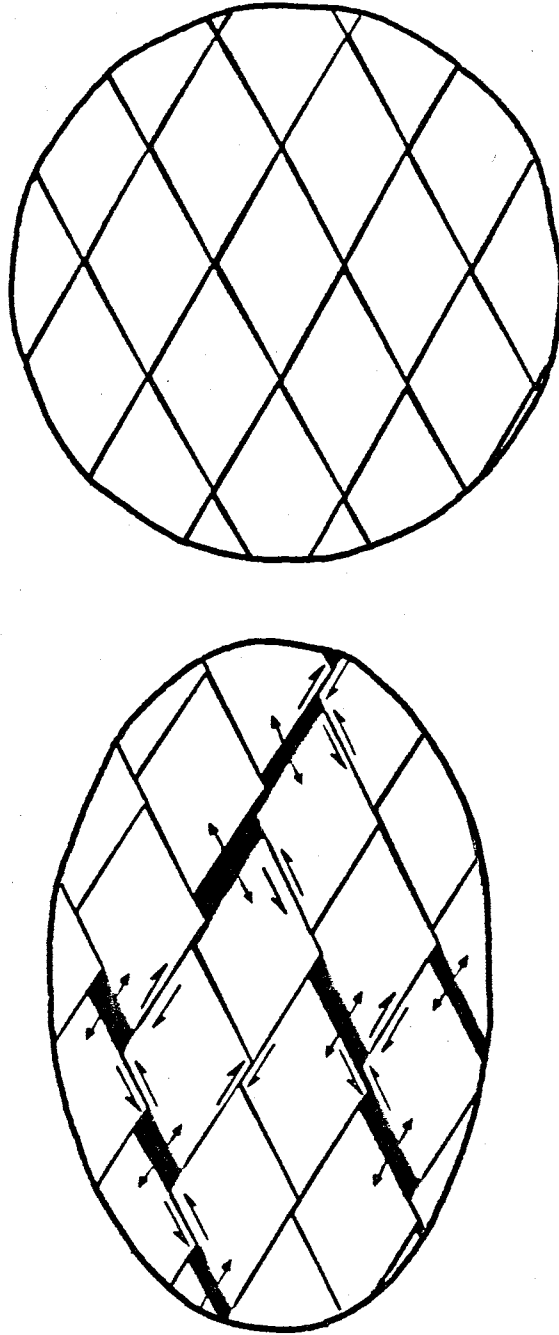
Figure 45. Diagrammatic representation of the
development of dilatant zones along
individual segments of a conjugate
fracture set (after Hodgson, 1989).

108
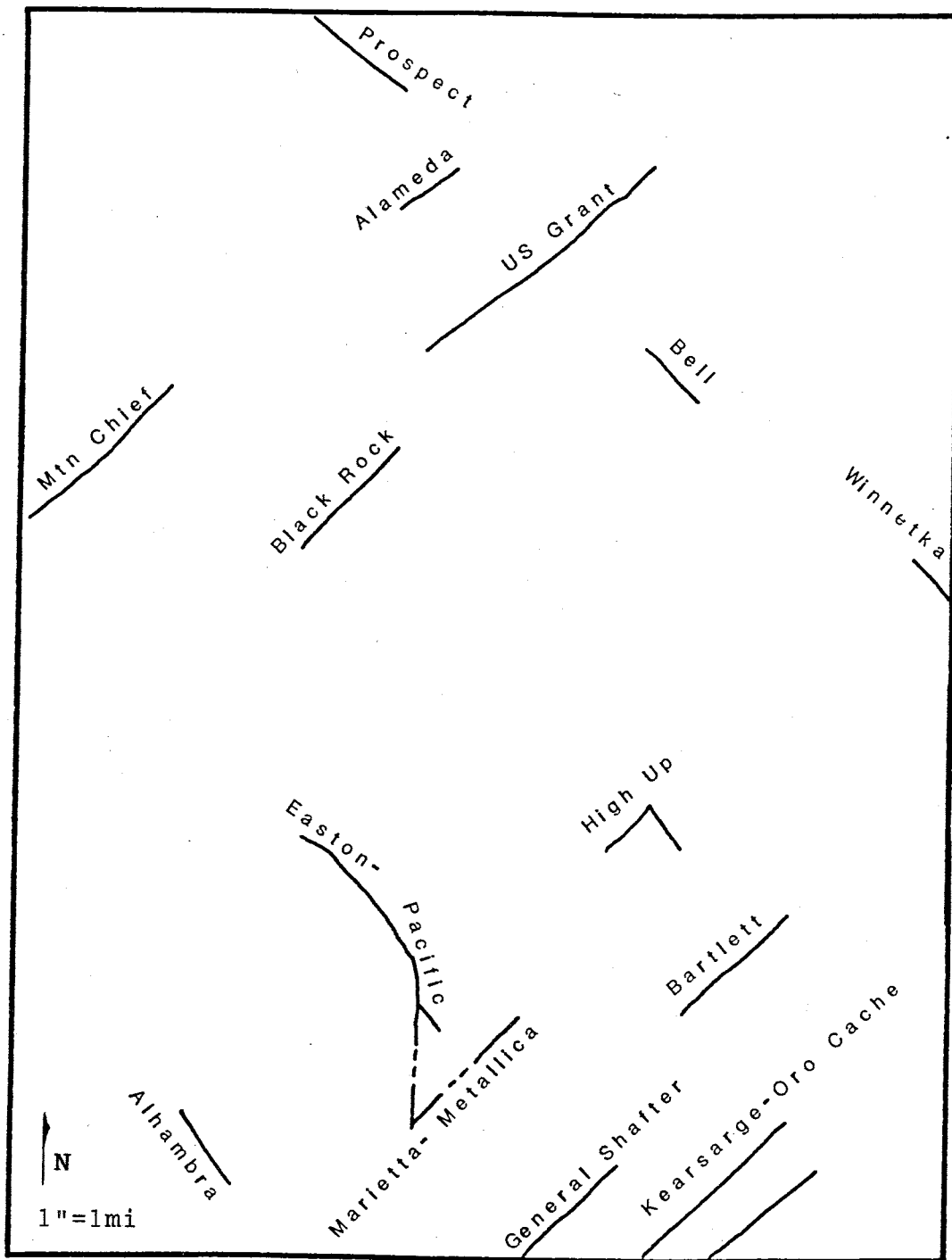
Figure 46. Plan veiw of mineralized segments of fracture
zones in the Virginia City district for
comparison with Hodgson's model of
in homogeneous shortening.

From the available data it appears that some of these fracture zones penetrated through the crust of the Earth. This is evidenced by the presence of NW-trending mafic dikes with isotopic signatures indicative of mantle derivation. The emplacement of the Tobacco Root batholith also indicates that the fracture system must be extensive, not only in a lateral sense but in the vertical direction as well.

The Easton-Pacific vein trend exhibits strong structural controls. Mineralization is restricted to fracture zones or immediately adjacent to them. Second order structures within these fractures appear to have facilitated the deposition ore minerals (fig. 47). Intersections, bends and jogs are the locus for high-grade mineralization. Dilatancy caused by episodes of brecciation and brittle fracturing during and after Period 1 mineralization provided continued access for mineralizing fluids into the main fracture zone. This continued access was important in developing ore-grade mineralization. The large area of brecciation at the Pacific mine appears to be the result of strain accumulated during periods of left-lateral displacement along the Easton-Pacific structure. Brecciation is localized by right-stepping strike variations in the structure (fig. 48).

JOGS:

zone of dilation

BENDS:

dilatant   or
compressional depending
on active segment

TRANSPRESSION:

compressional

TRANSTENSION:

dilatant
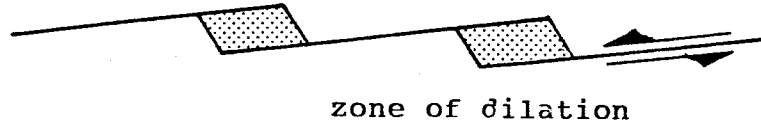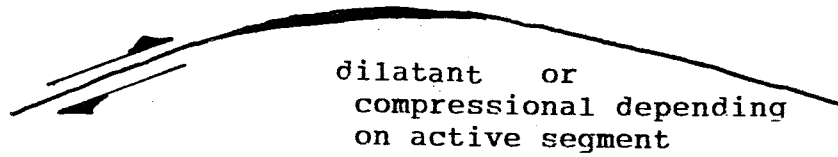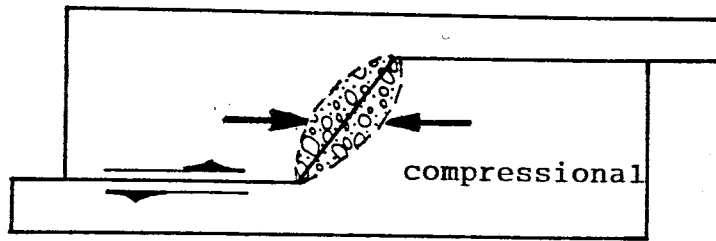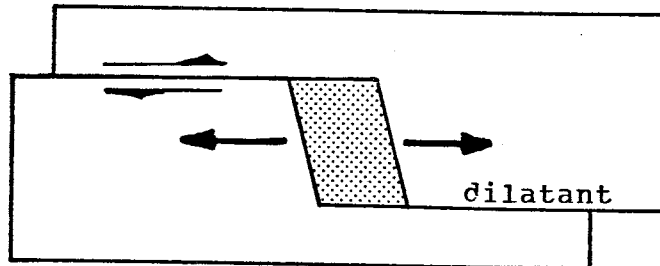
Figure 47. The nature of jogs, bends, and zones of
transpression and transtension (after
Hodgson, 1989).
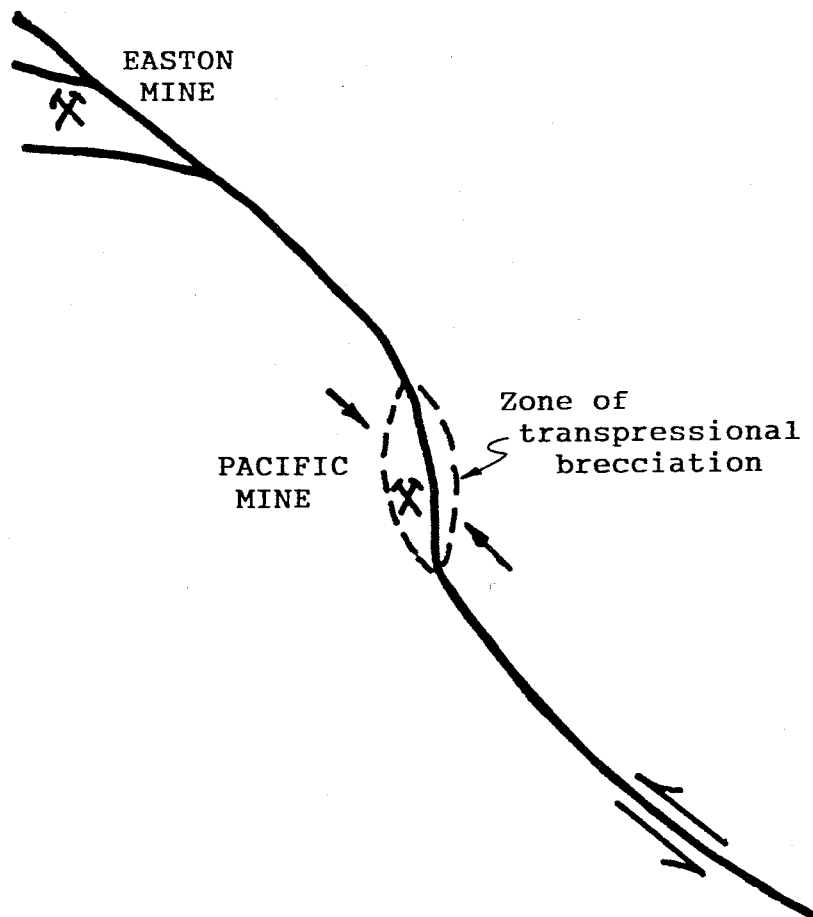
Figure 48. Schematic representation of structures in the area of the Easton and Pacific mines showing the development of transpressional breccia at the Pacific mine.

Fracturing of the wall rocks in some areas has lead
to very limited disseminated mineralization. Brecciation in
the area of the Pacific mine has facilitated the
development of argillic alteration over a large area.

Kelly and Goddard (1969) documented the structural controls
on telluride mineralization in Boulder, Colorado. They
reported that economic concentrations of ore minerals occur
at intersections of veins, and irregularities along the
vein related to movement along the veins. They also noted
the importance of brecciation and shearing in the veins for
the development of secondary open-space.

Plutonic Association

Precious metal deposits of the Tobacco Root mining region
appear to be genetically associated with the
Cretaceous-aged Tobacco Root batholith (Kinley, 1987; Cole,
1983; Vitaliano, 1979; Lorain, 1937). Deposits of this
type, throughout the world, show similar characteristics
(Newberry et.al, in press).

Following is summary of data on plutonic-related gold
deposits of the vein and replacement type compiled by
Newberry et.al (in press):

Intrusive type - reduced, mid to late Cretaceous, granitic.

Ore mineralogy - arsenopyrite, pyrite, ± pyrhotite,
stibnite, tellurides, molybdenite and Bi and W
minerals.

Geochemical expression - Au-As-Bi-Sb-Te (Zn,Cu,Ag,B,Sn,Be).

Morphology - vein and breccia bodies; replacement bodies
occur where carbonate-bearing rocks are present.

Attempts have been made to explain gold-enrichment in
plutons through various mechanisms. Tectonic setting of
gold-enriched plutons was investigated by Kesler (1973),
his data suggests that porphyry copper deposits in island
arc settings are more gold-enriched. Keith and Swan (1987)
used the oxidation state of the plutons to show that
reduced plutons favored gold-enrichment. A review of the
geochemistry of plutons with associated gold deposits was
compiled by Mutschler et al. (1985) showing that a variety
of gold deposits are associated with alkaline intrusives.
The combination of the alkalinity and oxidation state of
plutons appears to be a valid empirical method of
determining the "gold favorability " of plutonic rocks
which was proposed by Leveille et al. (1988). In their

114
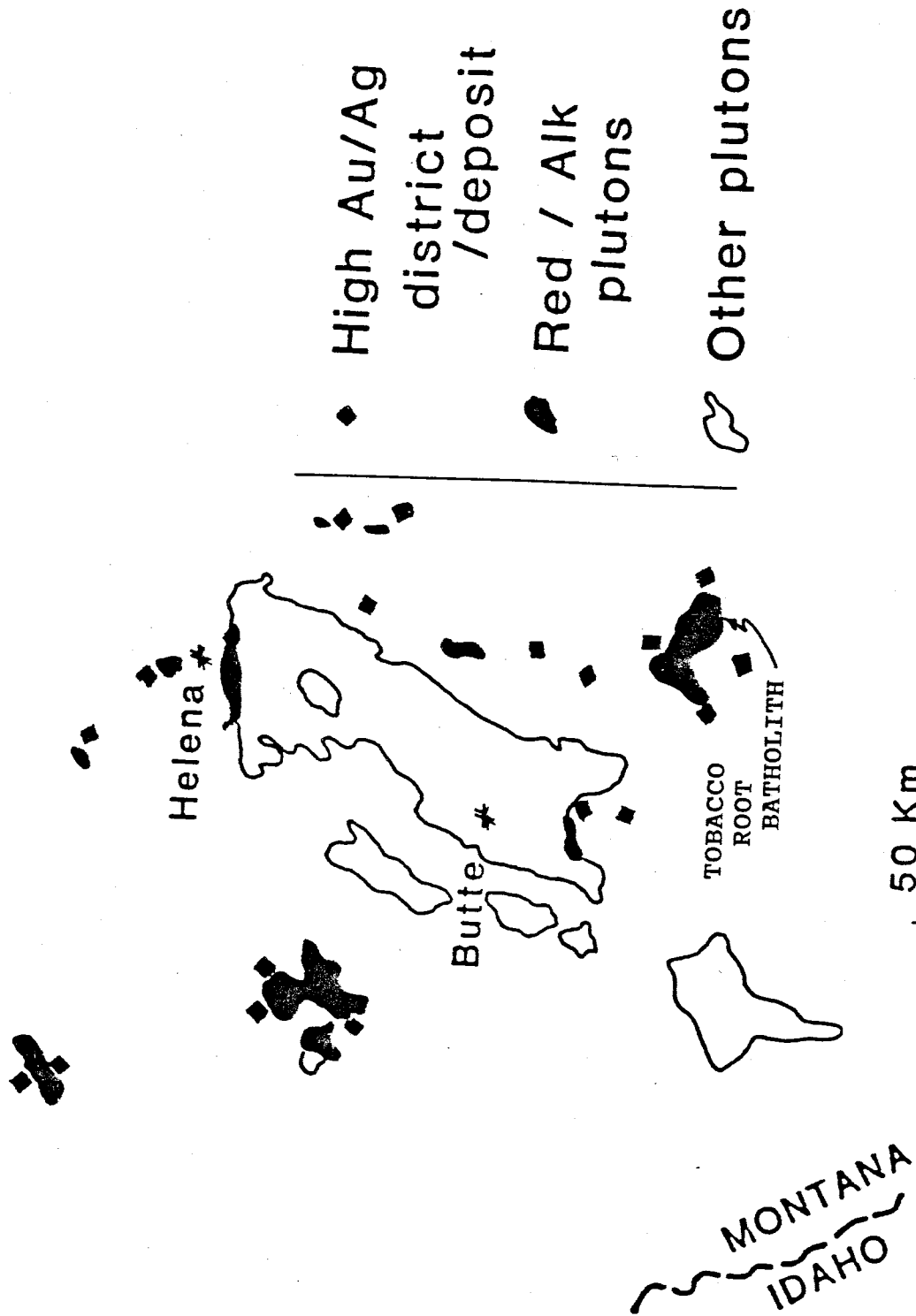
Figure 49. Distribution of reduced/ alkaline plutons and gold deposits in western Montana (from Leveille, Newberry, and Bull, 1988)

compilation the alkalinity/oxidation state of the plutons
in western Montana was investigated. They determined that
the Tobacco Root batholith was of the "gold-favorable",
reduced variety (fig 49).

Ore minerals present in the Tobacco Root mining region are
indicative of plutonic related deposits. Kinley (1987)
reported the association of gold and bismuthinite at the
Red Pine mine in the Sheridan district. Winchell (1914)
reported the occurence of huebnerite ($MnWO_4$) and
molybdenite at the Bismark mine in the Pony district. In
the Virginia City district, arsenopyrite and stibnite are
reported to occur at the Easton-Pacific mines and at the
Marietta mine (Winchell, 1914).

General Deposit Type

The comparison of the precious-metal veins of the Virginia
City district with other well-documented precious-metal
vein deposits throughout the world is a useful way of
determining the genetic implications of the observed
characteristics. Although these deposits occur in a variety
geologic environments, their chemical characteristics are
similar enough to indicate a commonality (Barnes, 1979).
Research in the area of vein deposits has uncovered a wide

range of conditions at which ore minerals are deposited. The variety of conditions possible is expressed in the wide variety of deposit types observed. The goal of this discussion is not to pigeon-hole the Virginia City deposits into a rigid category but to contrast them with the continuum of hydrothermal deposits.

Table 1 shows the generalized characteristics of epithermal deposits after Eimon (1988), mesothermal deposits after Nesbitt et al. (1986), Korean-type deposits after So and Shelton (1987) and the Virginia City deposits. From this comparison it can be seen that the Virginia City deposits do not fit perfectly into any one category but rather they span the gap between several deposit types.

The host rocks in the Virginia City district are Precambrian gneisses and Cretaceous monzonite. In contrast host rocks of epithermal deposits are typically Tertiary volcanic and sedimentary rocks (Eimon, 1988). Mesothermal deposits are typically hosted in metamorphosed greenstone belts (Nesbitt, 1988). The Precambrian gneissic and Cretaceous intrusive host rocks of the Korean deposits most closely resemble those of the Virginia City district.

The strong structural control of the deposits of the

TABLE 1. Comparison of Virginia City deposits with other hydrothermal deposits.

	EPITHERMAL	VIRGINIA CITY	KOREAN-TYPE	MESOTHERMAL
Age	Tertiary; late Jurassic	late Cretaceous	early Cretaceous	Jurassic to Tertiary
Host Rocks	Inter. to felsic volcanics, seds; unmetamorphosed	Archean gneiss, Cret. monzonite	pЄ gneiss, Jur.-Cret. granites	greenschist metamorphosed volcs.& seds.
Structural Setting	Fractures and faults assoc. w/ volcanic centers	Second order structures along regional scale structures	Major fault zones	Major trans-current fault zones
Morphology	Stockworks, vein fillings, comb structures, crustiform	Composite veins, breccia zones	Composite veins	Massive or ribboned veins
Ore Minerals	Sulphides, tellurides, sulfosalts	py, cp, gl, sph Au^0, Ag^0, tellurides	py, asp, sph, gl	py, cp, gl
Alteration	Adv. argillic, silicification, potassic, propylitic	Argillic, potassic, late calcite	Argillic, potassic, pyritization, late calcite	Carbonatization, silicification, seritization
Fluid Chemistry	Temp. 250°C low CO_2 3-4 eq wt% NaCl	Temp. 275°C low CO_2 1-13 eq wt% NaCl	Temp. 225-285°C moderate CO_2 3-9 eq wt% NaCl	Temp. 300°C high CO_2 3-6 eq wt% NaCl

Virginia City district is common in all the deposits,
however the structural styles vary greatly. Epithermal
deposits are localized in shallow structures associated
with volcanic centers (Eimon, 1988). Mesothermal deposits
are typically located along regional scale strike-slip
faults, and many show brittle and ductile textures on a
local scale (Bursnall, 1989). The Korean-type deposits are
localized in brecciated regional-scale fault zones similar
to those of the Virginia City district.

The morphology and mineralization of the precious-metal
deposits of the Virgina City district are characterized by
composite quartz veins restricted to fracture zones with a
relatively simple assemblage of sulphides, tellurides
native precious-metals. Textures of the quartz vary from
subhedral syntaxial crystals with poorly developed
open-space to silicified breccias. Sulphides occur as blebs
and stringers within the quartz. Minor late calcite
crosscuts earlier quartz. In contrast mineralization in
epithermal deposits occurs as stockworks, disseminations,
breccia pipes and irregular pods. On a small scale, ore
textures include open-space fillings, drusy cavities,
crustification, comb structure and colloform banding
(Eimon, 1988). Epithermal mineral assemblages include
sulphides, tellurides, selenides, sulfosalts with gangue

minerals of quartz, barite, flourite, rhodochrosite and adularia (Eimon, 1988). Mesothermal deposits are characterized by a simple assemblage of sulphides contained in a gangue of quartz and carbonate with tourmaline, and muscovite. Mineralization of the Korean-type deposits show the greatest similarity to that of the Virginia City district. They are characterized by a simple assemblage of sulphides in composite quartz veins with minor open-space texture.

The geochemical and physical conditions that prevailed at the time of ore deposition can be estimated using a variety techniques such as fluid inclusion and isotopic investigations (Skinner, 1979). Fluids responsible for the deposition of precious-metals in epithermal deposits appear to consist mainly of shallowly circulated meteoric waters which range in temperature from 50 to 250°C, contain low concentrations of CO_2 and NaCl (3-4 eq wt%). Mesothermal fluids contain high concentration of CO_2 (4-30 wt%), moderate amounts of NaCl (3-6 eq wt%) and range in temperature from 250 to 370°C. Isotopic values indicate that mesothermal fluids evolved from deeply circulated meteoric waters (Nesbitt, 1986). The Korean-type deposits appear to bridge the gap between the two end-member deposit types (Shelton, 1988). The fluids which formed the

Korean-type deposits appear to have evolved from high temperature (400°C) to low temperature (200°C). Salinities of the fluids also evolved from moderate salinity (3-9 eq wt% NaCl) to a more dilute solution (3-4 eq wt% NaCl). Characteristics of the fluids which deposited ore minerals in the Virginia City deposits evolved from a high temperature (275°C), low salinity fluid (3-6 eq wt% NaCl) to a lower temperature (175°C), higher salinity fluid (10-12 eq wt% NaCl).

Alteration patterns appear to reflect the physical and chemical conditions under which ores where deposited (Rose and Burt, 1979). Alteration assemblages of epithermal deposits typically contain minerals indicative of argillization, silicification and propylization (Eimon, 1988). This alteration is usually pervasive. Alteration associated with mesothermal deposits is dominated by carbonization, sericitization, chloritization and pyritization. At Virginia City as well as the Korean-type deposits alteration is restrict to narrow selvages around the veins and zones of intense brecciation. The alteration assemblage is characterized by argillic and potassic alteration.

The Easton-Pacific vein trend was the largest lode producer

in the Virginia City district. Characterization of the mineralizing events at the Pacific mine indicate that the deposit formed in the deep portion of an epithermal system (approximately 350 meters) as evidenced by mineralogical, textural, geochemical and fluid inclusion data. The correspondence of temperatures determined by illite:smectite ratios and fluid inclusions indicates a pressure correction for the fluid inclusion data is not needed, confirming this shallow depth of formation. Ore deposition was spacially associated with the Brown's Gulch stock and appears to post date its emplacement. Crosscutting relationships at the El Fleeda mine indicate that the mineralization in the Virginia City district predates the emplacement of a 51 m.y. old andesite plug (Cole, 1983). Mineralizing fluids appear to have evolved with time from a high temperature, low salinity fluid to a lower temperature, higher salinity fluid. Structural controls on ore deposition range from large scale regional fracture zones to small scale dilatant zones within these regional structures. Alteration is restricted to narrow selvages because of the lack of permeability in the host rock.

CONCLUSIONS

1. The host rock lithology of the Virginia City mining district in southwestern Montana does not favor the development of bulk-tonnage low-grade precious-metal deposits. The low primary permeability of the gneisses and intrusive rocks limits the occurrence of deposits to areas of increased secondary permeability such as fractures and brecciated zones.

2. The mineralization of the Virginia City district is localized along throughgoing regional-scale fractures that have been reactivated through time. Second order structures within these large scale structure are important sites of ore deposition. The limited extent of these mineralized zones does not favor bulk-mining.

3. Morphological evidence indicates that the Virginia City deposits are spacially and possibly genetically related to the Brown's Gulch stock, a satellite of the larger Cretaceous-aged Tobacco Root batholith.

4. Fluid inclusion data suggests that ore-forming fluids evolved from a high temperature ($275^{\circ}C$), low salinity (3-6 eq wt% NaCl) solution to a lower temperature

(175°C), high salinity (10-12 eq wt% NaCl) solution possibly indicating a mixing of fluids from different sources.

5. Temperatures estimated by illite/smectite ratios are consistent with those estimated by fluid inclusions. Illite/smectite ratios indicate that a zoning of high illite proximal to the vein with increasing smectite distal to the vein is present at the Pacific mine.

6. Comparison of the Virginia City deposits to other hydrothermal deposits worldwide reveals a continuum of deposit types. The Virginia City deposits most closely resemble the deposits of the Cheonan area in Korea studied by So and Shelton (1987). The deposits of both of these districts appear to bridge the gap between epithermal and mesothermal deposits.

124

REFERENCES CITED

Anon., 1889, The 1st report of the State Mine Inspector:
State of Montana.

Anon., 1894, A new departure in milling: Madisonian,
February 17, 1894.

Anon., 1900, The 12th report of the State Mine Inspector:
State of Montana

Anon., 1947, Mining convention addresses current activities
in County: Madisonian, December 5, 1947.

Burger, H. R., 1966, Structure, petrology, and economic
geology of the Sheridan district, Madison County,
Montana: Unpub. Ph.D. Dissertation, Indiana State
University, Bloomington, Indiana, 156 p.

Bursnall, J. T., 1989, Introduction: Reveiw of mechanical
principles, deformation mechanisms, and shear zone
rocks, in Bursnall, J. T., ed., Mineralization and
shear zones: Geological Association of Canada, Short
Course Notes, Volume 6, p. 1-27.

Chadwick, R. A., 1981, Chronology and structural setting of volcanism in southwestern and central Montana: Montana Geological Society 1981 Field Conference Guidebook.

Cole, M. M., 1983, Nature, age, and genesis of quartz -sulfide-precious metal vein systems in the Virginia City mining district, Madison County, Montana: Unpub. M.Sc. Thesis, Montana State Univ., Bozeman, MT., 76 p.

Cordura, W. S., 1973, Precambrian geology of the southern Tobacco Root Mountains, Madison County, Montana: Unpub. Ph.D. Dissertation, Indiana State Univ., Bloomington, Indiana, 247 p.

Eimon, P. I., 1988, Epithermal gold silver deposits: Commonwealth International Inc., Amarillo, 102 p.

Eslinger E. V., Savin S., 1973, Mineralogy and oxygen isotope geochemistry of hydrothermally altered rocks of the Ohake-Broadlands, New Zealand geothermal area: Am. Jour. Sci. v. 273, p. 240-267.

Gilette, B. J., 1966, Isotopic ages from southwestern Montana: Journal of Geophysical Research, v. 71, no. 16, p. 4029-4036.

Hadley, J. B., 1969, Geologic map of the Varney Quadrangle,
    Madison County, Montana: USGS Map QG-814, 1:62,500
    scale.

Hamilton, W., 1981, Plate tectonic mechanism of Laramide
    deformation: Contributions to Geology, University of
    Wyoming, v.19, no.2, p. 87-92.

Hodgson, C. J., 1989, Patterns of mineralization, in
    Bursnall, J. T., Mineralization and shear zones:
    Geological Society of Canada, Short Course Notes,
    Volume 6, Montreal, Quebec, p. 51-88.

Horton, D. G., 1985, Mixed-layer illite/smectite as a
    paleotemperature indicator in the Amethyst vein
    system, Creede district, Colorado, USA: Contrib.
    Mineral. Petrol., v. 91. p. 171-179.

Inoue, A., Utada, M., 1983, Further investigations of a
    conversion series of dioctahedral mica/smectites in
    the in the Shinzan hydrothermal alteration area,
    Northeast Japan: Clays and Clay Miner., v. 31, p.
    401-412.

James, H. L., and Hedge, C. E., 1980, Age of basement rocks of southwest Montana: Geological Society of America Bulletin, v.91, p. 11-15.

Keith, S. B., and Swan, M. M., 1987, Oxidation state of magma series in the southwestern U.S.: Implications for geographic distribution of base, precious, and lithophile metal metallogeny: Geological Society of America, Abstracts with Programs, p. 723.

Kelly, W. C., and Goddard, E. N., 1969, Telluride ores of Boulder County, Colorado: Geological Society of America, Memoir 109, 197 p.

Kesler, S. B., 1973, Copper, molybdenum and gold abundances in porphyry copper deposits: Economic Geology, v. 68, p. 106-112.

Kinley, T. K., 1987, The occurence and timing of gold mineralization at the Red Pine Mine, Western Tobacco Root Mountains, southwestern Montana: Unpub. M.Sc. Thesis, Montana State Univ., Bozeman, MT, 129 p.

Koehler, S. W., 1972, Petrology and petrogenyof the diabase
    dikes of the Tobacco Root Mountains, southwestern
    Montana: Unpub. M.Sc. Thesis, Indiana State
    University, Bloomington, 60 p.

--------------, 1976, Petrology of the diabase dikes of the
    Tobacco Root Mountains, Montana, in Tobacco Root
    Geological Society, 1976, Field Conference Guidebook:
    Montana Bureau of Mines and Geology Special
    Publication 73, p. 27-36.

Levandowski, D. W., 1956, Geology and mineral deposits of
    the Sheridan-Alder area, Madison County, Montana: Ph.D
    Dissertation, University of Michigan, Ann Arbor,
    University Microfilms 19.707. 318 p.

Leveille, R. A., Newberry, R. J., and Bull, K. F., 1988, An
    alkalinity-oxidation state diagram for discriminating
    some gold-favorable plutons: an empirical and
    phenomenalogical approach [abs.]: Geological Society
    of America, Abstracts with Programs, Denver, p. 142.

Lorain, S. H., 1937, Gold lode mining in the Tobacco Root
    Mountains, Madison County, Montana: USBM Information
    Circular 6972, 74 p.

McDowell, S. D., Elders, W. A., 1980, Authigenic layer silicate minerals in borehole Elmore 1, Salton Sea geothermal field, California, USA: Contrib. Mineral. Petrol., v. 74, p. 293-310.

Moore, D. M., and Reynolds, R. C. Jr., 1989, X-ray diffraction and the identification and analysis of clay minerals: Oxford University Press, 332 p.

Mueller, P., and Cordura, W. S., 1976, Rb-Sr whole rock age of gneisses from the Horse Creek area, Tobacco Root Mountains, Montana: Isochron/West, no.16, p. 33-36.

Mutschler, F. E., Griffen, M. E., Stevens, D. S., Shannon, S. S., Jr., 1985, Precious metal deposits related to alkaline rocks in the North American cordillera: An interpretive review: Transactions of the Geological Society of South Africa, v. 88, p. 355-377.

Newberry, R. J., Burns, L. E., and Pessel, G. H., 1990, Probabilistic estimate of mineral resources in the Valdez Creek mining district, Alaska: in press, 49 p.

Nesbitt, B. E., Murowchick, J. B., Muelenbachs, K., 1986, Dual origins of lode gold deposits in the Canadian Cordillera: Geology, v. 14, p. 506-509.

Pearle, A. C., 1896, Geologic atlas of the United States, no. 24, Three Forks Folio, Montana: USGS 7p. 3 maps.

Rose, A. W., and Burt, D. M., 1979, Hydrothermal alteration, in Barnes, H. L., ed., Geochemistry of Hydrothermal Ore Deposits: New York, Wiley Intersci., p.173-235.

Runner, J. J., and Thomas, L. C., 1928, Stratigraphic relationships of the Cherry Creek Group in the Madison Valley, Montana: Geological Society of America Bulletin, v. 39, 202 p.

Ruppel, E. T., 1985, The association of Middle Cambrian rocks and gold deposits in southwest Montana: USGS Open-file Report 85-207, 26 p.

Samuelson, K. J., and Schmidt, C. J., 1981, Structural geology of the western Tobacco Root Mountains, southwestern, Montana: Southwest Montana, Montana Geological Society Field Conference and Symposium, p.191-199.

Schmidt, C. J., Garihan, J. M., 1986, Laramide tectonic development of the Rocky Mountain foreland of southwestern Montana, in Lowell, J. D., Gries, R., eds., Rocky Mountain foreland basins and uplifts: Rocky Mtn. Assoc. of Geologists, Denver, CO, p. 271-294.

Shelton, K. L., So, C. S., and Chang, J. S., 1988, Gold-rich mesothermal vein deposits of the Republic of Korea: Geochemical studies of the Jungwon Gold Area: Economic Geology, v. 83., p. 1221-1237.

Sillitoe, R. H., 1985, Ore-related breccias in volcanoplutonic arcs: Economic Geology, v. 80, p.1467-1515.

Skinner, B. J., 1979, The many origins of hydrothermal ore deposits, in Barnes, H. L., ed., Geochemistry of Hydrothermal Ore Deposits: New York, Wiley Intersci., p.1-21.

Smith, J. L., 1970, Petrology, mineralogy and chemistry of the Tobacco Root batholith, Madison County, Montana: (abst.) Dissertation Abstracts, v. 31-B, p. 5429-B.

So, C. S., and Shelton, K. L., 1987, Stable isotope and
    fluid inclusion studies of gold- and silver-bearing
    hydrothermal vein deposits, Cheonan-Cheongyang-Nonsan
    mining district, Republic of Korea: Cheonan area:
    Economic Geology, v. 82, p. 987-1000.

Steiner, A., 1968, Clay minerals in hydrothermally altered
    rocks at Wairakei, New Zealand: Clays and Clay Miner,
    v. 16, p. 193-213.

Tansley, W., Schafer, P. A., Hart, L. H., 1933, A
    geological reconnaissance of the Tobacco Root
    Mountains, Madison County, Montana: Montana Bureau of
    Mines and Geology Memoir 9. 55 p.

Tendall, B. A., 1978, Mineralogy and petrology of
    Precambrian ultramafic bodies from the Tobacco Root
    Mountains, Madison County, Montana: Unpub. M.Sc.
    Thesis, Indiana State University, Bloomington,
    Indiana, 126 p.

Tooker, E. W., 1963, Altered wall rocks in the central part
    of the Front Range mineral belt, Gilpin and Clear
    Creek Counties, Colorado: USGS PP 439, p.1-102.

White, D. E., 1981, Active geothermal systems and
    hydrothermal ore deposits, in Skinner, B. J., ed.,
    Economic Geology, 75th Anniversary Volume: The
    Economic Geology Publishing Company, p. 392-424.

Wooden, J. L., Vitaliano, C. J., Koehler, S. J., and
    Ragland, P. C., 1978, The late Precambrian mafic dikes
    of the Tobacco Root Mountains, Montana: Geochemistry,
    Rb-Sr geochronology, and relationship to Belt
    tectonics: Canadian Journal of Earth Sciences, V. 15,
    p. 467-479.

Vitaliano, C. J., Cordura, W. S., Hess, D. F., Burger, H.
    R., Hanley, T. B., and Root, F. K., Geologic map of
    the southern Tobacco Root Mountains, Madison County,
    Montana: Geological Society of America Map and Chart
    Series, MC-31, 1:62,500 scale, 1 map, 8 p. text.

----------------, Kish, S., Towell, D. G., 1980, Potassium-
    Argon dates and strontuim isotopic values for rocks of
    the Tobacco Root batholith, southwestern Montana:
    Isochron/West, no. 28, p. 13-15.

Weir, K., 1982, Maps showing geology and outcrops of part

of the Virginia City and Alder Gulch quadrangles,

Madison County, Montana: USGS Map MF-1490, 1:12,000

and 1:4750 scales.

Winchell, A. N., 1914, Mining district of the Dillon

quadrangle, Montana, and adjacent areas: USGS

Bulletin 574,

191 p.

Appendix I.

Ore and gangue minerals historically reported in the districts of the Tobacco Root mining region.

Appendix I.

MINERAL	DISTRICT					
	VIR.CITY	PONY	SHERDN.	TDLWV.	NORRIS	RENOVA
Argentite	X	X			X	
Arseno-pyrite			X		X	
Azurite		X				
Barite				X		
Bornite			X	X	X	
Calcite	X	X	X	X	X	X
Cerargy-rite					X	
Cerussite				X	X	
Chalcan-thite						X
Chalcocite				X	X	
Chalcopy-rite	X	X	X	X	X	X
Chlorite	X				X	
Chryso-colla		X		X	X	
Copper				X		
Cuprite			X	X	X	
Dolomite			X	X		X
Flourite		X				
Galena	X	X	X	X	X	X
Gold	X	X	X	X	X	X
Hematite	X	X	X	X	X	X
Huebnerite		X				
Limonite	X	X	X	X	X	X
Magnetite		X		X	X	
Malachite	X	X	X	X	X	X
Melaconite			X	X		
Melanterite						X
Microcline	X					
Molybden-ite		X				
Nagyagite	X					
Pyrargyrite	X	X				
Pyrite	X	X	X	X	X	X
Pyrolusite	X	X	X	X	X	X
Quartz	X	X	X	X	X	X
Siderite			X	X		
Silver	X	X			X	
Sphalerite	X	X	X	X	X	X
Stibnite	X					
Sylvanite	X					X
Tetrahedrite	X		X	X	X	

(from Cole, 1983)

Appendix II.

Photomicrographs of polished sections with location, hand-sample description, and sequence of mineralizing events.
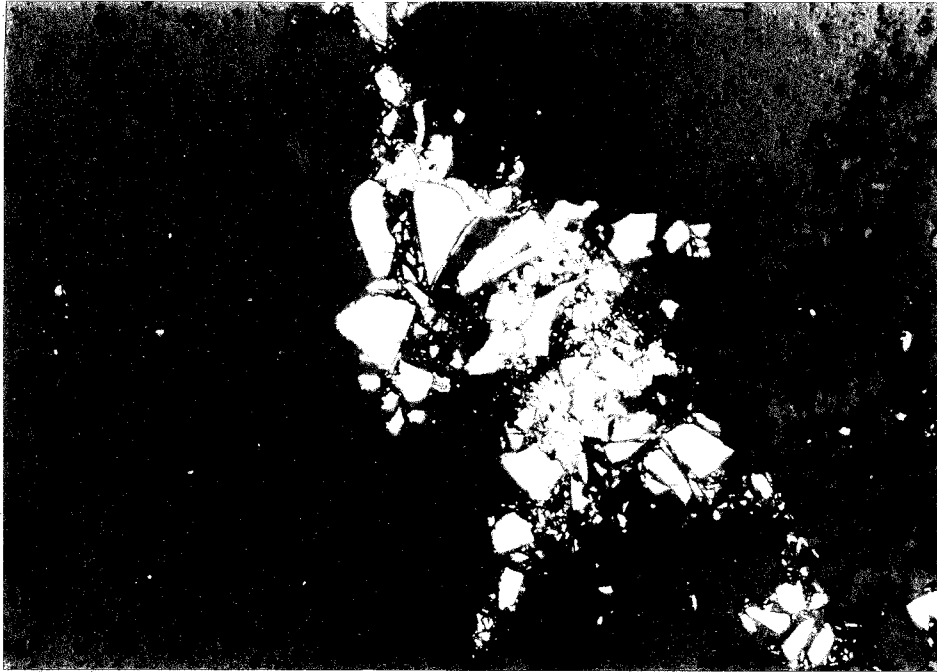
f.o.v.= 0.6mm

<u>89 ms1 018A</u>- High Up mine dump; light gray, brecciated
quartz with rounded to subangular clasts
with quartz matrix and minor sulphide
blebs (1%).

quartz + pyrite ——▶ brecciation ——▶
chalcopyrite.
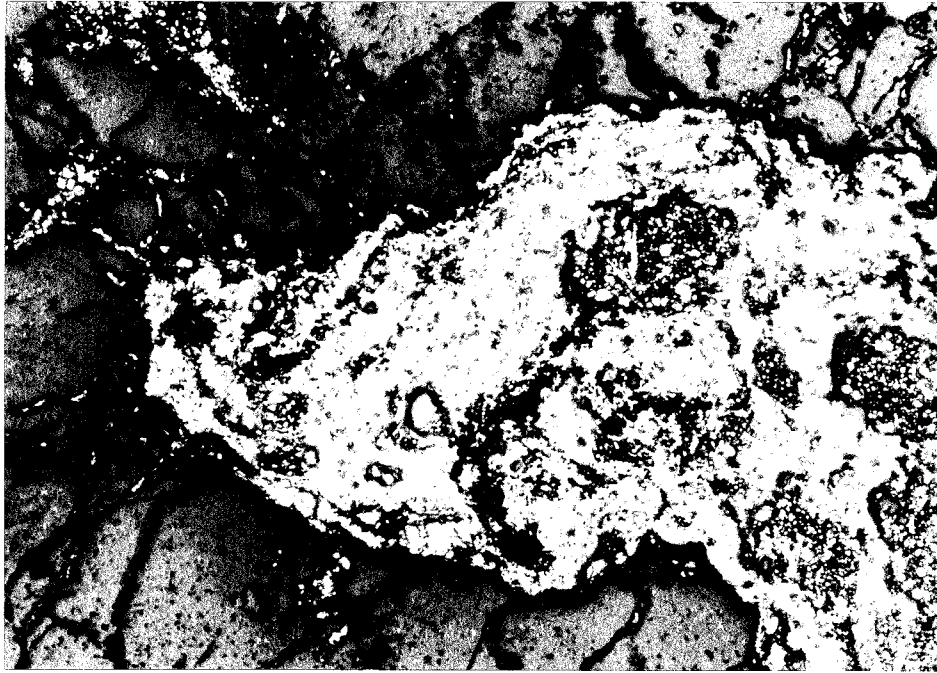
f.o.v.= 1.2mm

<u>89 msl 026</u>- Northern Pacific vein; brecciated quartz with
dark sulphide matrix (30%), clasts are
angular to subangular.

quartz + pyrite ⟶ brecciation ⟶ chalcopyrite
+ tetrahedrite

f.o.v.= 0.6mm

89 msl 028- Surface sample of the "South Vein" at the Easton mine; massive, milky quartz with fractures filled by sulphides (2%).

quartz + pyrite ⟶ brecciation ⟶ chalcopyrite + acanthite.
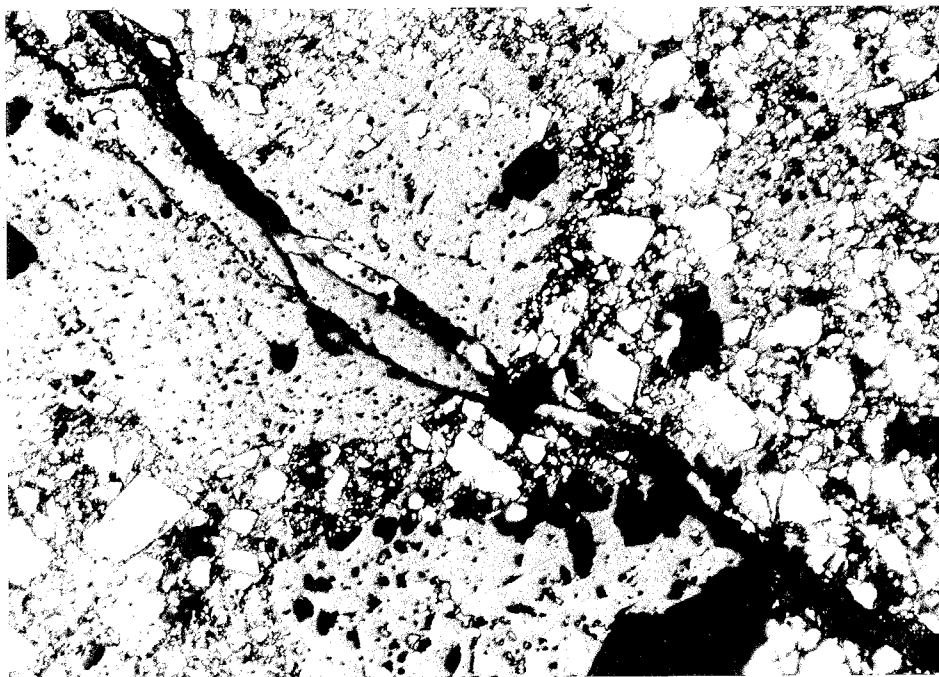
f.o.v.= 0.6mm

89 msl 052- Eastern most vein in the Pacific Pit; light
gray brecciated and massive quartz with
minor sulphides (3%).

quartz + pyrite ⟶ brecciation ⟶ sphalerite
⟶ quartz + acanthite + galena + chalcopyrite
veinlets.

f.o.v.= 1.2mm

89 ms1 070- Lower Easton dump, position on dump suggests
sample represents lowest level in Easton mine;
light gray, brecciated quartz with minor
sulphides (3%).

quartz + pyrite ⟶ brecciation ⟶ galena ⟶
deformation (bending) ⟶ chalcopyrite ⟶
quartz veinlets.
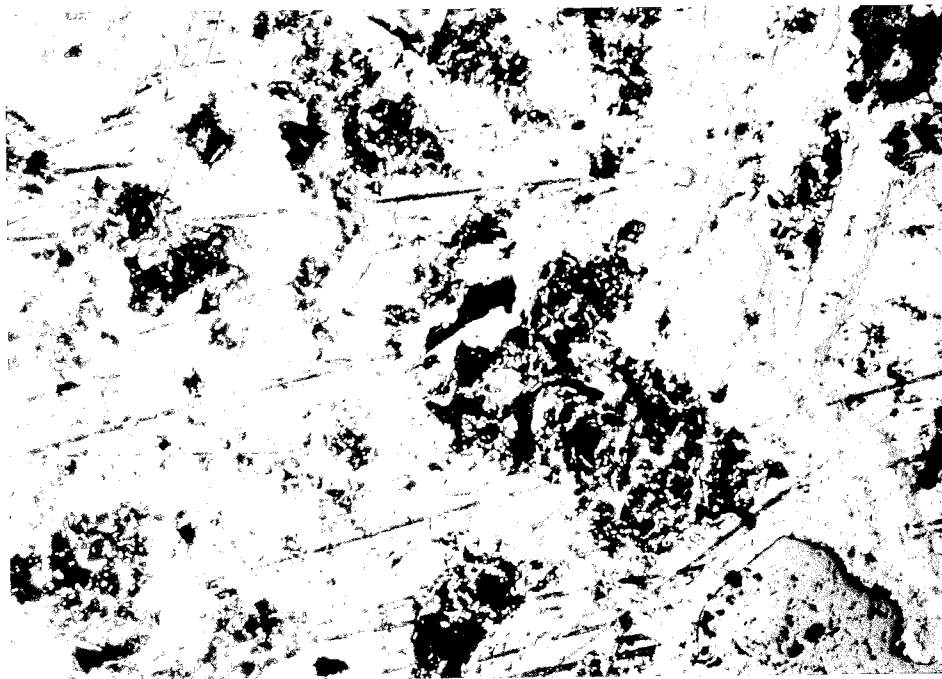
f.o.v.= 1.2mm

<u>89 ms1 071</u>- Section 16 prospect dump; massive milky quartz
with sulphide blebs (5%) and abundant malachite
staining on fractures.

quartz + chalcopyrite ⟶ chalcocite ⟶
goethite ⟶ malachite.

f.o.v.= 1.2mm

<u>ML-G1-</u> Little Lode mine; light gray to milky massive
quartz with blebs of native gold and sulphides
(3%).

quartz + gold + acanthite.

Appendix III.

Trench sample geochemistry.

TRENCH #1 (values in ppm)

footage	Au	Ag	As	Hg	Sb
5	0.380	6.300	13.000	2.000	0.001
8	2.500	57.700	31.000	1.000	0.001
13	0.630	7.900	18.000	5.000	0.001
18	0.013	0.500	10.000	4.000	0.001
23	0.900	28.800	10.000	3.000	0.001
26	1.170	68.000	10.000	5.000	9.000
28	3.200	96.900	10.000	4.000	8.000
32	0.142	1.900	10.000	1.000	0.001
37	0.009	0.400	31.000	6.000	48.000
42	0.026	1.200	19.000	5.000	0.001
47	0.063	1.400	10.000	4.000	0.001
52	0.050	2.300	29.000	6.000	106.000
57	0.114	1.000	27.000	1.000	0.001
58	16.100	250.000	67.000	7.000	0.001
59	14.500	320.000	10.000	2.000	9.000
64	0.132	1.500	10.000	3.000	0.001
69	0.310	3.500	17.000	2.000	0.001
74	0.490	4.700	17.000	1.000	0.001

TRENCH #10   (values in ppm)

footage	Au	Ag	As	Hg	Bi	Sb
5	0.066	0.300	10.000	5.000	0.001	0.000
15	0.078	0.900	10.000	2.000	0.001	0.000
25	0.220	1.500	10.000	3.000	0.001	0.000
35	0.009	0.001	10.000	3.000	0.001	0.000
45	0.039	0.001	10.000	3.000	5.000	0.000
55	0.086	1.700	10.000	3.000	13.000	0.000
65	0.180	0.900	10.000	1.000	0.001	11.000
75	0.430	1.000	10.000	6.000	5.000	0.000
85	0.380	2.800	10.000	3.000	0.001	33.000
95	3.650	22.500	25.000	5.000	5.000	24.000
105	3.500	14.600	23.000	4.000	6.000	0.000
115	0.650	0.300	25.000	5.000	0.001	0.000
125	0.076	0.001	10.000	4.000	14.000	0.000
135	0.033	0.300	10.000	4.000	0.001	0.000
145	0.015	0.001	10.000	2.000	0.001	0.000
155	0.016	0.001	10.000	3.000	9.000	0.000
165	0.010	0.001	10.000	3.000	0.001	0.000
175	0.010	0.300	18.000	3.000	0.001	0.000
185	0.001	0.001	10.000	2.000	0.001	0.000
195	0.051	0.600	10.000	3.000	0.001	0.000

Appendix IV: Equations for quantitative determination of clay mineral species.

The calculations are as follows and reported in parts in 10:

$$\text{Illite} = \frac{I_{(1G)}}{T} \times 10$$

$$\text{Smectite} = \frac{\frac{S_{(1)}}{4}}{T} \times 10$$

$$\text{Chlorite} = \frac{C_{(3)}}{I_{(2)}} \times \frac{I_{(1G)}}{T} \times 10$$

$$\text{Mixed-layer I/S} = \frac{I_{1H} - I_{(1G)} - \frac{S_{(1)}}{4}}{T} \times 10$$

$$\text{Kaolinite} = \frac{K_{(1)}}{T} \times 10$$

or, if chlorite is present

$$= \frac{K_{(2)}}{2C_{(4)}} \times \frac{C_{(3)}}{I_{(2)}} \times \frac{I_{(1G)}}{T} \times 10$$

where T is equal to "total counts"

If chlorite is not present

$$T = I_{(1H)} + K_{(1)}$$

or, if chlorite present

$$= I_{(1H)} + \frac{C_{(3)} I_{(1G)}}{I_{(2)}} + \frac{K_{(2)} C_{(3)} I_{(1G)}}{2C_{(4)} I_{(2)}}$$

References for clay mineral identification:

Austin, G. S., and Leininger, R. K., 1974, Effects of heat-treating sedimented mixed-layer illite-smectite as related to quantitative clay mineral determinations: Journal of Sedimentary Petrology, v. 46, p. 206-215.

Brindley, G. W., Quantitative X-ray mineral analysis of clays, *in* Brindley, G. W., and Brown, G., eds., Crystal structures of clay minerals and their X-ray Identification: Mineralogical Society, London, Monograph 5, p. 411-438.

Drever, J. I., 1973, The preparation of oriented clay mineral specimens for X-ray diffraction analysis by a filter-membrane peel technique: American Mineralogist, v. 58, p. 553-554.

Schultz, L. G., 1960, Quantitative determination of some aluminous minerals in rocks: Clay and Clay Minerals, v. 7, p. 216-224.

This thesis is accepted on behalf of the faculty
of the Institute by the following committee:

William X. Chavez, Jr.   5 December, 1990
<div align="center">Adviser</div>

Andrew Campbell

Paul J. Eimon

Dec 5 1990
<div align="center">Date</div>